Table of Contents / Table de matières

Nuclear Journal of Canada

Volume 1 No. 3 Sept. 1987 sept.

Journal Nucléaire du Canada

Canadian Nuclear Society
Societé Nucléaire Canadienne

Nuclear Journal of Canada
Journal Nucléaire du Canada

Volume 1 No 3 Sept. 1987 sept.

Published by University of Toronto Press
for The Canadian Nuclear Society
111 Elizabeth Street, Toronto, Ontario, Canada, M5G 1P7

Annual Subscription Rates:
Institutional in Canada $90.00 Canadian
outside of Canada $90.00 U.S. (includes postage and handling)
Single issue in Canada $25.00 Canadian
outside of Canada $25.00 U.S. (includes postage and handling)
Replacement Issue in Canada $20.00 Canadian
outside of Canada $20.00 U.S. (includes postage and handling)
Note: Supplements to the journal will be published periodically
and will be priced separately
Designed and Printed University of Toronto Press
ISSN 0833-1758

Second Class Mail Registration number 74171 (Sept.) 1987

Editorial

Alan Wyatt
Editor

With work well advanced on the fourth issue of the *Journal* we are approaching completion of the first volume. The launching of any new journal often involves a 'chicken-and-egg' situation. Researchers would often prefer to have their papers published in established journals; but how does a new journal become established without a steady flow of papers? The *Nuclear Journal of Canada* is fortunate in having the support of a large number of people in the nuclear field in Canada and elsewhere, and in being able to draw on the many excellent papers presented at conferences and seminars sponsored by the Canadian Nuclear Society.

Conference papers often describe work in progress. For a journal paper it is usually best to complete the work; the resulting paper is then essentially a different paper from the earlier one. In order to cater to the wide interests of the *Journal*'s readership it is appropriate to include a couple of broad review papers in each issue. As the *Journal* becomes more firmly established, it is planned to increase the proportion of original research papers in each issue. Word-of-mouth and personal contact are the most effective ways of promoting the *Journal*. All of our readers should consider the *Journal* as the first place to send their papers for possible publication, and to urge their colleages to do likewise.

Although, during its first year, the *Nuclear Journal of Canada* has published papers on a wide range of subjects, including food irradiation, the Chernobyl accident, medical applications, reactor design and operation, health risks, waste management, etc., there are other areas that have not been covered. In the next issue we expect to have our first paper in the fusion energy field, but we have still to receive our first paper in the uranium area.

In order to encourage reports of preliminary work, extensions of previously reported work, and shorter papers on a wide range of technical items, it is planned to start a Technical Notes section in the *Journal*. Normal length would be in the range of 500 to 4,000 words, compared to the full papers of 5,000 words and more. Items for inclusion in this section should be typed, double-spaced, on plain paper. Abstracts are not required. The original and two copies should be addressed to the Editor, *Nuclear Journal of Canada*, 111 Elizabeth Street – 11th Floor, Toronto, Ontario, Canada, M5G 1P7. Submissions for inclusion in the Technical Notes section will be subject to a less formal review process.

Chernobyl – A Canadian Technical Perspective

J.Q. Howieson
Thermohydraulics Branch
V.G. Snell
CANDU 300 Safety
Atomic Energy of Canada Limited
CANDU Operations
Sheridan Park Research Community
Mississauga, Ontario L5K 1B2

Abstract

On 26 April 1986, the unit 4 reactor at the Chernobyl Nuclear Power Station in the Soviet Union suffered a severe accident which destroyed the reactor core. The reactor design, as it relates to the accident sequence, is reviewed in detail, using information presented in Soviet literature and at the International Atomic Energy Agency Post-Accident Review Meeting in August 1986. The aspects of the design which, in our view, exacerbated the accident are presented and compared to the CANDU[1] reactor design. Key Chernobyl design aspects examined are (in order of importance): capability of shutdown, containment, and the variation of void reactivity with operating state. A number of design issues have been raised for Chernobyl which are less relevant to the accident and which we feel are less important. These include: the sign of the void coefficient, pressure tubes, use of computers in control, multi-unit containment, and fire protection. These are discussed briefly, and compared with the CANDU approach. It is concluded that the Chernobyl shutdown system design was deficient in that it did not provide an adequate level of safety for *all* plant operating states, and the plant safety depended too heavily on the skills of operators in maintaining many reactor parameters, especially reactor power and power shape, within a certain operating envelope. By contrast, the ability of the CANDU shutdown systems to shut down the reactor is independent of the operating state of the plant and, in that sense, the design is much more forgiving. Nevertheless, as a prudent response to Chernobyl, Atomic Energy of Canada Limited (AECL) is undertaking two areas of design review for CANDU: 1) a re-examination of all possible core configurations to ensure these do not impede shutdown capability, and 2) a review of fire protection featu presence of high radiation fields. Reviews of o aspects are underway by the Canadian electrical util review by the Canadian regulatory agency (the Aton Control Board) has also been performed.

Résumé

Le 26 Avril 1986, un grave accident s'est produit à du réacteur no. 4 de la centrale nucléaire de Tcher URSS: Le coeur du réacteur a été entièrement c conception du réacteur et son rapport avec le déroul l'accident sont étudies en détail dans le présent doc l'aide des documents soviétiques et de renseig présentés lors de la Réunion d'analyse de l'acc l'Agence Internationale de l'Énergie Atomique, en a Les aspects de la conception et du fonctionneme notre avis, ont aggravé l'accident, sont présentés parés avec ceux de la conception du CANDU.[1] Les asp de la conception de Tchernobyl étudiés dans le document sont les suivants (par ordre d'importance ité de mise à l'arrêt, confinement, et variation de la due au coefficient de vide selon la configuration c D'autres questions relative à la conception ont été s en relation avec Tchernobyl, mais elles sont moins tes à l'accident et nous semblent moins importantes du signe du coefficient de vide, des tubes de f contrôle-commande par ordinateur, de l'enceinte de ment multi-tranches, et de la protection contre les in Il a été conclu que le système d'arrêt de Tchernc insuffisant dans la mesure où il n'était pas capable de un niveau de sûreté suffisant pour chacun des fonctionnement de la centrale, et que la sûreté de la dépendait trop des opérateurs, c'est-à-dire de leur h maintenir plusieurs paramètres du réacteur, et s niveau et forme de puissance, à l'intérieur de cer maines de fonctionnement. Par contre, dans le cas d le fonctionnement des systèmes d'arrêt est indépe l'état de fonctionnement de la centrale: en ce conception est beacoup plus tolérante. Cependant tenir compte des erreurs de Tchernobyl, l'EACL reve études de conception du CANDU: 1) un réexamen de t

Keywords: safety, accident, nuclear reactors, nuclear reactor accidents, accident analyses, safety engineering, radio heavy water reactors, graphite-moderated reactors.

configurations possibles du coeur, afin d'assurer qu'elles n'entravent pas sa capacité de mise à l'arrêt, et 2) une révision des caractéristiques de protection anti-incendie, dans des champs de rayonnement. Les compagnies d'électricité canadiennes effectuent actuellement l'analyse des aspects de fonctionnement et une étude a aussi été executée par la Commission de Contrôle de l'Énergie Atomique, l'organisme réglementaire canadien.

Introduction

On 26 April 1986, the unit 4 reactor at the Chernobyl Nuclear Power Station suffered a severe accident. The core and much of the building were destroyed; all of the noble gases and several per cent of other fission products were released to the environment.

The reactor design and the accident sequence have been studied extensively since then. While a reasonable amount of information on the reactor design was publicly available, [Semenov 1983; Levin and Kreman 1983; Dubrovsky *et al.* 1979; Turetskii *et al.* 1984; Babenko *et al.* 1980; Dollezhal and Emel'yanov 1986], the specific features of unit 4 design and the accident sequence were presented by the Soviets at an International Atomic Energy Agency (IAEA) meeting in Vienna in August 1986. The related reports [USSR 1986; INSAG 1986] are the most authoritative documents available to date, and this information is now being used by all countries with a nuclear power program to examine the robustness of their plant design and operation in light of the events at Chernobyl, and to see what lessons can be learned.

In this paper the design review done to date in Canada by Atomic Energy of Canada Limited (AECL) is presented. From the Canadian point of view it covers:

1 relevant information on the Chernobyl design and the accident, both as presented [USSR 1986; INSAG 1986; Dastur *et al.* 1986] by the Soviets at the Post-Accident Review Meeting (PARM) held in Vienna from 25–29 August 1986, and as deduced from publicly available Soviet documentation;

2 details of AECL's technical review of the Canadian Deuterium Uranium Pressurized Heavy Water Reactor (CANDU PHWR) against the background of the Chernobyl accident; and

3 implications of the Chernobyl accident.

Reviews of operational aspects are underway by the Canadian electrical utilities, and a review by the Canadian regulatory agency (the Atomic Energy Control Board) has also been performed.

Other related reports produced in Canada to date are a technical review [Howieson and Snell, 1987], an executive summary of the technical review [Snell and Howieson 1987], and a less technical summary for the general public [Snell and Howieson 1986].

Brief Review of the Accident

Accident Sequence

The Post-Accident Review Meeting (PARM) for Chernobyl took place from 25 to 29 August 1986. At the meeting and during the following week, the Soviets presented detailed information on the accident sequence [USSR 1986; INSAG 1986], accident recovery, radiological consequences, and planned design / operational changes for other reactors of the same type. In this section the information presented is summarized.

Accident Sequence

In the process of performing a safety-related test just prior to a scheduled shutdown, a sequence of events occurred which took the reactor outside the permissible operating range, and at the same time led to the ineffectiveness of emergency shutdown. The combination of operating conditions, control rod configuration, operator violations of procedures, and the inherent core characteristics, led to a large reactivity transient and rapid power rise.

The fuel energy reached a mechanical breakup level, causing rapid fuel fragmentation in the bottom portion of the core: this resulted in an overpressure in the cooling circuit. Pressure tube failures led to pressurization of the core vessel and loading of the 1,000-tonne reinforced-concrete top shield slab, expelling it from the reactor vault. Burning fragments were ejected from the core, starting 30 fires in the surrounding area.

Immediate Effects of Power Runaway

The core expanded into the surrounding space in the reactor vault (i.e., there was destruction of the radial reflector and the water shield), and dispersal of the fuel and the graphite moderator resulted in the core becoming subcritical. The severing of reactor inlet pipes and outlet pipes and the destruction of the upper portion of the reactor building led to air access to the core. The graphite began to burn locally; ultimately 10% was oxidized.

Radioactive Releases

Fragmented fuel and fuel aerosols were expelled in the explosion, and taken high (0.8–1 km) into the atmosphere by the thermal plume from the hot core. This continued for several days as the graphite burned and the fuel oxidized, with the rate of release falling as the fuel cooled.

To stop the release the Soviets dropped about 5,000 tonnes of material, including boron carbide (to ensure shutdown), dolomite (to produce carbon dioxide to try to smother the fire), lead (to absorb heat and provide shielding), and sand and clay (to create a filter bed). This led to a rise in fuel temperature as the convective cooling was cut off. The core reached a hot, oxidizing

condition (peaking on May 4), and fission product release rates increased again.

At this stage the Soviets fed nitrogen to the bottom of the reactor cavity, cutting off the ingress of oxygen and extinguishing the graphite fire. The fuel temperatures dropped, with a corresponding sharp reduction in releases. The core was now in a stable air convective cooling mode.

Total releases were estimated by the Soviets to be: 100% of the noble gases, 10–20% of the volatile fission products, and approximately 3.5% of the long-lived fission products. It was acknowledged that there is substantial uncertainty associated with these estimates.

Accident Recovery

Firefighting started immediately and external fires were brought under control in four hours. Extensive cleanup and decontamination began. A 'sarcophagus' (reactor burial structure), utilizing a forced-convective air-cooled system with open ventilation and a filtration system, was built around the reactor and turbine hall. The sarcophagus surrounds the reactor and turbine of unit 4 and reduces the radiation level so that reactor units 1, 2, and 3 can be operated.

Core meltdown was a Soviet concern during the days following the accident, but did not occur. To prevent molten materials from falling into the water suppression pools below the reactor, they were drained and replaced by concrete. To prevent ground water contamination, a concrete barrier was built deep into the ground around the area.

As of April 1987, units 1 and 2 have been restarted. The timing of startup of unit 3 is less certain, due to the higher level of radioactivity and the need to check the condition of the equipment.

Radiological Consequences

Onsite staff. There were 2 immediate deaths as a result of the accident. Over the next few weeks there were 29 fatalities from high radiation doses and burns received by station staff trying to bring the accident under control. The dose distribution for these people was as follows:

Dose (rads)	*No. Patients*	*No. Deaths*
600–1,600	22	21
400–600	23	7
200–400	53	1

Offsite – effects of the accident on the surrounding population. Emergency response measures included: 1) distribution of iodine tablets to the population around Pripyat, apparently successfully and with minor side effects; 2) sheltering for residents of Pripyat before evacuation; and 3) evacuation once the plume shifted towards Pripyat.

The Soviets estimated the collective dos *ment*[2] in the USSR as:

31×10^6 person-rem *external* (over 50 years),
210×10^6 person-rem *internal* (over 70 years).

In both cases the dose commitment is mc caesium. The latter figure is a conservative which was acknowledged verbally as perhap too *high* at the PARM and more recently in Sov reports [Nuclear News 1987].

Design / Operational Changes for Chernoby Reactors

A number of design and operational changes nobyl-type reactors were presented by the S the meeting.

Design:

1 Improved effectiveness of emergency shutdov achieved in the short term by increasing from 3 equivalent number of control rods normally inse core, and also by limiting their uppermost rem tion to 1.2 m from the top of the core.
2 Additional operating information will be made a the operator in the control room.
3 In the longer term the fuel enrichment will be in 2.4%. This should reduce void holdup but w more reactivity from the control rods (more sorbers).
4 Also, in the longer term, a faster shutdown syste added. Poison injection (liquid, gas or solid) i control rod channels was mentioned as a possil

The above mentioned changes were statec the maximum reactivity below prompt critica most severe accident) and also to provide rapi shutdown.

Operational. The areas that will receive empl 1)adherence to operating procedures, 2)clarifi command responsibilities, and 3)improveme man-machine interface.

Design Aspects Relevant to the Accident

This section identifies aspects of the Chernob design and operation relevant to the accide detailed descriptions of the design are given i presented in August 1986 [USSR 1986; INSAG 1

Conceptual Basis

Chernobyl unit 4 is of the RBMK (roughly tran 'large reactor with tubes') type, and the most the 1,000 MW(e) series. It is a graphite-mo boiling-light-water-cooled, vertical pressure sign, using enriched (2% U-235) UO_2 fuel power refuelling. It utilizes a direct cycle, to electricity from twin turbines (see Figure 1).

The reactor core is shown in Figure 2. One o

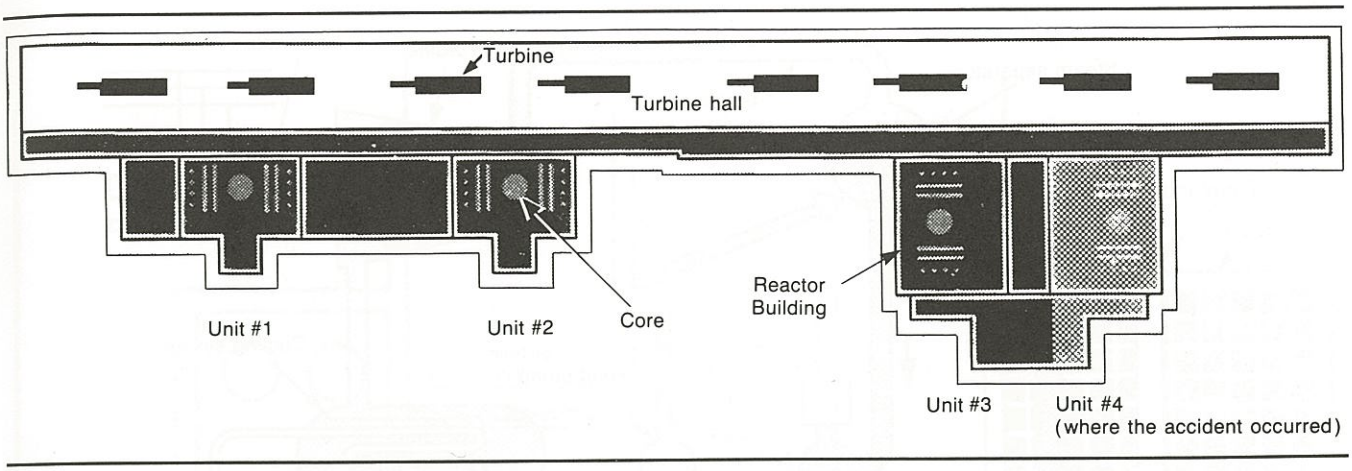

Figure 1 Layout of four reactor units.

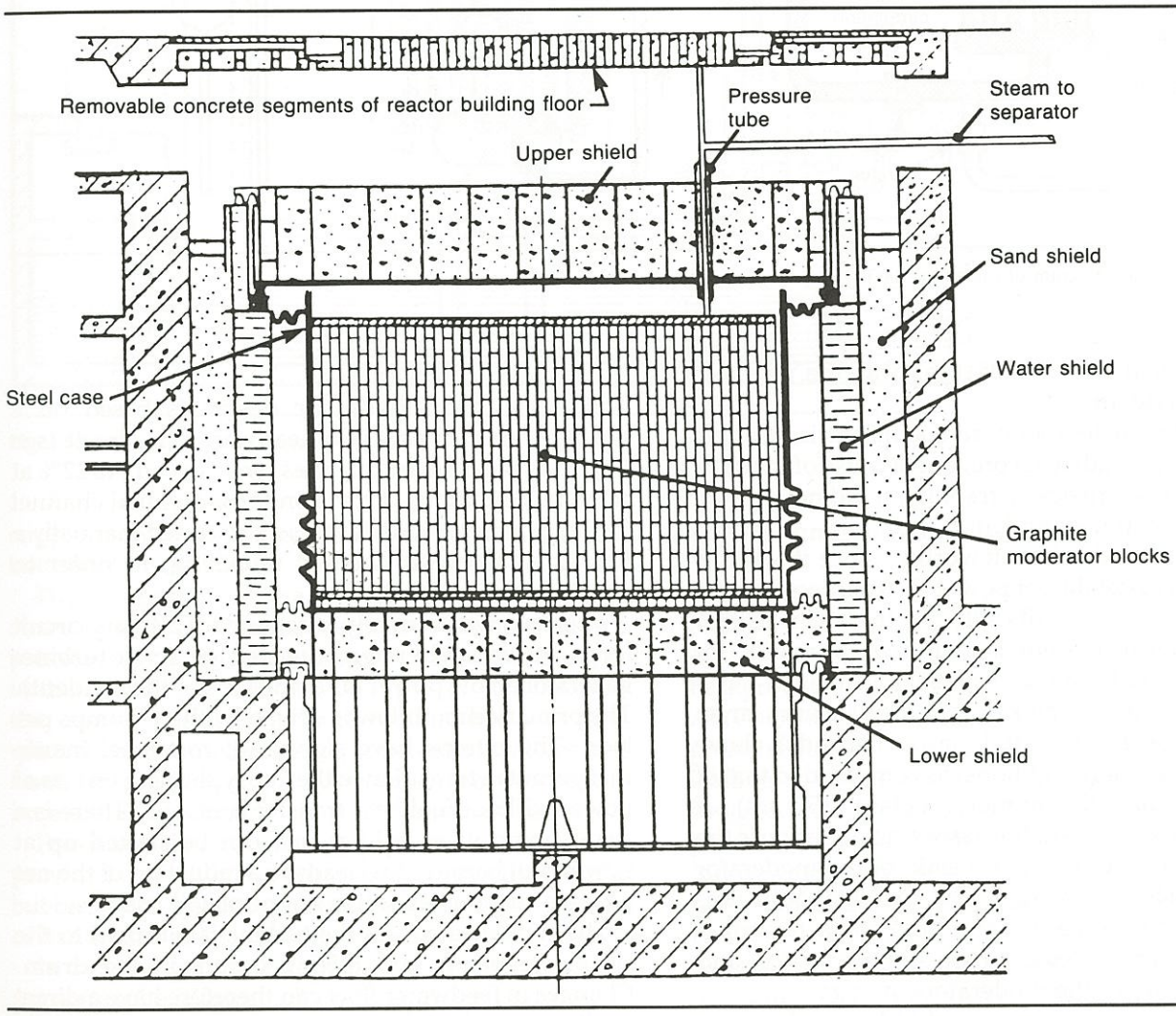

Figure 2 Cross-sectional view of reactor vault.

reactor physics parameters in the equilibrium fuel state is a positive void reactivity with a strong dependence on the operational configuration of the reactor. The design basis called for a maximum void reactivity coefficient of 0.2 mk / % void, whereas at the accident conditions it was reported to be 0.3 mk / % void. (Note that at their *normal* operating conditions, i.e., above 20% full power, the void coefficient is about 0.05 mk / % void.) Thus the overall fast power coefficient (which includes both the positive void coefficient and the negative effect of fuel temperature increase) is negative under normal high-power conditions, but positive

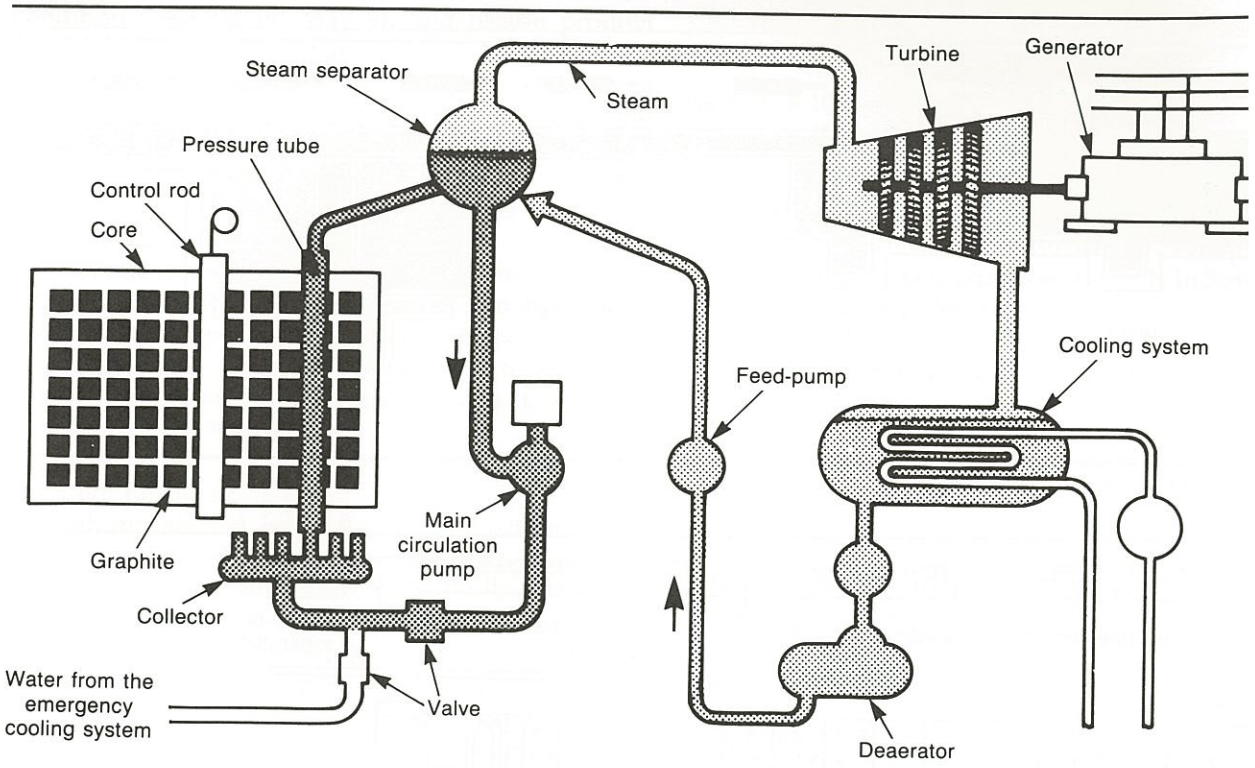

Figure 3 Schematic Diagram of the RBMK-1000.

at low power (below ~ 20%), as was the case just before the accident.

The moderator temperature coefficient is strongly positive for the irradiated core, but because of the slow response characteristics of graphite, it did not play an important role in the accident.

The large core size is noteworthy, since it leads to the potential instability of power distribution, and, in the extreme, to local criticality. In the RBMK reactor a spatial control system is required, primarily for feedback-reactivity-induced spatial instabilities.

The graphite moderator heat capacity is very large, being at least 400 FPS (full power seconds) above ambient at nominal conditions, as compared to that of fuel (11 FPS) and the primary coolant (150 FPS). A distinguishing feature of the RBMK reactor design is the use of the primary circuit as a sink for the moderator heat (5.5% of fission energy). Considerable sophistication has gone into the design of the contact conductance between the pressure tube and moderator, and the conductivity of the moderator cover gas.

With respect to emergency shutdown, the most important features are a slow rate of negative reactivity insertion and a dependence of that rate on the control rod configuration. Administrative controls were required to ensure at least 30 equivalent rods were in the core at all times. This heavy reliance on administrative control was traced to early USSR experience in which operators were more reliable than automatic systems.

Thermalhydraulic Design

The RBMK thermalhydraulic design is base
boiling water, direct-cycle heat transport cir
Figure 3). Steam mass qualities range from 11 t
nominal conditions. Provision for individual
flow adjustment is made and is performed ma
few times between channel refuelling, in
match flow to power.

There are two normally independent primar
loops, which can be interconnected to a single
generator at low power (as at the time of the ac
The primary circuit flow is driven by three pu
loop. The pumps have significant rotationa
that permits a transition to thermosyphoning o
power without fuel heat transfer concerns. Tl
spare pump in each loop that can be starte
power, but because this leads to a reduction o
positive suction head, it is not normally used

The condensate from the turbine is returne
steam separator, and mixing occurs in the
Changes in feedwater flow can therefore have
feedback on core inlet temperature (separated
only by a transport delay).

Containment Design

The containment 'localization' system at Ch
was a recent RBMK design (see Figure 4). In thi
the containment was divided into local compa
with distinct design pressures and relief / p

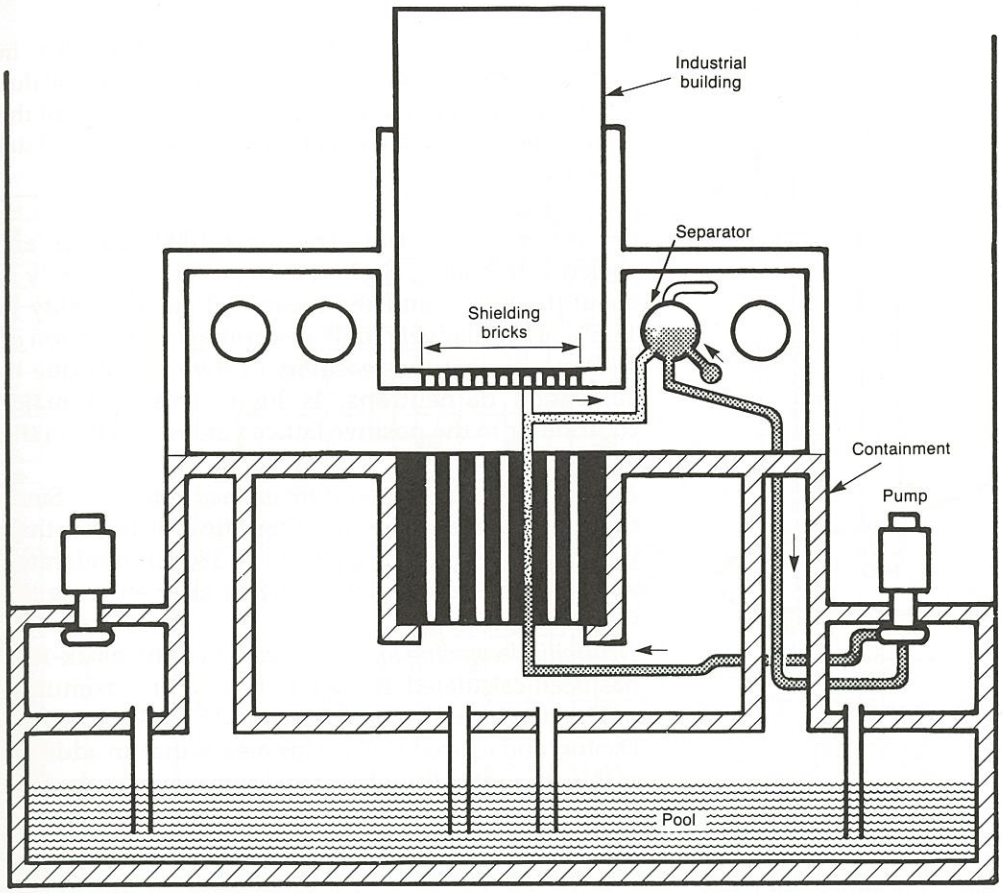

Figure 4 Chernobyl containment.

suppression to the water-filled 'bubbler pond' in the bottom of the building.

The top portion of the reactor (risers, separators, steam lines, fuelling machine room) was not within a pressure-retaining containment. For small pipe breaks in this group (e.g., a riser tube rupture), it is believed that the Soviets felt the large fuelling hall was adequate for the limited discharge rates and low expected levels of radioactivity. In any case, they stated the impracticality of building a containment of this size.

Pressure relief for the graphite core vessel was provided by eight 30-cm pipes connected to the bubbler pool. Relief capacity was stated to be capable of handling a single channel rupture.

In the accident, the steam explosion led to multiple pressure tube failures, which caused a pressure rise in the reactor vault, well beyond design capacity. Thus, the containment localization system played no real role in accomodating the accident. The basic structural integrity of the lower 'containment' compartments was preserved. The upper portions of the building were designed for modest loadings and suffered dramatically from the thermal, and possibly chemical, explosions that occurred.

Key Design Issues for Chernobyl

Variation of Void Reactivity with Reactor Operating State

Background

At Chernobyl, if coolant is lost (voids) from the pressure tubes, there is a positive reactivity addition leading to a rise in power. In fact, the plant was designed to cope adequately with this effect at high power. It was *not* designed to cope with the effect at low power, because the *size* of the void reactivity effect was strongly dependent on reactor operating parameters. Because of the unusual conditions of the reactor just prior to the accident (i.e., low reactor power; only 6–8 control and shutdown rods equivalent in the core, versus 30 required; high coolant flow through the core), there was an abnormally high void reactivity holdup.

Simulations done at AECL and at the U.S. Department of Energy suggest that *positive reactivity was also added by the shutdown system* [Chan *et al.* 1987; U.S. DOE 1986]. Normally, the absorber rods are attached to graphite displacers or followers, to increase their worth. As

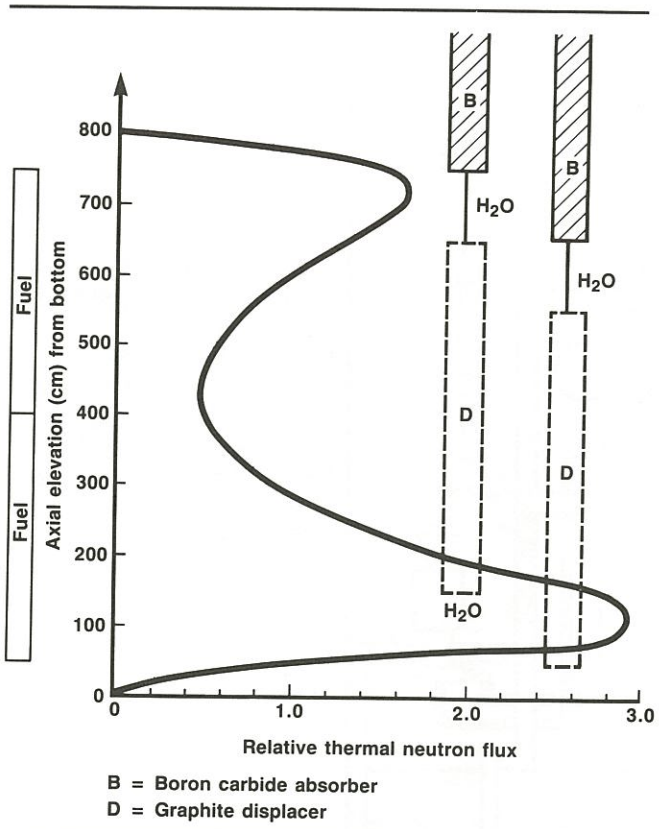

Figure 5 Axial flux distribution preceding accident.

they are inserted, the absorber rods move into the high-flux region in the centre of the core, which was previously occupied by the graphite, so the absorber rod effectiveness is enhanced (see Figure 5). If there were no graphite, the rod would displace water – also an absorber – so the change in reactivity with insertion would not be as great. But in the accident, most of the absorbers were well removed from the core. The flux was peaked at the top and the bottom, where most of the reactor power was being generated. Thus, when insertion of the absorbers first started, the *water* in the high-flux region at the bottom of the core *was first displaced by the graphite follower*, leading to a reactivity increase. Thus operating the plant in an abnormal condition resulted in an unusually large holdup of void reactivity, exacerbated by a deficient shutdown system design (see below, Shutdown Systems and Reactor Control), which led to the large power excursion and the resultant core damage.

Chernobyl Design

The characteristics of the RBMK-1000 design that affect void reactivity are:

1 the use of H_2O coolant;
2 the relatively high temperature of the moderator (~700°C), compared with that of the coolant (280°C);
3 a large and hence neutronically decoupled core (i.e., one which behaves like a number of independent reactors), and which, indeed, just before the accident, v pled into top and bottom halves; and
4 the requirement of significant reactivity hol solid absorber rods due to the use of enriched fu to the need to be able to override xenon build impracticality of using soluble poison in a solid moderator.

The use of H_2O coolant. The RBMK-1000 rea cooled with boiling H_2O. The mean coolant about 0.5 kg / L and the mean exit steam 14.5%. The relatively high absorption cross- H_2O means that the reactivity of the coolar absorption of neutrons, is high. This is contributor to the positive lattice void reactiv RBMK-1000.

Effect of moderator temperature on void reactiv the moderator temperature is significantly hi the coolant temperature (700°C vs 280°C), m neutrons are slowed down further after ent fuel channel.

Neutronic decoupling and void reactivity. The R has been calculated at AECL to have a first a mode subcriticality of between 6 and 7.5 mk [(Dastur, and Chexal 1987]. This means that an of this amount to the lattice reactivity would n radial half of the reactor critical, and result i cant power redistribution between the tw i.e., the reactor is fairly close to behaving independent reactors. This was particularly just prior to the accident. (By comparison, th ponding value for the CANDU 600 is 17 mk 1981]; i.e., the reactor behaves much more un The same phenomena are true for other ha Therefore, void reactivity addition in the R results in a complex power shape requiring trip logic to recognize the accident in time.

Effect of absorber rods on void reactivity. In th literature [USSR 1986] on the RBMK-1000 des stated that the designers have used the effe and spectrum changes due to the presence of rods (see Figure 6) to reduce void reactivity achieved by the combined use of manually absorber rods and coolant flow valves (t channel void fractions) and proper fuel mana the purpose is to adjust the neutron flux dis such that, on voiding, the flux increases in th sets of absorber rods and the role of the c moderator are enchanced. This leads to an in neutron absorption in the rods compared to th fuel and thereby produces negative reactivity

The magnitude of the void reactivity c changes with fuel burnup. According to the for fresh fuel the void reactivity coefficient is r For equilibrium fuel it is positive (about 0.0 void) for normal operating conditions, i.e., w 80 absorber rods partially inserted into t

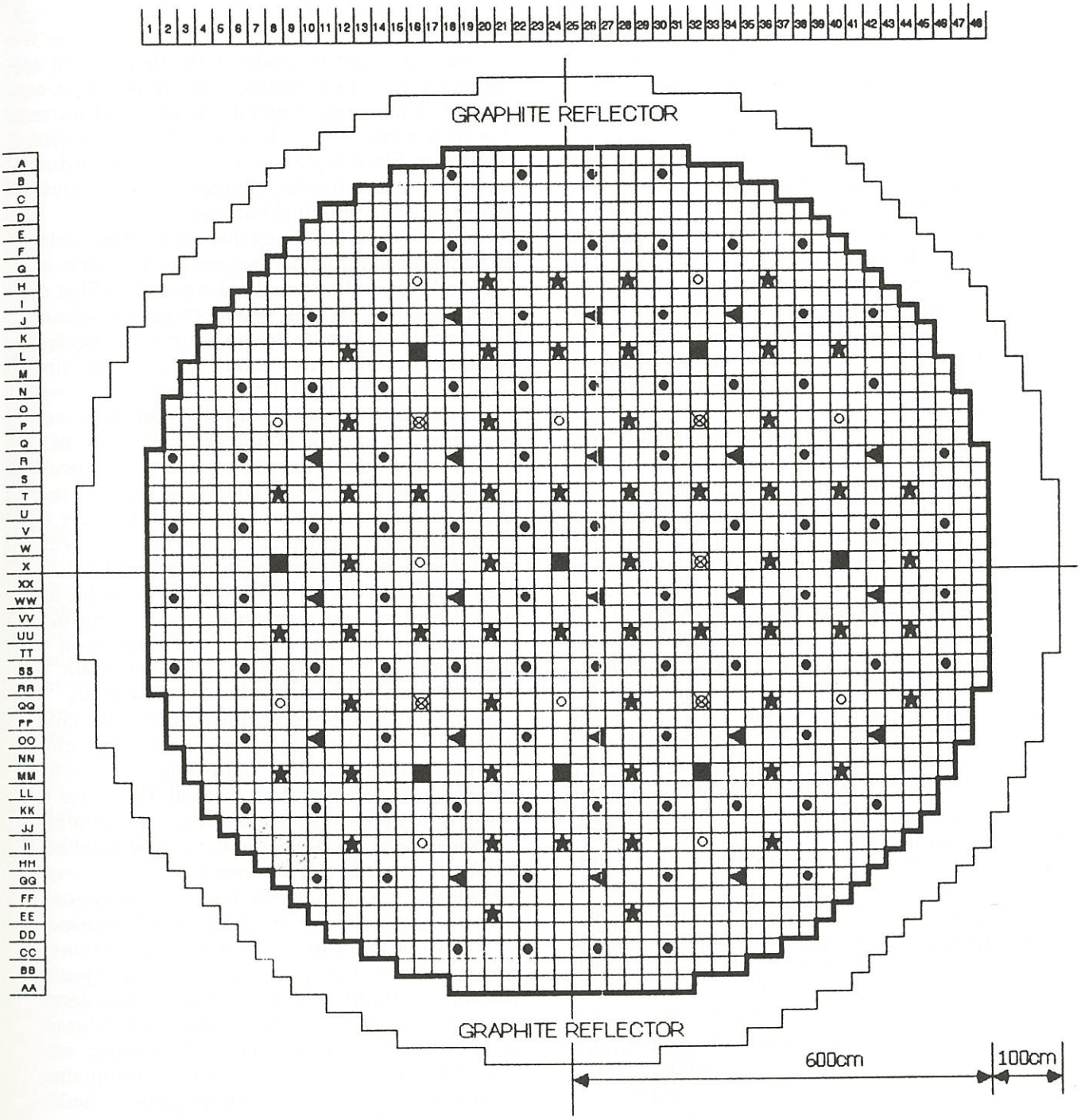

Figure 6 Reactor physics model of RBMK-1000 core.

The maximum possible void reactivity coefficient is 0.2 mk / % void at normal operation with a minimum of 30 equivalent rods inserted in the core. The coefficient was as high as 0.3 mk / % void before the accident, as there were only 6 to 8 equivalent rods in the core.

Comments on the Chernobyl Design

The size of the system void reactivity in the RBMK-1000 reactor can be controlled to a large extent by operational constraints. The safety of the reactor, therefore, is dependent on the competence of the reactor operators and on their adherence to these constraints. The system void reactivity in this reactor can become significantly higher under abnormal operating conditions. Such conditions include: a) reduction in the number of in-core absorbers with concurrent increase in fuel burnup, which is plausible during loss of refuelling capability; and b) reduction in reactor power level without a matched decrease in coolant flow rate.

In particular, the RBMK-1000 reactor is very sensitive to item b. In order to maintain a similar coolant void level in the reactor core, the flow is normally reduced as the power is reduced. However, at low powers (i.e., less than 20% full power), the flow cannot be reduced to match the power, and small changes in coolant conditions can have large effects on coolant void.

To summarize, then, the weakness of the Chernobyl design is that the void reactivity and the capability of the shutdown system depend significantly on the operating state of the reactor (and the ability of the operators to maintain the reactor within an allowable operating envelope). The Soviets themselves have indicated that operating procedures did not allow sustained operation (other than startup or shutdown) below 20% power.

CANDU Design

Void reactivity. The heavy water (D_2O) coolant, the heavy water moderator, and the natural uranium fuel are the major determinants of the void reactivity of the CANDU lattice.

Changes in neutron spectrum on voiding. The CANDU lattice pitch, which sets the volume of D_2O associated with a fuel channel, is chosen by mechanical considerations to facilitate on-power refuelling, and by economic considerations to maximize fuel burnup by adjustment of the rate of neutron absorption in U-238 (initial conversion ratio), and thereby of plutonium production. As a result, the standard CANDU lattice consists of a 10-cm inside diameter fuel channel arranged on a square pitch of 28.6 cm.

The amount of moderator contained in the lattice produces a well-thermalized neutron spectrum in the fuel. Over 95% of the neutron population in the fuel has energies below 0.625 eV. Thus, the role of the D_2O coolant as moderator is not that significant. If the coolant is lost from the fuel channel, there is a small reduction in the energy (or velocity) of th population in the fuel.

This shift in neutron spectrum in the fuel fuel neutron absorption rates in the therma thermal ranges. In particular, the resonanc tion in U-238 decreases, and there is a 6.3-m due to the increase in the lattice resonan probability. Since depletion of U-238 is minin the life of the fuel, this contribution to void re almost constant with fuel burnup.

Loss of neutron scattering due to loss of co increases the neutron flux and reaction rates 1.4 MeV fast-fission threshold for U-238. tributes 5.2 mk to void reactivity for the 37-element fuel bundle design. Due to the depletion of U-238, this contribution is al constant over the life of the fuel.

The changes in spectrum affect the therma rates because of the non-linear behaviou uranium and plutonium cross-sections witl velocity. On voiding there is a 3% increa U-235 neutron production rate, which is la the increase of 2.5% in its absorption rate. Th production per absorption increases by 1. plutonium cross-sections behave differently presence of several resonances; the coolir spectrum on voiding reduces the absorp production rates in the fuel. The net re decrease in neutron production per absorpti

So the contribution to void reactivity of th in thermal reaction rates depends on the irra the fuel because of the role of the plutonium and of the fission products. In total, the la reactivity in the CANDU reactor is 16 mk when fresh and decreases with irradiation. At eq fuel burnup it is 11 mk [Rouben 1987].

Effect of absorber rods on void reactivity. In th design, the mechanism that leads to a chang reactivity due to the presence of absorber roc different from that at Chernobyl. Voidin coolant in the CANDU reactor results in a small in the thermal neutron flux in the modera means that if there are absorbers preser moderator (such as adjusters), their neutron tion rate will drop. This effect is included in t of void reactivity given above (see Changes ir spectrum on voiding).

Comments on the CANDU Design

In direct contrast to the key weakness in the yl reactor design, the CANDU reactor physic that void reactivity does not depend on state, and therefore the shutdown systems down the reactor, essentially independent operating state of the reactor. To confirm this, reactor trip effectiveness studies for the full initial power levels and reactor states ha

performed for each shutdown system acting alone [CANDU 600 Safety Report 1984].

Compared to the Chernobyl design, CANDU has a *smaller* void coefficient under abnormal conditions, and the capabilities of the shutdown systems are more successfully matched to the reactivity coefficients (see below).

Shutdown Systems and Reactor Control

Background

The accident was characterized by a power excursion and an ineffective shutdown; the former, as noted above, may also have been initiated or worsened by the shutdown system design.

Chernobyl Design

Overall philosophy. Reactivity protection (shutdown) and control in the RBMK reactor is complex and requires manual involvement (see Figures 7 and 8). The control function of the RBMK-1000 reactor is divided into:

1 bulk reactivity control for power manoeuvering and for maintaining criticality in the presence of perturbations caused by absorber rod movement or by feedback reactivity,
2 control of flux and power distribution in the radial plane to limit channel power,
3 emergency reduction of total reactor power to safe power levels when necessary,
4 emergency reduction of local reactor power to safe power levels when necessary, and
5 emergency shutdown of the reactor with the insertion of all absorber rods at their maximum speed.

Demands on the absorber rods are made according to certain rules. The automatic control system attempts to meet these demands. If the operator finds that the automatic control system is insufficient, he inserts or removes 'supplementary' absorbers manually. The number of supplementary absorbers present at any time depends on a combination of factors. Some of these are: 1) the extent of power shaping required, 2) the neutron poison override capability that was required, and 3) the operating value of the coolant void reactivity.

As the demand on the automatic control system increases, supplementary absorbers are driven in or out by the operator to keep the automatically controlled absorbers in their range of travel. However, 24 absorbers are normally kept outside of the core to provide reactivity depth on reactor shutdown.

Required absorber rod positions. A significant feature of this mode of operation is that the maximum negative reactivity rate achieved in an emergency shutdown depends on the *number* of supplementary absorbers present in the core, and in *which locations* they are inserted. For this reason, the equivalent of at least 30

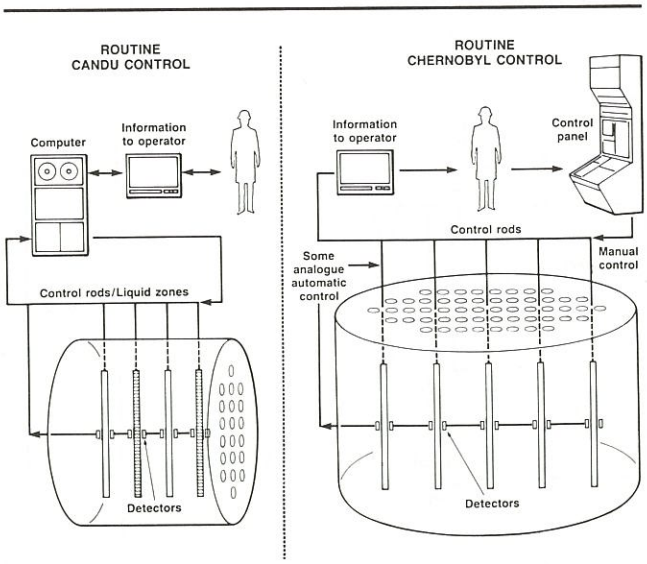

Figure 7 Controlling the power.

absorber rods are always required to be inserted at least 1.2 m into the core and spread reasonably uniformly over the reactor diameter. This rule was violated prior to the accident.

A significant feature of the rod design is the ingress of water into the bottom of the core that occurs when the absorber and its graphite displacer are pulled out of the reactor.

Bulk control. Automatic control of total reactivity (or total power) is provided over a range of about 0.5% to 100% full power. The control system appears to be entirely analog rather than digital.

Spatial control. The majority of the spatial control rods (139) were *manually* operated. The operator would use recommendations from the plant monitoring computer as well as direct indication of flux distribution from 130 radially distributed and 84 axially distributed (7 at each of 12 locations) in-core flux detectors (see Table 1). The Chernobyl design also had a limited number of spatial control rods (12) which were automatically controlled (see Table 2).

The automatic spatial control rods were designed to stabilize the most important radial and azimuthal flux modes. The 12 control rods are moved in such a way that the signals from 2 fission chambers near each control rod remain at a specified value. This system can operate between 10% and 100% of full power and also controls the total reactor power when it is active.

Emergency shutdown. The emergency protection (shutdown) is designed for both bulk and spatial power excursions. Protection is based on three types of signals:

1 Ion chambers outside of the reflector are used for high flux and high rate trips. One description states that rate is monitored only below 10% full power. Some degree of

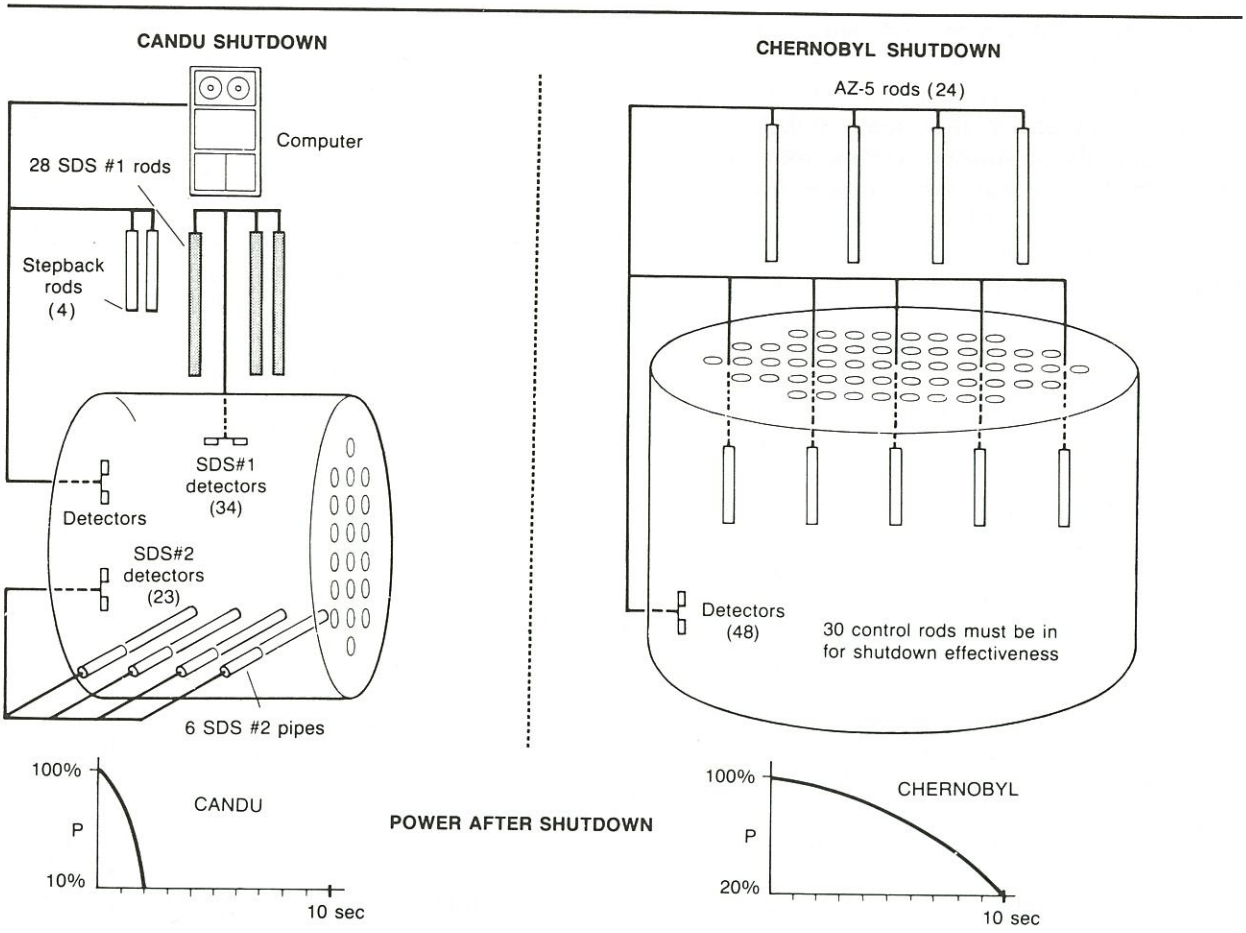

Figure 8 Shutting down the reactor.

spatial protection is afforded by tripping if setpoints are exceeded at 2 ion chambers on the same side of the reactor. A total of 8 ion chambers is used by the protection system.

2 Two fission chambers are located near each of the automatic spatial control rods. Both chambers near one rod must exceed their setpoint to initiate protective action. There is no reference to a rate trip on these measurements, nor any indication of the power range over which the instruments are effective.

3 One hundred and thirty radially distributed in-core flux detectors (using a silver emitter) are compared to appropriate pre-calculated setpoints, and a partial forced power reduction is initiated by the protection system if the setpoint is exceeded. This system is stated to be effective only above 10% full power. The detectors have a slow response (25-second time constant), so this system would be of no use during a fast excursion in power.

In summary, the ion chambers give only poor spatial protection, but their response is prompt. The fission chambers give better coverage, but there are only a few detectors to cover a large core. Fission chambers are usually also prompt in their response. The in-core detectors give very good coverage, but have a slow response.

Comments on the Chernobyl Design

The RBMK protection (shutdown) system is fur tally different from the CANDU shutdown syst Figure 8). In the RBMK design the action necessarily a full shutdown; under some co only a partial power reduction is initiated (si the CANDU power control action called stepba

The emergency rods are complex devices w be inserted at various rates, the fastest of whic slow (about 10 seconds) compared with CANDU rods (less than 2 seconds). This speed limitatic to the hydraulic drag as the rods are driven or c into their water-filled guide tubes. Trips do no to be locked in; when a flux reading is no long rod insertion is interrupted. Rods do not appe rigidly assigned to the control or protection s some appear to serve a dual role.

Physics assessments at AECL show that the C yl reactor is potentially subject to very local, ve flux perturbations [Gulshani, Dastur, and 1987]. Less than 10% of the core can sustain cr From what we know of the protection system those which are widely distributed are very respond and would not adequately protect aga reasonably fast power increase, while thos

Table 1: Summary of Flux Measurement Devices at Chernobyl

3	Start-up counters
3	Low-power ion chambers
12	Ion chambers for control of total power (used 4 at a time)
8	Ion chambers used for protection
130	Radially distributed silver flux detectors for – computer monitoring – alarm on relative deviation (above 5% full power) – alarm and protection action on absolute limit (above 10% full power)
84	Axially distributed silver flux detectors for – computer monitoring – alarm on relative deviation
24	Fission chambers for – automatic spatial control – local protection

(1) The silver flux detectors have a full-power current of 15 microamps; except for electronic equipment limitations, they should be good down to a few percent of full power. Their response is about a 25-second time constant for 90% of the signal and as 2.4-minute time constant for 10% of the signal. The burnout rate is about 20% per year, and the expected life about 3 years.

Table 2: Summary of Control / Shutdown Rods at Chernobyl

12	Rods for automatic control of total power (used 4 at a time)
12	Rods for automatic spatial control
24	'Short' rods for manual axial control
139	Regular rods for radial / azimuthal manual control
24	Emergency protection

respond quickly are small in number and would not adequately detect a very local power increase.

Finally, and most significantly, the protective system action is very slow, so that a power excursion is likely to experience a significant overshoot before it is turned around. In addition, as noted earlier, given certain analysis assumptions on fuel burnup distribution and shutdown system design, it is possible that the shutdown system itself may have exacerbated the accident by inserting positive reactivity during the first few seconds of its initiation [Chan *et al.* 1987; U.S. DOE 1986].

CANDU Design

CANDU stations control reactor power automatically over the entire range from 6 or 7 decades below full power up to full power. Spatial control is done only above about 15% full power, because the reactor is spatially stable up to about 25% full power. At low powers, up to about 10% full power, control is based on ion chambers, while at high powers flux detectors are used. Both types of measurement are totally prompt for all practical purposes.

Reactivity control at all power levels, both for bulk and for spatial purposes, is based on the 14 zone controllers (see Figure 7). If their worth is inadequate, mechanical control rods are available for both positive and negative reactivity addition, again under totally automatic control. Manual reactivity adjustments are limited to poison addition to, and removal from the D_2O moderator, both of which are very slow and relatively rarely required.

Protection against reactivity insertion accidents is provided partly by the control system itself, via stepbacks on high lograte and high flux, but mostly by powerful, rapid shutdown. In CANDU 600, shutdown system No. 1 consists of 28 gravity-operated, spring-assisted absorber (shutoff) rods, and shutdown system No. 2 consists of 6 liquid injection pipes containing over 200 nozzles (see Figure 8). Each system is, independently, fully capable of shutting down the reactor for all accidents. Each system has its own detectors, amplifiers, relays, logic, and actuating mechanisms, and is independent of the control system and of the other shutdown system. Because the shutoff units act in the liquid moderator, they can be inserted very quickly. For example, the shutoff rod guide tubes are full of holes to allow the water to escape as the rods are inserted, reducing hydraulic drag.

In particular, each system has high rate and high flux trips. These trips have been studied quite extensively in terms of their trip coverage (i.e., the range of initial power level and reactivity rate for which trips are effective), and are found to be fully comprehensive [CANDU 600 Safety Report 1984]. Any fast power increase would be terminated by the rate trips, while slow increases continue until the high power trip is exceeded, without core damage.

The emphasis on shutdown performance, and independence from reactor control, are hallmarks of Canadian safety philosophy going back to early days of power reactor development in Canada. The design has evolved since then. The Pickering A units (the first full-size CANDU reactors), put into operation in the early 1970s (near Toronto, Ontario), have 2 different shutdown mechanisms (shutoff rods and quick draining of the heavy water moderator). The shutdown is fully independent of the control, and, unlike the Chernobyl units, capable under any accident conditions of shutting the reactor down. The two shutdown mechanisms were made more powerful in later CANDU designs (Pickering B, Bruce A and B, CANDU 600, and Darlington A), and the logic was fully separated. Offsetting this, the measured reliability of shutdown in Pickering A is much better than called for in the original design requirements, and shutdown is effective in preventing serious consequences even if a few of the rods do not work. Even the NPD reactor, a 25 MW(e) demonstration of the CANDU pressure tube concept, which went into operation in 1962, has a single shutdown system that is fully independent of

Table 3: Summary of Flux Measurement Devices in CANDU 600

3	Start-up counters (installed temporarily only for initial startup and after very long shutdowns)
3	Ion chambers for control at low power
3	Ion chambers for SDS-1 emergency shutdown
3	Ion chambers for SDS-2 emergency shutdown
28	Platinum in-core flux detectors for control at high power (total power plus flux tilts)
102	Vanadium in-core flux detectors for – calculation of reactor flux shape by the computer every 2 minutes – automatic power reduction on high local flux
40	Platinum in-core flux detectors for SDS-1 emergency shutdown
23	Platinum in-core flux detectors for SDS-2 emergency shutdown

the reactor control system, and with an availability target of greater than 9,999 out of 10,000. There have been no shutdown system failures on test in NPD in 27 years of operation, and the predicted future availability approaches the combined target for plants with two independent shutdown systems.

The required response speed and reactivity depth of the shutdown systems is set by the large loss-of-coolant accident. As a result, the systems are more than capable of handling any conceivable reactivity insertion due to loss of reactivity control, from any initial power level.

Comments on CANDU Design

The CANDU design is especially sound in the area of spatial control (at all ranges of power level) and protection. The CANDU ion chambers and flux detectors give full trip coverage in both shutdown systems; the measurements are very fast; the shutdown action is very fast (less than 2 seconds) and inserts a large negative reactivity; the shutdown systems are totally independent of the control system.

Containment

Background

As an immediate consequence of the accident, the roof of the reactor building (primarily that portion away from the turbine building) was blown away during the explosion, and much of the structure of the reactor building was damaged. The lower pressure suppression chambers housing the pumps and inlet manifolding remained intact. (The pump motors, which are outside containment, were intact and exposed to view by the destruction.)

Photographs of the installation show substantial destruction. The upper shield (1,000 tonnes) can be seen on edge at the top of the reactor in the fuelling machine hall, with shreds of channels attached to it.

Table 4: Summary of Control / Shutdown Rods in CAN

14	'Liquid Rods' (water-filled chambers) for control of and flux tilts
21	Adjuster Rods for control (normally fully inserted, driven out, in banks, for extra positive reactivity)
4	Mechanical Control Absorbers for control (normall serted, but can be driven or dropped in for extra n reactivity)
28	Shutoff Rods for SDS-1 emergency shutdown
6	Liquid Poison Injection Pipes into moderator for si gency shutdown

All of the steam outlet (riser) lines were brok lifting of the lid. Most of the larger debris building fell quite close to the reactor build clear that the Chernobyl containment was byp the accident.

Chernobyl Design

The Chernobyl unit 4 RBMK 1000 reactor w with (Figure 9) a containment consisting o closures covering parts of the reactor and system, designed to withstand approximate 400 kPa(g); 2) a pressure suppression syste functions by forcing discharged steam throu pools; 3) a sprinkler cooling system; 4) h removal systems intended to cope with limite gen production; 5) ventilation and filtering and 6) a very tall stack.

The upper end of the reactor and fuelling m not within a pressure-retaining containmer sure. There is a conventional building cove fuelling machine area. This building and its ve system play a role in collecting small discharg area.

Core Container. Information provided indicate core of the reactor, including the channels graphite, is contained in a low-design-pressu 200 kPa) tank filled with inert gas. This tank with relief valves which lead down into the pond. A helium/nitrogen mixture is circulated this tank during normal operation.

Reactor building. The fuelling machine and th the reactor were enclosed in a building of conv structure, which was blown away during the c the accident.

Containment. The Soviets indicated [USSR 198 1986] that the Chernobyl containment includ features as:

1 double water pools (bubbler ponds) which c steam from main steam safety valves, as well accidents;
2 a complex valving arrangement between comp that swaps the 'wet well / dry well,' depending c location, and whose design is aimed at minimi tainment volume and design pressure;

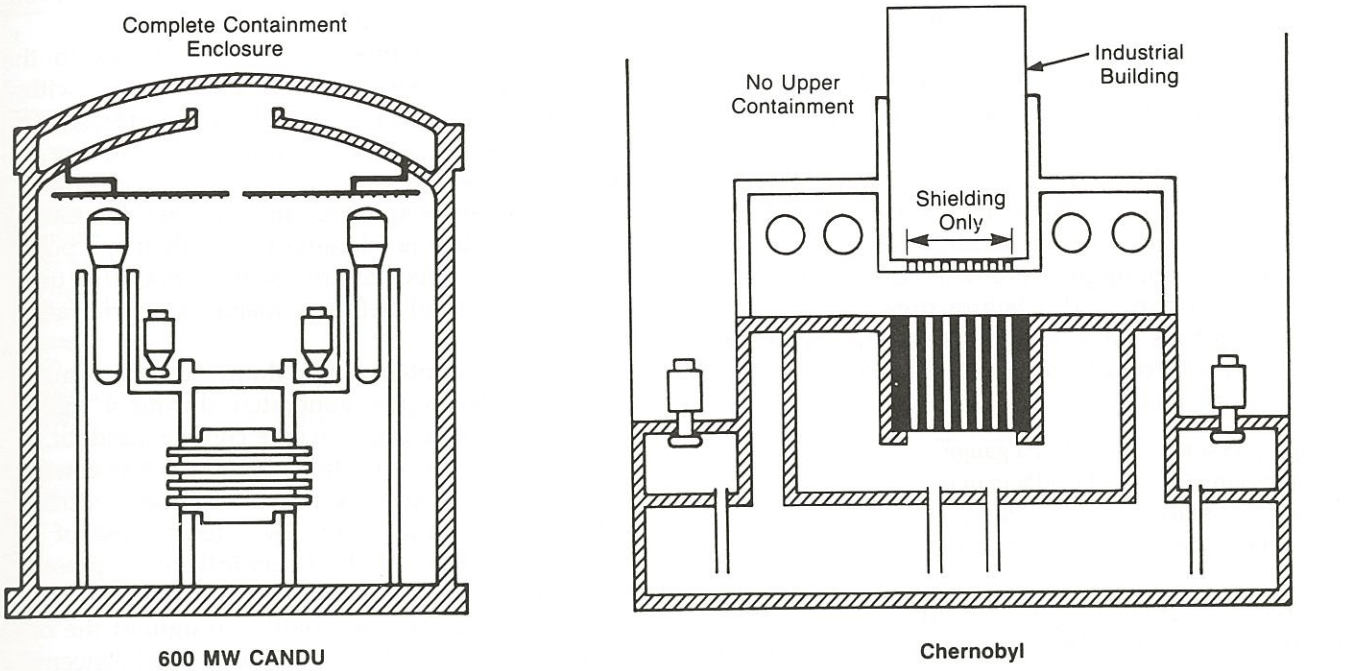

Figure 9 Containment structures.

3 a sprinkler cooling system for cooling of air during normal operation and after accidents; and
4 a system to remove hydrogen from the enclosure. Sources of hydrogen are controlled by catalytic combustion. The system has a capacity of 800 m^3/h and is designed for a postulated release of hydrogen from the oxidation of 30% of the fuel sheaths.

Comments on the Chernobyl Design

There are a number of pathways by which activity released from fuel in the reactor core could directly affect the reactor operators or public:

1 Failures in the steam separators or reactor outlet piping can allow fission products to escape via the removable shielding blocks which form the floor of the reactor hall. It is possible to assume that the Soviet rationale is that large piping (and the steam separators) is unlikely to fail, and would likely leak before break in any case. Breaks in the reactor outlet piping would be limited to one channel, and the affected channel and other channels could reasonably be expected to be cooled by the emergency core cooling system. If so, significant numbers of fuel failures would be unlikely.
2 Since the reactor is of a direct-cycle design, failures in steam lines or main steam safety valves can allow fission products to escape. There are no obvious ways to isolate the reactor from these pathways (e.g., main steam isolation valves). Failing open of the main steam safety valves is covered, as they relieve to the pressure suppression pool, which could handle the discharge for some period of time.
3 Failures of the cooling of irradiated fuel in the fuelling machine would not be contained, but the consequences would be limited to one or two channels' worth of fuel.

CANDU Design

There are 3 different containment designs used for CANDU plants:

1 The single-unit containment envelope (see Figure 9) encompasses the reactor core, all major components of the primary and secondary coolant systems, the moderator system, and the refuelling mechanisms. Some lines (such as ventilation) may be open to the outside atmosphere during normal operation. These lines are closed should an accident condition be detected.
2 The multi-unit reactor stations all have negative-pressure containment systems, with a vacuum building which takes the enclosure below atmospheric pressure after an accident.

   The Pickering *reactor* containment is similar to CANDU 600. Bruce and Darlington designs have a smaller reactor containment which encloses most of the reactor auxiliary equipment. The primary coolant pumps and primary piping systems are inside the containment enclosure, but the pump motors are outside containment and the drive shaft seals form the containment boundary.
3 The containment system for the NPD reactor is a pressure suppression / *relief* system rather than a pressure suppression / *containment* design. Its dousing system suppresses pressure and washes out fission products as in all CANDUS. However, for large piping failures which exceed the capacity of the pressure suppression, steam overpressure

is initially relieved to atmosphere. Following relief of the initial discharge of steam, the building isolates to trap any fission products which may be generated as a result of an accident. Release of these from the fuel is delayed relative to the steam release because of its low power rating.

The CANDU 600 containment has significant capability beyond its design basis. It has a defined design pressure, a test pressure about 15% above design pressure, a cracking pressure when the first through-wall cracks occur, and a failure pressure when the reinforcing bars yield. In the case of the CANDU 600 reactors (e.g., Point Lepreau), these values are [MacGregor *et al.* 1980]:

design pressure	:	124 kPa gauge
test pressure	:	143 kPa gauge
cracking pressure	:	~330 kPa gauge
failure pressure	:	~530 kPa gauge

The containment is designed for rupture of the largest main cooling pipe. The maximum pressure inside containment for this accident is predicted to be less than 70 kPa(g), well below the design pressure.

A hypothetical power runaway in a CANDU 600 (as occurred at Chernobyl) could only happen if there were:

- failure of a normal control system,
- *plus* failure or incapability of stepback,
- *plus* failure of shutdown system No. 1,
- *plus* failure of shutdown system No. 2.

Such an accident has an estimated frequency of less than 1 in 10 million years per reactor in CANDU 600 – much less frequently than in the Chernobyl reactor because of CANDU's stepback and its redundant and independent shutdown systems [Snell 1986]. Accidents of such low frequency are not specifically designed for anywhere in the world; for example, in a light water reactor (LWR), used in many countries in the world, the core melt frequency is between one in 100,000 and one in 1,000,000 years, and no specific design provision is made or required, as the frequency and consequences together are judged an acceptable social risk [U.S. NRC 1975; U.S. NRC 1987]. Nevertheless, although a hypothetical severe power excursion could damage the CANDU 600 reactor core, the energy would be released into a large containment volume (for the CANDU 600 the volume is about 50,000 m^3 compared to about 100 m^3 for the core container at Chernobyl) and pressures in the CANDU 600 containment would be much lower. Analysis of such events is quite speculative and depends on the containment design, but even if the CANDU 600 containment cracking pressure were exceeded, the resulting pressure relief would make it unlikely to attain the failure pressure [MacGregor *et al.* 1980]. The CANDU 600 containment thus is likely to retain much of its effectiveness, even for suc and improbable accident.

The CANDU 600 moderator tank relieve containment enclosure through 4 relief pip total relief area of 0.66 m^2. The relief pipes are rupture discs with a 138 kPa gauge break pre CANDUs employ the same concept and have similar relief areas and pressures. In fact, tl moderator system is tolerant of more than o lated pressure tube failure. Several press would have to fail before a major calandı could occur.

In CANDU 600 containments, the maximum quantity of hydrogen generated during coolant / loss of emergency core cooling acc lead to average concentrations of about 3% i ment [CANDU 600 Safety Report 1984]. The p of hydrogen is limited by the effectivene moderator heat sink, so that very little of the tube zirconium reacts. Buoyancy flow and co mix the hydrogen quite rapidly throughout tainment volume and quickly reduce local c tions in compartments below flammability lin if flammable concentrations were generated, pressure from a burn would not result in con cracking.

The multi-unit stations have a more comple geometry and a lower design pressure. Mos stations are now equipped with hydrogen igr the remaining ones will be similarly outfitte The objective of the igniters is to burn any flammable mixtures before their concentratio to the level at which a burn might rep significant challenge to the multi-unit con integrity. Table 5 provides a comparison of tl and Chernobyl containments.

Comment on CANDU Containment

The enclosure provided by CANDU containr tems is much more complete than that of the C system in that all of the major primary cooli and the reactor core are within the cont Refuelling is also accomplished inside the ment. The Pickering and CANDU 600 reac include much of the secondary cooling sys auxiliary systems inside the containment e although this is for layout convenience rat safety necessity.

The containment enclosures of Bruce and ton are surrounded by buildings of con structure housing auxiliary systems. The vessel extension boundary coincides with the ment boundary in the housing for the mechanisms. A rotating seal on the pump sha containment at the coolant pumps. Thus, CANDU reactors are fitted with an enclosure co surrounding the systems containing fuel.

Table 5: Containment Comparison Summary

Containment item	Multi-unit CANDUs				Single-unit CANDUs	
	Pickering A and B	Bruce A	Bruce B	Darlington A	Gentilly-2	Lepreau
Containment volume (m^3) (2)	594,700	212,900	212,900	305,100	48,500	48,500
Reactor building design pressure: cracking pressure: (kPa gauge)	41	69	82.7	96.5	124 331	124 331
Wall condensation area (m^2)	61,300	57,500	57,500	61,100	22,300	22,300
Dousing water volume (m^3)	9,200	9,900	9,900	10,000	2,500	2,500
Sensible cooler capacity (MW) (3)	21.3	11.8	11.8	9.2	2.9	2.9

Chernobyl data on next page.

Notes: 1 Some data are approximate.
2 Includes vacuum building volume × 1.9.
3 Only coolers on Class III electric power are credited.

Containment item	Chernobyl					
	Main cooling pump compartment	Lower space water piping volume	Steam separator + outlet piping space	Relief tunnel + suppression pool space	Reactor hall	Total
Containment volume (m^3)	14,000	8,700	13,900	25,400	67,000	129,000
Design pressure (kPa gauge)	350	180	0	350	~7	
Wall condensation area (m^2)						200,000
Supression pool water (m^3)				5,000 × 2		10,000

Reactor vault (Chernobyl) or calandria (CANDU) data	CANDU				Chernobyl*
	Pickering	Bruce	Darlington	600 MW	
Relief pressure (kPa gauge)	138	138	138	138	185
Yield pressure	Estimated 1.01.2 MPa				Estimated 0.7 MPa

*Chernobyl design pressure 200 kPa.

Heavy Objects Above the Core

Background

One mechanism of severe core-wide damage that could potentially affect a number of systems is mechanical damage due to falling objects. The Soviets have stated that the refuelling machine at Chernobyl fell over due to the explosion.

Chernobyl Design

The fuelling machine is located above the reactor core in the fuelling hall and is moved over the face of the core and to the spent fuel storage pool in the same building by a gantry. The walls of the fuelling hall are 1.2-m-thick concrete for a height of 17 m, to support the weight of the fuelling machine and the gantry whose rails are attached at this level. The gantry rails have a span of 23 m, and the weight of the fuelling machine is 200 tonnes. In addition, near the top of the refuelling hall, 28 m above the face of the reactor, there is a 50-tonne capacity service crane.

The fuelling machine duty in RBMK-1000 reactors can be as much as 4 to 5 channels a day, so that, in equilibrium operation, the fuelling machine is suspended over the core for much of the time.

Comments on Chernobyl Design

The boundary between the reactor core and the fuelling machine is for shielding and not containment purposes. Thus an accident in the refuelling hall has the potential to propagate into the core, or vice versa.

CANDU Design

CANDU reactors have a service crane that is entirely

within containment for Pickering and CANDU 600, and outside containment for Bruce and Darlington. The service crane in the steam generator room handles such heavy items as a primary heat transport pump motor (45–65 tonnes) and reactivity mechanism / cobalt adjuster flasks of 25 to 30 tonnes. These are infrequent uses and normally the crane is parked away from the top of the reactivity mechanisms deck.

Comments on CANDU Design

The fuelling machines in CANDU access the side of the reactor and are entirely within the containment structure. Thus, even severe mechanical failure of a fuelling machine would not affect more than a few channels and the release would be inside the containment.

Dropping a heavy object on the reactivity mechanism deck during power operation would combine two infrequent events – moving a heavy object over the core and failure of the crane. Damage of the mechanism deck is possible if a heavy object were dropped onto the core, so administrative controls are in place to limit any such movements across the top of the deck.

Graphite Moderator

Background

The moderator had two roles in the accident. It acted as a heat storage mechanism once the fuel reached temperatures higher than the graphite. However, once the graphite started burning, in addition to being a heat sink, it provided a continuing source of energy to distribute fission products up to 1,000 metres above the reactor.

Chernobyl Design

The moderator consists of 1,700 tonnes of graphite bricks stacked in the shape of a vertical cylinder 11.8 m in diameter. Each graphite column is composed of 25 cm by 25 cm blocks. The main blocks in the core are 60 cm high; shortened blocks 50 cm high are installed in the top and bottom reflectors for a total graphite height of 8.0 m. The graphite blocks have vertical holes to accommodate fuel channels (about 1,670), control rods (211), and instrumentation (142). The reflector is cooled through 156 channels in the peripheral row of the graphite columns. Twenty vertical holes of 45-mm diameter contain thermocouples to monitor graphite temperature.

The moderator and reflector columns are located in a sealed vessel which serves as a gas barrier and structural restraint for the graphite. The atmosphere is a circulating mixture of 40% helium and 60% nitrogen at a pressure of 1.5 kPa. For startup, it is understood that the composition of this mixture is changed to pure nitrogen, to decrease the cooling, so that the graphite temperature is similar to that at full power operation. This avoids the large reactivity changes resu changes in graphite temperature as power i

In normal operation, heat is removed graphite, partly through gas cooling in channels, but mainly by conduction to the tubes and to the primary coolant, i.e., the gr heat source for the channels. Conduction is in by a series of graphite rings on the pres which are alternately tight on the moderato and tight on the pressure tube. It is likel pressure tubes are inserted and removed wit graphite rings attached, so that even for which fit tight on the bulk graphite, there come clearance – some papers suggest a 0.04- gap. The maximum local graphite temper been stated to be 750°C. It is reported tha pressure tubes can be detected by sam moderator gas.

Comments on Chernobyl Design

The effectiveness of heat removal from the must be very dependent upon local conditi graphite rings on the pressure tubes. On hand, it can be postulated that dimensional c these rings and in the bulk graphite, as th ages, alter the heat transfer conditions – thi point made by a U.K. review of RBMK 11 years 1976]. In addition, the bulk graphite is poo with temperature monitors – 20 thermocoup 1,700 tonnes, or one per 85 tonnes, sug difficult to detect local graphite hotspots. On hand, the Soviets have had lengthy experi the RBMK type and have not declared any related to graphite overheating.

The fact that the graphite is a heat sour channels affects the course of postulated a The graphite has a large amount of stored must be removed during cooldown after coolant accident. On the other hand, fo accidents involving potential pressure tube tion, the graphite can actually act as a heat s channel temperature rises above local graphit ature, because of its large mass. This is prob there was no 'meltdown' at Chernobyl after explosion. In contrast to CANDU, the chann higher temperatures for a severe accident (e. coolant / loss of emergency core cooling), and more of the zirconium is able to react with stea hydrogen. Of course, this is exacerbated if th ite catches fire.

The response to a pressure tube rupture i not well understood. On the one hand, pres rupture has been considered in the design, a strated by design provisions for relief from th vessel, and the Soviets acknowledge ha channel failures and having replaced them [u The restraint provided by the graphite ring

preclude unstable rupture of the tube but not necessarily the growth of a large leaking crack. On the other hand, it is difficult to see how the steam pressure from anything other than a small leak could be relieved – because of the very small clearances between the pressure tube and the surrounding graphite and the fact that escaping liquid from the ruptured tube, on hitting the hot graphite, flashes to steam and increases the pressure in the tank. The U.K. review points out that in the absence of a clear escape path for the steam, it would go between the graphite bricks and cause radial and axial forces on the moderator structure. There appears to be no published Soviet accident analysis on pressure tube rupture.

Combustion of the graphite has been highlighted as a contributor to the severity of the accident. Simple kinetics calculations done by Whiteshell Nuclear Research Establishment (AECL) show that graphite oxidation in air is exothermic, with ignition around 650 to 750°C. In steam, the reaction is endothermic, becoming significant around 1,100 to 1,200°C, but requiring an external heat source to keep going. The latter reaction produces hydrogen and carbon monoxide, which burn exothermically in air. In contrast, tests on Hanford reactor graphite cubes (heated in air in a furnace) and bars (heated by an oxyacetylene torch until white hot), and crucibles heated by thermite, showed no flame and slow sublimation at the highest temperatures. This suggests geometry (heat losses through conduction) could be significant in any extrapolation of small-scale tests to a large essentially adiabatic graphite block; access of air could also be limiting, and this would depend on the extent and nature of the damage to the core.

The graphite has a large positive reactivity coefficient with temperature. This influences reactor control strategies but not fast accidents, due to the large heat capacity of the graphite mass (bulk heatup is slow). For severe accidents, with graphite overheating, it imposes a requirement on the reactivity depth of the shutdown systems – it is not know how this is dealt with.

CANDU Design

The CANDU moderator is heavy water at an average temperature of 60°C, and a low normal operating pressure up to 21 kPa(g). It is cooled by a separate system of pumps and heat exchangers, since normal heat flow is from the channels to the moderator, and from direct gamma and neutron heating. The total amounts to about 100 MW(th) in the CANDU 600, or about 5% full thermal reactor power.

The moderator is separated from each pressure tube by an annulus filled with an insulating gas, and a Zircaloy calandria tube. The annulus gas is monitored for moisture, to detect a pressure tube leak. The localization is not to each individual tube, but to groups of tubes, whereafter other methods are used to locate the specific leaking tube.

The calandria is provided with 4 relief pipes, which discharge into containment and have rupture disks set at a calandria pressure of 138 kPa. They are sized based on a sudden double-ended rupture of a pressure tube and associated calandria tube, with no credit for the strength of the surrounding calandria tube.

Comments on CANDU Design

The amount of heat removed from the moderator in normal operation is the same as fuel decay heat a few tens of seconds after reactor shutdown. Thus, the moderator is capable in emergencies of removing fuel heat following a loss of coolant and loss of the emergency core cooling. In such a circumstance, the pressure tube either sags on to the surrounding calandria tube as it overheats, providing a conduction heat path from fuel to moderator (in addition to radiant heat transfer), or, expands under the influence of residual coolant pressure in the channel. The expansion is arrested by the cool calandria tube, and the tube-to-tube contact provides a conduction path to remove decay heat.

In either case no significant melting of the UO_2 fuel occurs and the channels remain intact. Equally important, the pressure tube temperatures are limited by heat conduction and radiation to the calandria tube, so that the amount of hydrogen that can be produced from fuel sheaths or pressure tubes is limited by the metal temperature. For a loss of coolant / loss of emergency core cooling accident, CANDU 600 analysis indicates that about 35% of the sheaths and less than 1% of the pressure tubes can be oxidized [CANDU 600 Safety Report 1984].

A spontaneous pressure tube failure at normal operating pressures may or may not cause a failure of the surrounding calandria tube. If the calandria tube does fail, the steam discharge will be largely condensed by the moderator liquid, i.e., the moderator reduces the potential overpressure in the calandria instead of increasing it. In addition, for a severe pressure tube failure, some calandria tubes can absorb some of the energy in the pressure wave by collapsing onto their internal pressure tubes. Thus a pressure tube failure is not predicted to cause further pressure boundary or calandria failures.

Source Term Considerations

Background

The accident at Chernobyl pointed out a significant effect of the lack of a complete containment. During the accident, oxidizing conditions occurred, such that fission products that are volatile at 1,700°C (iodine, caesium, tellurium) were released as elemental gases. In the case of a severe accident in CANDU it is expected

Table 6: Three Mile Island and Chernobyl Releases Compared

	TMI-2		*Chernobyl*
	Outside the core	*To environment*	*To environment*
Noble Gases (Xe, Kr)	48%	1%	100%
I	25%	3×10^{-5}%	20%
Cs	53%	not detected	10–13%
Ru	0.5%	not detected	2.9%
Ce(group)	nil	not detected	2.3–2.8%

that reducing conditions would occur and that these fission products would be released to containment as chemical compound aerosols.

Chernobyl Phenomenology

In general, the composition of the aerosols released during the accident was reported to be characteristic of the irradiated fuel composition, except for enhanced release of elemental iodine, caesium, and tellurium.

The initial reactivity excursion is reported to have shattered the fuel in the bottom 30% of the reactor. The hot fuel and cladding particles interacted violently with the coolant. The explosion probably released fuel particles and fission products into the air. Once the reactor vessel was breached, oxygen entered the core and some of the remaining fuel may have oxidized. Oxidization could have destroyed the fuel matrix and could have led to the production of small fuel particles containing fission products. The fission products that are volatile at 1,700°C (I, Cs, Te) would be released as gases, while other less volatile species would be released as aerosols.

A further effect of oxygen is on fission product behaviour. The hot, oxidizing conditions in the core region would either destroy CsI or would prevent its formation, and a substantial fraction of the released iodine would likely be volatile I_2 gas. As the I_2 cooled, it would attach to aerosols (for example, from combustion of the graphite) and would be transported along with other core material.

Another phenomenon that could have had some effect on the releases at Chernobyl is the potential interaction of graphite with fuel. The explosion could have mixed graphite and hot fuel particles. At high temperatures (i.e., 1,500°C), graphite and fuel can react to form a uranium oxy-carbide. This could have contributed to the destruction of the fuel matrix and further enhanced the release of fission products.

CANDU Phenomenology

The releases during the accident at Chernobyl are in marked contrast with the release of iodine and caesium in a heavy water reactor (or light water reactor), where the hot reducing conditions in the core would result in CsI formation. The CsI would encounter oxidizing conditions only in the containment building, where temperatures are too low for extensive oxidat CsI. Thus, large quantities of volatile I_2 wou expected to form in a CANDU containment sy

CsI is easily absorbed into water in the cont thus significantly reducing (10 to 100 ti amount of caesium and iodine released. The the wet atmosphere inside a containment is strated by the differences between the releas environment from Three Mile Island unit 2 (the Chernobyl unit, even though the forme completely isolated from the environment for part of the accident.

Although there was a similar level of re containment for TMI (Table 6) [Collier and Davies 1986], there was a significant attenuati for all forms of fission products released. The and physical processes connected with a 'wet ment, like TMI, would also occur for an acci CANDU reactor. Even if the containment build leaking, major attenuation of the biologicall cant radioactive releases would occur.

Other Concerns Raised

Pressure Tubes

Background

In this section the pressure tube design Chernobyl unit and of CANDU are discussed.

Chernobyl Design

In the Chernobyl unit the channels are locatec ly in the graphite moderator and either con enriched uranium oxide fuel or are used as for control rods and instrumentation.

The pressure tube has an 88-mm outside with a wall thickness of 4 mm. A series of rings are stacked and fitted alternately arc pressure tube to improve heat transfer graphite blocks to the outer surface of the tube.

A mixture of helium and nitrogen, fed bottom end of the reactor, flows between the columns. It provides a heat conducting me transmitting the graphite heat to the fuel cha is also monitored for moisture to detect leak the tubes.

The top end of the fuel channel is welded to the top housing sleeve and, at the other end, a stuffing box assembly seals between the extension pipe and the bottom housing sleeve. Small changes in the length of the pressure tube are accommodated by movement through the stuffing box seal.

The outlet top end of the channel is sealed by a nozzle plug which can be removed by rotation during the refuelling operation. The inlet end of the channel is connected directly to the coolant pipe by means of a welded connection.

The service life of the fuel channel is estimated to be 25 to 30 years (reactor design life is 30 years) and the channel is said to be replaceable during shutdown with remote tooling.

Comments on Chernobyl Design

There are several key features of the Chernobyl reactor pressure tube design:

1 Heat is removed from the graphite to the channel. The graphite is always hotter than the coolant in the channel (graphite is about 700°C, and transfers heat to the channel coolant at a temperature of about 280°C).
2 The diffusion joint appears to limit maximum allowable heating and cooling rates to from 10°C to 15°C / hour. This is likely required to ensure a long design lifetime.
The joint is quite strong; however, it is uncertain whether the diffusion joint or the transition section is as strong as the remainder of the pressure tube.
3 As noted in the previous section, the response of the surrounding structure to a pressure tube rupture is important, yet not well understood.

CANDU Design

CANDU is a pressure tube, heavy-water-moderated, heavy-water-cooled reactor. The fuel channels consist of *two* concentric tubes, the pressure tube and calandria tube, with a space in between. These channels are located horizontally in the heavy water moderator, and contain natural uranium fuel. The channels and heavy water moderator are all contained in a large tank called a calandria vessel.

Fuel bundles are typically made of 37 elements of short length (about half a metre), and there are typically 12 bundles in each fuel channel. The fuelling machines refuel by coupling onto a fuel channel at both sides of the core (thus the machines are never over the core). CANDU design has typically about 380 to 480 fuel channels. Each fuel channel is made of a zirconium-niobium pressure tube (similar in composition to that at Chernobyl), and is connected by 'rolled joints' (i.e., no welding), to stainless steel end fittings which serve as a connection to the fuelling machine and to the external feeder piping through a side part.

In CANDU reactors, the annular space between the pressure tube and calandria tube is filled with an inert gas, which is monitored to detect any moisture in the space. The dewpoint of the gas provides a preliminary indication of a pressure tube leak. Monitors in segments of the reactor annulus system aid in locating a leaking channel.

Comments on CANDU Design

1 For many conditions, pipes, including pressure tubes, leak before they break. The CANDU design has *two* separate tubes, the pressure tube and the calandria tube. The calandria tubes can withstand a very high (basically, full-system) pressure. Thus, should the pressure tube leak, the leak can be detected by the gas in the space between the tubes, the reactor can be shut down, and the pressure tube replaced. The moderator vessel is nevertheless designed to withstand a sudden channel rupture (both pressure and calandria tube).
2 Surrounding each of the channel assemblies is the cool (about 70-80°C) water moderator. If the pressure tube heats up to temperatures in the range of 650°C to 800°C, it expands or sags to contact the surrounding calandria tube, and heat is transferred to the cool water. Subdividing the core into many pressure tubes allows this possibility. This cool surrounding water provides an inherent safety defence to prevent significant fuel melting. It also means that fuel and pressure tube temperatures are kept low, so that there is little formation of hydrogen for a large range of severe accidents [CANDU 600 Safety Report 1984].
3 Severe fuel heatup or fuel melting due to channel blockage or flow reduction in a channel is an unlikely event, since it could only occur in a highly unusual combination of circumstances. Flow blockage severe enough to damage the channel requires a blockage area greater than 90% of the channel flow area [CANDU 600 Safety Report 1984] and has never occurred in a CANDU reactor. Such a blockage could fail both pressure tube and calandria tube, and result in discharge of coolant to the moderator. The calandria and other channels are designed to remain intact following such a failure.
4 There have been 2 pressure tube ruptures due to defects; one at Pickering A and one at Bruce A. In both cases the damage was limited to one channel, which was replaced.
5 The rolled joints used in CANDU reactors have generally performed well. There were leaking pressure tube problems in the rolled joint area in Pickering A and Bruce A, associated with delayed hydride cracking of some tubes in highly stressed areas, resulting from improper rolling of the joint. Subsequent CANDU reactors have used an improved pressure tube installation procedure.

Finally, the first two units at Pickering A have been entirely retubed due to premature sagging of the Zircaloy-2 pressure tubes used in those units. The tubes were replaced with tubes of the zirconium-niobium material which is used in all other CANDU reactors. While retubing was not expected to be needed so soon, the contribution to the station lifetime

unavailability will be less than 10% and the fact that the core pressure boundary can be replaced is a unique feature of pressure-tube reactors.

Computer Control

Background
Direct computer control was not used at Chernobyl – the Soviets reportedly felt it was not sufficiently reliable based on their early exerience.

Chernobyl Design
The actual *control* of Chernobyl appears to be mostly analog; from 0 to 0.5% full power, the control is manual, with special low-power ion chambers; from 0.5% to 6% full power, the control is non-redundant automatic control of 4 rods, based on 4 ion chambers; above 6% full power, control is dual redundant automatic control, with each redundant portion having 4 rods and 4 ion chambers.

Spatial control is mostly manual, using 139 absorber rods, but there is a rudimentary automatic spatial control system using 12 absorber rods. For the latter, 2 fission chambers near each rod are used as feedback sensors.

There is an extensive *monitoring* programme (PRIZMA) in an on-line station computer (SKALA). This program monitors in-core flux measurements, individual channel flows, control rod positions, and many other variables, then calculates reactor power distribution, margins to dryout, etc., and issues instructions to the operator to guide him in manual spatial control and flow control. There is apparently *no* direct digital control of the devices. It also appears that there is only 1 such station computer. The PRIZMA program runs every 5 to 10 minutes, so is relevant for very slow power changes only.

Comments on Chernobyl Design
At Chernobyl, most of the basic spatial flux control is manual (i.e., 139 absorber rods). While it is possible to use this kind of control, it assumes a high reliance on the operator.

CANDU Design
CANDU stations make extensive use of direct digital control; this encompasses all reactor controls and all major process loops [for a detailed description see Ichiyen 1982]. The configuration consists of 2 identical computers running continuously in active / hot-standby mode. Internal self-checks and external checks transfer control if failure of the active computer is detected. If both computers fail, all control circuits are isolated and go to their designed state, which is either failsafe or neutral. For example, the reactivity control absorbers would be inserted and cause a rapid reactor power decrease if both computers failed. Flux mapping for purposes of refuelling is done at Chernobyl.

Comments on CANDU Design
The dual computer concept has served w
have been only a few instances of compu
[Ichiyen 1982; Ichiyen and Yanofsky 19
computer failure, although it has occurred
very rare and has always been ended
shutdown by the (independent) shutdown

From a safety point of view, the key i
shutdown systems are completely indepen
control computers, in terms of sensing d
shutdown mechanisms, and have the ca
overcome any computer-induced positive
insertion. Thus, even a massive adverse
failure (e.g., driving all reactivity devices in
direction) can be easily terminated.

Multi-Unit Containment

Background
Both the Chernobyl reactors and the m
current CANDU reactors are multi-unit plar
same site. The accident at the former forc
down of all other operating units at the site

Chernobyl Design
There are 4 operating units at Chernobyl, pl
under construction. There is no sharing o
ment facilities, but the operating units share
turbine hall and some electrical services.

Comments on Chernobyl Design
The *physical* damage was apparently restrict
4. However, an accident which spreads cont
as widely as Chernobyl did will restrict acce
units on the same site. An effective containn
in preventing such damage. Because the
direct cycle, there is a possibility of contami
common turbine hall, since there is appa
steam main isolation capability.

CANDU Design
The multi-unit plants in Ontario have a linke
ment structure, wherein the containment ar
reactor is linked by a large duct to a commo
building kept at reduced pressure. In the e
accident, steam and radioactivity are sucke
vacuum building, and the entire structure st
atmospheric pressure (leakage in *in*, not *out*)
hours.

Since the primary coolant does not run th
directly, the extent of contamination on th
side is limited to that from an accident wi
leaking steam generator tube.

Comments on CANDU Design

The vacuum concept has been analyzed for the usual spectrum of accidents, such as a large loss of coolant, but, as part of the Canadian safety philosophy, must also meet public dose limits for *dual* failures, such as a loss of coolant plus a failure of the emergency core cooling water flow, or plus an impairment in the containment envelope [Hurst and Boyd 1972; Domaratzki 1984]. The vacuum concept, because of its forced *in*-leakage, is very powerful in limiting short-term releases for such impairments. In the long term (hours to days), the emergency filtered air discharge system can be used to vent containment and, at the same time, to filter and remove activity from the containment atmosphere. Typically, 99.9% of the core inventory of iodine is contained.

Source terms from accident analysis are used to study the habitability of the control room after an accident; the units could also be safely shut down and monitored (if necessary) from the secondary control area in Pickering-B, Bruce-B, and Darlington.

Given the powerful containment and the severity of failures analyzed to meet the dose limits, it is very unlikely that damage in one unit would prevent effective control of the others by station staff.

There are other safety advantages to the multi-unit design: 1) an ability to use the electrical and water supplies of the *other* units in emergencies, and 2) the presence of a large operational staff familiar with all the units on site. These two factors were doubtless true for Chernobyl as well.

Fire Protection

Background

The dramatic graphite fire at Chernobyl, in combination with fires in the fuelling machine hall and turbine hall, has further raised awareness of fire as a reactor safety issue.

Chernobyl Design

The fire protection system consists of hydrants inside and outside of the turbine building and a system to cool the trusses and roof of the machinery room. An automatic water-spray fire-extinguishing system is provided in the cable and transformer rooms. The pumps and automatic valves of this system are connected in 3 independent subsystems, which are in turn connected to the emergency diesel generators. The water supply for each system consists of 3 tanks with a capacity of 150 m^3. These tanks are filled from the plant general fire-fighting system.

Comments on Chernobyl Design

The fire protection system in the Chernobyl design is of quite a high standard. Nonetheless, it is clear that the accident was well beyond the capability of the fire protection design.

CANDU Design

In CANDU there are no automatic fire suppression systems in the reactor buildings; fires there are expected to be limited in extent because of the absence of large quantities of flammable material, and are fought with portable fire extinguishers. Limiting the *safety* consequence of local fires is achieved by the 2-group philosophy: that is, the plant can be shut down and monitored and decay heat removed by either of 2 independent and spatially separated groups of systems. Fire suppression systems outside of the reactor building are conventional sprinkler systems, CO_2 systems, Halon systems, and fire standpipe systems. Manual firefighting using fire hoses and portable fire extinguishers are relied on for areas of lower fire hazards.

Comments on CANDU Design

Of course, there is no combustible graphite in the vicinity of the core. Combustible sources in the reactor building are mainly the lubricating oil in the pump motors, and the electric cables. Due to the physical separation of the combustible sources and the reactor core, it is improbable that a fire could induce direct core damage. The dousing system in single-unit containments could be used for some fires, e.g., a pump lubricating oil fire, but it does not cover the entire reactor building volume and has a severe economic penalty associated with its operation. Further review of the adequacy of firefighting systems in CANDU plants is underway.

Conclusions

The threat posed by reactivity accidents has long been recognized in nuclear programs worldwide. The 1952 NRX accident at Chalk River [Lewis 1953] spurred the development of fast, powerful, and independent shutdown systems in the Canadian nuclear program.

Nonetheless, it is prudent to review, in depth, the adequacy of our defences. In particular, a review is underway to ensure that there is no conceivable combination of distorted flux shape, reactor power, control system action (automatic or operator), coolant condition, etc., which could result in a reactivity excursion exceeding the capability of the CANDU shutdown systems.

The consequential fires (besides the graphite fire) at Chernobyl were well handled, under extreme circumstances (particularly radiation), by the firefighting crews. CANDUs all have fire protection programs included in the design and operation of the reactors. It is prudent, however, to review the fire protection design adequacy, particularly in the presence of radiation, to determine any possible lessons to be learned.

Acknowledgements

Acknowledgements are made to the following people who have contributed to the preparation and review of this report:

At AECL – A. Dastur, R. Osborne, D. Pendergast, D. Primeau, G. Brooks, D. Torgerson, W. Fieguth, J. Pauksens, K. Hau, S. Yu, E. Price, V. Bajaj, P. Gumley, S. Lee, C. Boss, J. Dick, D. Barber, and J. Van Berlo. Acknowledgements are also made to S. Grove, H. Gartner and D. Simpson for the excellent work done in typing this report.

At Ontario Hydro – W. Cichowlas, R.A. Brown, and G. Frescura.

At the New Brunswick Electric Power Commission – D. Wilson.

At Hydro Quebec – A. Duchesne.

Notes

[1]CANadian Deuterium Uranium.

[2]Expected future dose to be received for a person who remains in the western USSR, but outside of the evacuated area.

References

1. *Babenko EA*, et al. Development and introduction of hydrogen combustion facilities at an NPP (RBMK-1000 and WWER-440 Reactors), Nuclear Power Plants, Moscow, V3, 1980.
2. CANDU 600 Safety Report, Point Lepreau Unit 1 / Gentilly-2 Safety Report. Part 2. Accident analysis. November 1984. (These reports are not held in libraries but can be inspected by any member of the public at the offices of the Atomic Energy Control Board).
3. *Chan PSW*, et al. The Chernobyl accident: multidimensional simulations to identify the role of design and operating features of the RBMK-1000. Paper to be presented at Conference on Probabilistic Safety Assessment and Risk Management, Zurich, Switzerland, August 31 – September 4, 1987.
4. *Collier JG, Myrddin Davies L.* Chernobyl. Central Electricity Generating Board, Gloucester, England, 1986.
5. *Dastur A.* Dynamic flux synthesis with discontinuous trial functions. Proceedings of the 2nd Annual Conference of the Canadian Nuclear Society, Ottawa, June 1981.
6. *Dastur A*, et al. A quick look at the Post-Accident Review Meeting (PARM). Atomic Energy of Canada Limited Publication, AECL-9327, September 1986.
7. *Dollezhal NA, Emel'yanov IY.* The channel type nuclear power reactor. Moscow: Atomizdat, 1980 (in Russian; book translated into English by IAEA, draft 1986).
8. *Domaratzki Z.* CANDU containment systems – a regulatory perspective. Atomic Energy Control Board, paper presented at International Conference on Containment Design, June 17 – 20, 1984.
9. *Dubrovsky V*, et al. Construction of nuclear power plants. Moscow: MIR Publishers, 1979.
10. *Gulshani P, Dastur A, Chexal B.* Stability a spatial power distribution of the RBMK-10(Paper to be presented at 1987 ANS Annua Dallas, Texas, June 7 – 11, 1987.
11. *Howieson JQ.* CANDU moderator heat sink accidents. Paper presented to 2nd Internatio Meeting on Nuclear Power Plant Thermohyd Operation, Tokyo, Japan, April 15 – 17, 198
12. *Howieson JQ, Snell VG.* Chernobyl – a Canad cal perspective. AECL-9334, January 1987.
13. *Hurst DG, Boyd FC.* Reactor licensing and safe ments. AECB-1059, June 11, 1972.
14. *Ichiyen NM.* Computers in CANDU special safe Reprint from Nuclear Power Plant Control a mentation, IAEA-SM-265 / 92, 1982.
15. *Ichiyen NM, Yanofsky N.* Computers' key rol control. Atomic Energy of Canada Limite Engineering International, August 1980.
16. *International Nuclear Safety Advisory Group* (IN mary report on the Post-Accident Review M the Chernobyl accident, August 30 – Septem GC (SPL. 1) 13, IAEA, Vienna, September 24, 1
17. *Kugler G.* Distinctive safety aspects of the C reactor design. AECL-6789, January 1982.
18. *Levin YM, Kreman MC.* Particulars of startup, a on third generating unit of Chernobyl AES. heskoye Stroitel 'stvo. No. 6, June 1983.
19. *Lewis WB.* The accident to the NRX reactor on 12, 1952. Atomic Energy of Canada Limit AECL-232, July 1953.
20. *MacGregor JG*, et al. Concrete containment summary of findings. University of Alberta, A INFO-0031, May 1980.
21. *National Nuclear Corporation (NNC) Limited.* T Graphite Moderated Channel Tube Reacto Nuclear Corporation Limited, Report N March 1976.
22. Nuclear News, May 1987; 30: 55.
23. *Rouben B.* Power transient in a CANDU core f hypothetical large loss of coolant accident. sented at conference on Anticipated and Transients in Nuclear Power Plants, Atlant April 12 – 15, 1987.
24. *Sainsbury JD.* Overview of the research an ment programs in support of CANDU reacto AECL, paper presented at IAEA meeting on Rea Research, January 1984.
25. *Semenov BA.* Nuclear power in the Soviet U Bulletin, 1983; 25.
26. *Snell VG.* Probabilistic safety assessmen Canada. AECL-8761, 1986.
27. *Snell VG.* Safety of CANDU nuclear powe AECL-6329, January 1985.
28. *Snell VG, Howieson JQ.* Chernobyl – a Canad cal perspective: executive summary. Atomic Canada Limited, Report AECL-9334S, Januar
29. *Snell VG, Howieson JQ.* Chernobyl – a Canadi

tive. Atomic Energy of Canada Limited, Report PA-10, December 1986.
30. *Turetskii LI*, et al. A system for localizing failures of generating units with the RBMK-1000 reactor. Teploenergetika 1984; 31: 14-9 (one of four abstracts from Thermal Engineering).
31. *US Department of Energy*. Report of the US Department of Energy's team analyses of the Chernobyl-4 atomic energy station accident sequence. DOE / NE-0076, November 1986.
32. *US Nuclear Regulatory Commission*. An assessment of accident risks in US commercial nuclear power plants. Reactor Safety Study WASH-1400, October 1975.
33. *US Nuclear Regulatory Commission*. Reactor risk reference document, main report (draft for comment). NUREG-1150, February 1987.
34. *USSR State Committee on the Utilization of Atomic Energy*. The accident at the Chernobyl nuclear power plant and its consequences. Presented at the International Atomic Energy Agency Post-Accident Review Meeting, Vienna, August 25–29, 1986.

Seismic Qualification of CANDU-PHW Nuclear Power Plant Equipment

S.A. Usmani
Equipment Seismic Qualification and Process Piping
Atomic Energy of Canada Limited
CANDU Operations
Sheridan Park Research Community
Mississauga, Ontario
L5K 1B2

Abstract

CANDU-PHW (Canada Deuterium-Uranium, Pressurized Heavy-Water reactor) nuclear power plants, whether in Canada or abroad, are thoroughly qualified to resist potential earthquakes because of the great emphasis placed on nuclear safety. CANDU Plants have been seismically qualified dynamically since the mid-1960s, with ever-increasing requirements for each new plant. The approach now employed in Canada for seismic qualification of CANDU equipment and systems is described in this paper. While many of the Canadian technical requirements, criteria, procedures, and methods are similar to those developed by the U.S. NRC (United States Nuclear Regulatory Commission), they are uniquely suited to the CANDU system. In some cases, the Canadian approach differs from that applied in other countries, and in many ways is more conservative. This paper provides typical examples to show that the CANDU equipment and systems are seismically qualified using state-of-the-art techniques and methods.

Résumé

Qu'elles soient situées au Canada ou à l'étranger, les centrales nucléaires CANDU-PHW (Canada Deuterium Uranium, réacteur à eau lourde sous pression) sont qualifiées pour résister aux tremblements de terre en raison de l'importance accordée à la sûreté nucléaire. Les centrales CANDU sont qualifiées sismiquement (méthode dynamique) depuis le milieu des années soixante, et des critères de plus en plus sévères ont été appliqués à chaque nouvelle centrale construite depuis. Cet article décrit l'approche adoptée par le Canada pour doter le matériel et la filière CANDU des caractéristiques parasismiques nécessaires à sa qualification. Bien qu'un grand nombre des exigences, critères, procédés et méthodes techniques utilisés au Canada correspondent à ceux de la United States Nuclear Regulatory Commission, ils ont été établis tout particulièrement pour la filière CANDU. Dans certains cas, l'approche canadienne diffère de celle d'autres pays et est aussi plus prudente à plus d'un égard. L'article offre des exemples typiques démontrant les caractéristiques parasismiques du matériel et de la filière CANDU obtenues grâce à l'incorporation de techniques et de méthodes à la fine pointe de la technologie.

Introduction

Seismic design requirements for commercial structures and industrial plants have been invoked in Canada for many years through the National Building Code of Canada (NBCC). The seismic design of nuclear power plants requires special consideration because of concern for the nuclear safety of the public. The CANDU seismic design philosophy is based on principles established by the Atomic Energy Control Board (AECB) of Canada. The resulting requirements and criteria to ensure the integrity and safety of structures and equipment in the event of an earthquake have been developed by the Canadian Standards Association (CSA), and published as National Standards of Canada by the Standards Council of Canada (CAN3 N289 series). The design requirements, criteria, and methods for seismic qualification of CANDU systems and equipment will be described briefly in the following sections.

Seismic Design Requirements

The CANDU plant is designed to satisfy three general safety requirements [Duff and Usmani 1984]. These requirements must be met in the event of an earthquake to minimize the radiological risk to the public:

1. Means shall be provided to shut down the reactor safely and maintain it in the safe shutdown condition as required in the event of an earthquake.
2. Means shall be provided to remove residual heat from the core after reactor shutdown.
3. Means shall be provided to reduce the potential for release of radioactive materials and to ensure that any releases are within acceptable limits in the event of an earthquake.

Keywords: CANDU-PHW, seismic qualification, seismic categories, design basis earthquake, site design earthquake, National Building Code of Canada, Canadian Standard Association, response spectrum, dynamic analysis, shake testing.

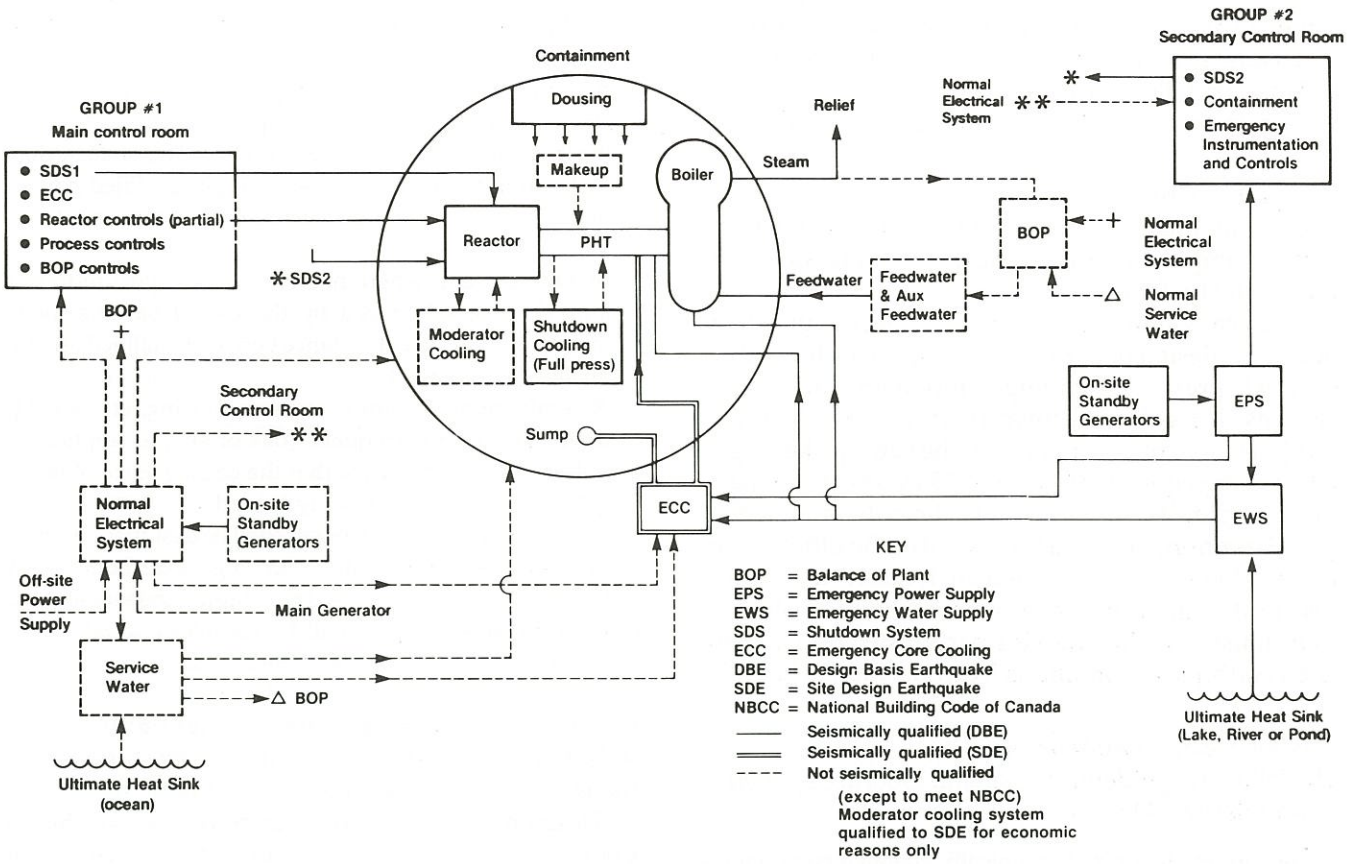

Figure 1: Seismic qualification and system separation for a CANDU 600 NPP on an ocean site.

These general safety requirements are met by seismically qualifying sufficient numbers of equipment and systems to ensure the following:

1. The reactor is capable of being safely shut down and being maintained in that state indefinitely.
2. Decay heat can be removed from the fuel during the shutdown period. As one requirement of this function, the primary coolant system pressure boundary shall not fail.
3. The containment building and associated isolation systems shall remain functional.

The major systems and structures requiring seismic qualification are shown in Figure 1. The plant systems are arranged in two independent, diverse, and widely-separated safety groups as shown.

Seismic Categories

Two categories of system components are defined [Duff and Usmani, 1984] as regards seismic qualification: category 'A' components are those whose pressure boundary or structural integrity must be maintained; category 'B' components are those which, in addition to category 'A' requirements, must also remain functional.

The particular seismic requirements for each system component usually cannot be adequately covered by the general definition of 'A' and 'B' classification. Therefore, the detailed seismic requirements for each component, including whether it is required to operate after an earthquake, or during *and* after an earthquake, are identified, and the components are designed accordingly.

Design Earthquake Levels – Definitions

The Canadian National Standards CSA-N289 require that nuclear power plant (NPP) structures and systems important to safety meet more restrictive design requirements than those imposed by the National Building Code of Canada (NBCC). CSA-N289.1 defines two levels of earthquake safety: 1) 'The Design Basis Earthquake (DBE),' an engineering representation of potentially severe effects at the site of earthquakes, applicable to the site, that have sufficiently low probability of being exceeded during the lifetime of the plant; and 2) 'The Site Design Earthquake (SDE),' defined as an engineering representation of the effects, at the site, of a set of possible earthquakes, with an occurrence rate based on historical records not greater than 0.01 per year (with a minimum level of 0.03 g). The SDE is always a more probable event, and therefore has a lower intensity than the DBE. Only one earthquake, the SDE or the DBE, is assumed to occur during the design life of

the NPP. Other structures and systems shall be designed to meet at least the NBCC, or equivalent, in order to ensure a minimum degree of resistance against collapse or failure, to mitigate the effects of earthquakes on nearby safety-related structures and systems.

Acceptance Criteria

The seismic qualification acceptance criteria for CANDU system components are as follows: strength, deformation, stability, fatigue, function.

Seismically-induced 'fatigue' is a special consideration in the design of CANDU-NPPS, especially for highly-stressed, pressure-retaining components and piping systems. It has been shown [Duff and Heidebrecht, 1979] that, for critical equipment, the earthquake fatigue effect is the equivalent of up to 25 cycles at the maximum amplitude or stress level. The criteria 'function' must be confirmed by testing, as all of the other acceptance criteria can be evaluated analytically. It is for this reason that important components, such as shut-off rods, must have their moving parts tested under simulated earthquake conditions [Kuroda and Duff, 1982].

Seismic Design Guidelines

The following guidelines [Usmani, 1986] are applied in CANDU Seismic Design:

- The random failures of seismically qualified components and structures coincident with an earthquake are incredible, and therefore need not be considered in the plant design.
- The plant design considers the most adverse effect of the non-qualified systems on the qualified systems.
- The instrumentation and control associated with the essential safety function of a system shall be qualified to the same level and category as the system.
- Cables, cable trays, conduit, and their supports for a system required for safe operation shall be qualified. They shall be routed separately from unqualified cable pans to avoid damage from such equipment.
- Fire protection systems shall be designed to avoid damage to seismically qualified systems through falling or spurious operation.
- An analysis, test report or other justification of seismic capability shall be prepared for all seismically qualified equipment and structures, to demonstrate that the safety requirements have been satisfied.
- All systems and structures of the plant shall be designed to comply with the latest codes.
- Site surveys [Duff and Stevenson, 1984] shall be conducted at an advanced stage of construction and system installation. This is to determine, both by inspection and by *ad hoc, in situ* testing, that the as-built, as-installed condition of the nuclear plant will be in a safe state during and following a severe earthquake.
- All control operations that must be completed within 15 minutes after an earthquake shall be automated.
- All monitoring and manual control functions required shall be exerciseable from a seismically qualified control area.
- All qualified systems and components shall be designed and located to minimize their exposure to hazards resulting from failure of unqualified systems. This shall be done by locating the majority of seismically qualified components in an area where surrounding components are qualified.
- In addition, and where necessary, the exposure to hazards shall be minimized by the use of barriers, or by maintaining sufficient distance between qualified and unqualified components.
- As a minimum, supports, anchors, bracing, etc., shall be designed for an earthquake (DBE or SDE, as applicable), unless it has been shown that the consequence of failure would not constitute a safety hazard.
- The Main Control Room (MCR) shall be designed to ensure operator safety during and following an earthquake. The Secondary Control Area (SCA), including the access routes from the MCR to SCA, shall be seismically qualified for post-earthquake plant operation.

Canadian Approach vs. Others – Highlights

As befits an active participant in the NUSS program of the IAEA, Canada's seismic design criteria meet [Duff and Usmani, 1984] the requirements of the IAEA Safety Code on siting, 50-C-S, the IAEA Safety Guide on earthquakes with respect to nuclear power plant siting, 50-SG-S1, and the IAEA Safety Guide on seismic analysis and testing, 50-SG-S2.

Table 1 is derived from the IAEA criteria, where only two levels of earthquake, S_2 and S_1, are specifically defined. The S_2 is comparable to the Canadian DBE, whereas the S_1 is more in line with the Operating Basis Earthquake (OBE), frequently applied in other countries. Table 2 illustrates the same information in terms of the Canadian seismic design criteria. The specific design requirements are drawn from CSA, ASME, and the NBCC Standards. In general, these design requirements differ from those used in other countries; for example, the ASME level 'C' stress limit [ASME, 1983] is applied for both the DBE and SDE, whereas the U.S. NRC permits stresses for the SSE (Safe Shutdown Earthquake, corresponding to the DBE or S_2) to meet the level

Table 1: IAEA Earthquake Design Levels

System category	*Earthquake level*	*Design requirement*	*Plant status (post-earthquake)*
Major process and safety systems	S_2 (DBE)	Nuclear Code	Serviceable
Safety-related systems	S_1 (OBE)	Nuclear Code	Operable
Other systems	$\leq S_2$	National Building Code	Non-collapse

Table 2: Canadian Earthquake Design Levels

System category	*Earthquake level*	*Design requirement*	*Plant status (post-earthquake)*
Reactor and reactor building major process and special safety systems and their supporting structures	DBE	CSA-N285 -N287 -N289 and ASME level 'C' stress	Safe and serviceable
Emergency core cooling system	SDE	CSA-N285 -N289 and ASME level 'C' stress	Safe and serviceable (following LOCA)
Other systems and structures	NBCC	National Building Code of Canada	Non-collapse

'D' limit. The design of a system to level 'C' of the ASME Code, Section III, for the DBE (S_2), is the equivalent of designing for at least six, S_1-level earthquakes of one-half the S_2 intensity, in terms of shakedown and fatigue damage [Duff and Heidebrecht, 1979].

The Operating Basis Earthquake (OBE) as such is not applied in Canada. This is entirely in keeping with the IAEA Siting Guide. As the Canadian approach applies the DBE to all structures and systems essential to ultimate plant safety, the only requirement for an OBE, will be economic reasons such as plant operation and availability. For these reasons, all non-safety-related structures and systems are designed to the NBCC, using more conservative methods than called for by that code, and cascading effects are minimized. The proof of the inherent capability of CANDU NPPS to continue operating through low-level earthquakes is borne out by the fact that there have been no failures of any operating CANDUS, including some in an advanced stage of commissioning, during actual earthquakes estimated to range from 0.01 to 0.1 g.

Seismic Qualification Methods and Selection

Seismic Qualification Methods

Seismic qualification can be demonstrated by analysis, testing, and a combination of analysis and testing. Of the above methods, full dynamic analysis is the most common and acceptable.

Testing is necessary when a system or component is too complex to model and analyze reliably. Testing is especially important when it is necessary to demonstrate that the equipment can perform a function reliably (electrical or mechanical) during and / or following an earthquake.

Testing may be performed at a low level of excitation for obtaining suitable dynamic characteristics to enable a meaningful dynamic earthquake analysis to be carried out. It may also be used to confirm analytical results for increasing the level of confidence. Testing may also be performed on scale models where full-scale testing is out of the question or would be performed too late to permit necessary changes to be made.

Seismic qualification may be claimed where a piece of equipment has been selected that is identical with, or similar to equipment that has already been seismically analyzed or tested for similar conditions, or has safely survived an actual earthquake of equal severity under equivalent operating conditions.

Analytical Methods

The analytical methods that are available are the time-history method by direct integration, the time-history method by modal superposition, the response-spectrum method, and the equivalent static-load method.

The time-history methods are the most rigorous and costly. These are used in limited cases where other methods yield unacceptable results. A suitable time-history of the required DBE, either at ground level or at floor level, is used as seismic input.

The response-spectrum method is the most common, as well as being the cheapest to apply. The Ground Response Spectrum (GRS) is used to represent, on a mode-by-mode basis, the response of the building or other structure to ground motion, while the Floor Response Spectrum (FRS) is used to determine, in a similar manner, the response of equipment. Proper care must be taken to determine the responses in each mode and in each direction of earthquake excitation, and to combine the results appropriately.

The equivalent static-load method is a simplified, but usually conservative way of determining and applying horizontal seismic design loads to simple systems or components without having to perform a full-scale dynamic analysis.

Typical Examples

Seismic qualification of CANDU equipment and components is established by analysis, testing, and combination of analysis and testing, as appropriate. Some typical equipment and their qualification methods are described briefly in the following section.

A Heat Transfer System (HTS) pump (Figure 2a) is required to maintain pressure boundary integrity and must remain free wheeling during and after a DBE. This

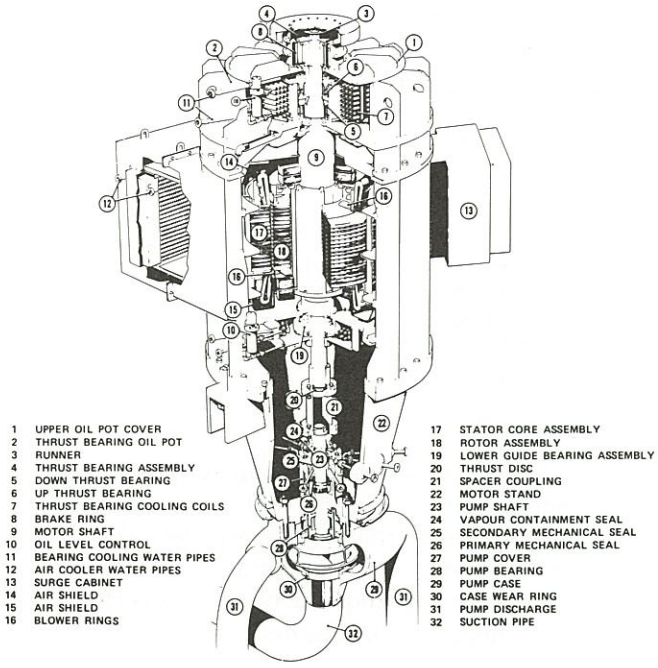

Figure 2a: Heat transport system pump.

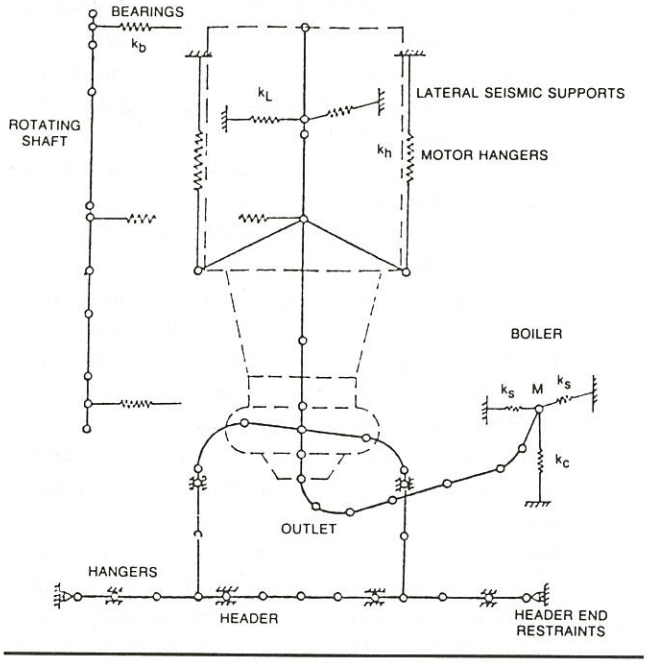

Figure 2b: Schematic dynamic model of pump.

is demonstrated by dynamic analysis, along with testing of parts such as the bearings and the motor. A typical dynamic model of the pump and the rotor-bearing system is shown in Figure 2b. From the analysis it is shown that, due to seismic-loading, the bearing does not fail, the clearance between the rotor and the stator does not close, and the structural integrity of all components is maintained.

A steam generator (Figure 3a) is required to maintain

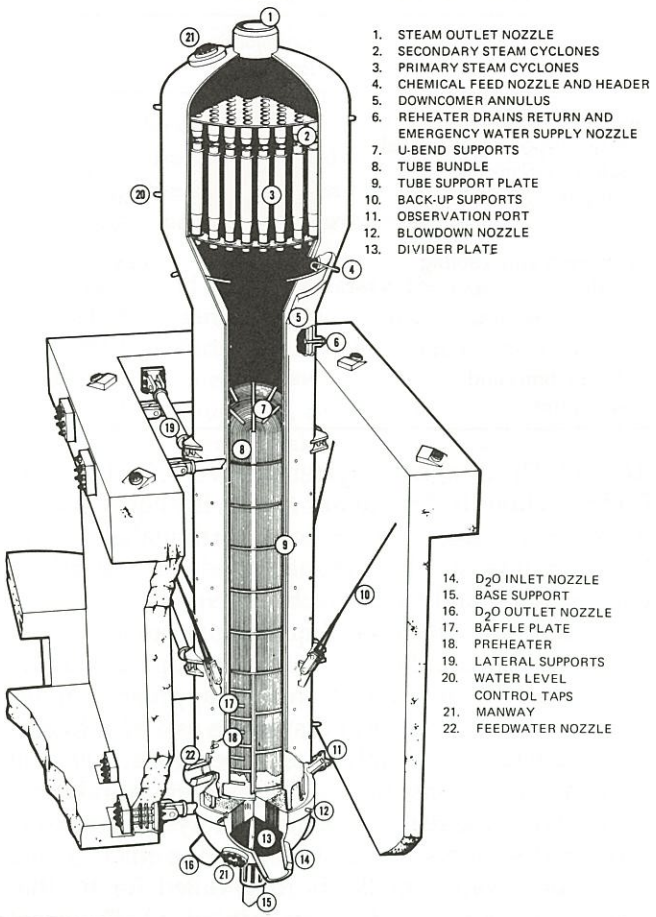

Figure 3a: Steam generator for 600 MW(e) NPS.

heat rejection capability and the pressure boundary integrity. This is demonstrated by dyanamic analysis. The typical model (Figure 3b) includes all the internal components. The dynamic properties, such as damping and stiffnesses of some components, are established by testing.

Piping systems are qualified by extensive dynamic analysis, taking into account both inertia and seismic anchor movements. Multiple-support excitation techniques are applied, when necessary, to cut down the over conservatism of the envelope Floor Response Spectrum (FRS) approach. A typical model of CANDU feeder piping is shown in Figure 4.

Valves are seismically qualified by analysis and testing. Safety related valves, such as the quick-opening valve in the second shutdown system, are shake-tested to demonstrate operability. Other valves are tested by simulating the worst seismic loading by an equivalent side-load test.

The fuelling machine (Figures 5a, 5b) is qualified [Banwatt *et al.*, 1985] by dynamic analysis. The dynamic characteristics, non-linear effects, and model verifications are based on extensive dynamic test results.

Control and instrumentation equipment is seismically qualified by shake-testing. The stand-by diesel

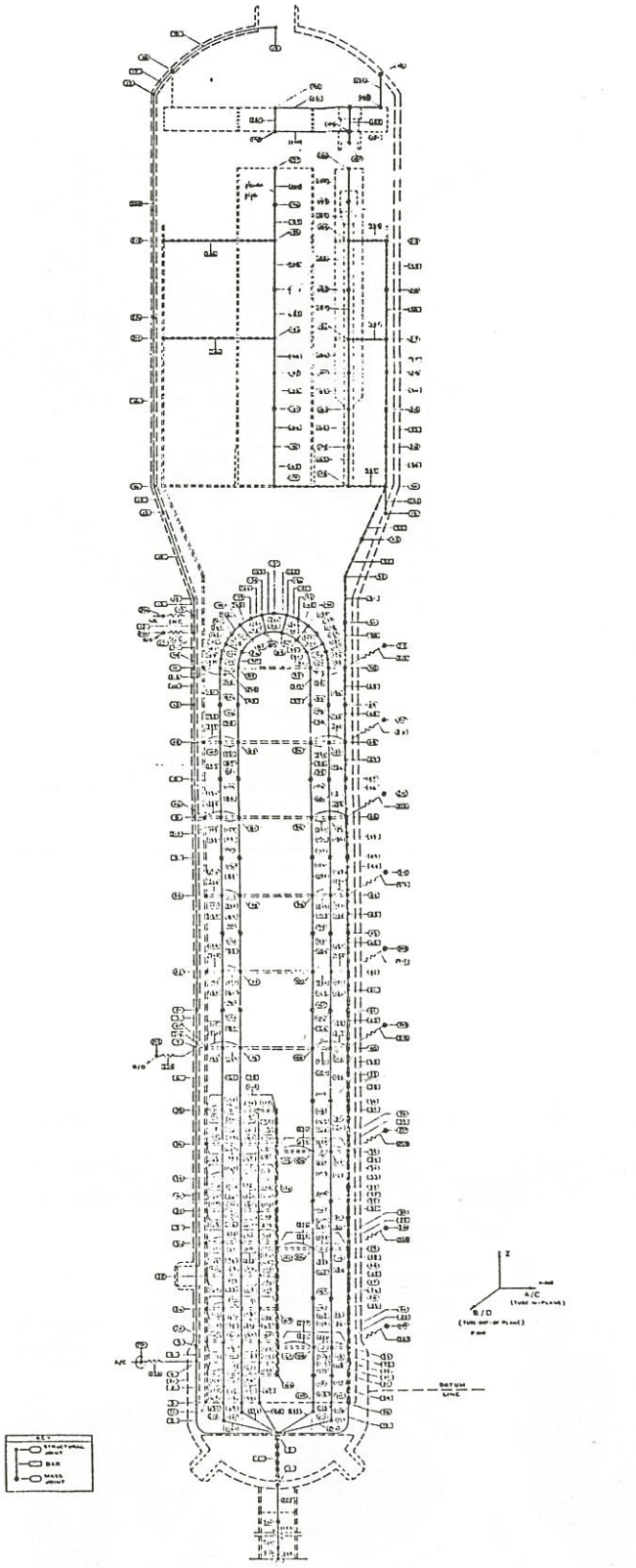

Figure 3b: Mathematical model of steam generator and its internals.

generators (Figure 6) have been qualified by shake-testing as well.

The core, including the shut-off rod mechanisms,

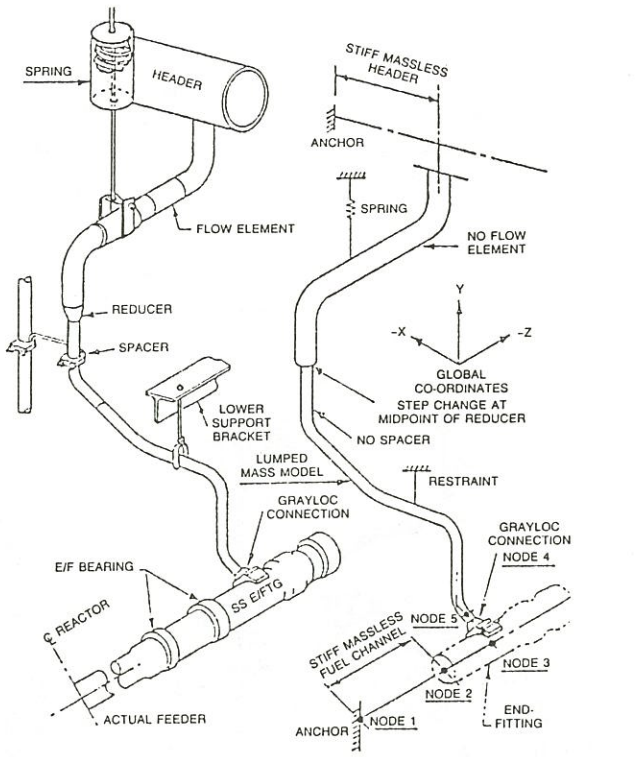

Figure 4: Analytical model of feeder.

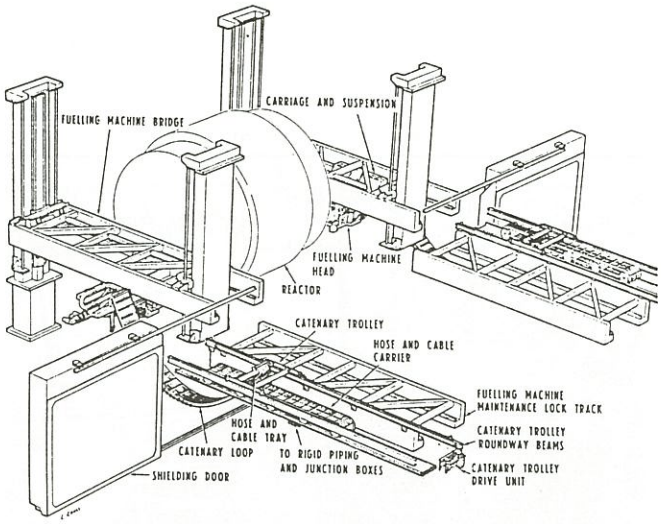

Figure 5a: Fuelling machine.

have been seismically qualified [Kuroda and Duff, 1982] by testing full and partial scale models (Figures 7a, 7b) under very severe seismic motions simulated on a shaker table.

Conclusion

The Canadian seismic design approach and methods for seismically qualifying the CANDU-PHW nuclear power

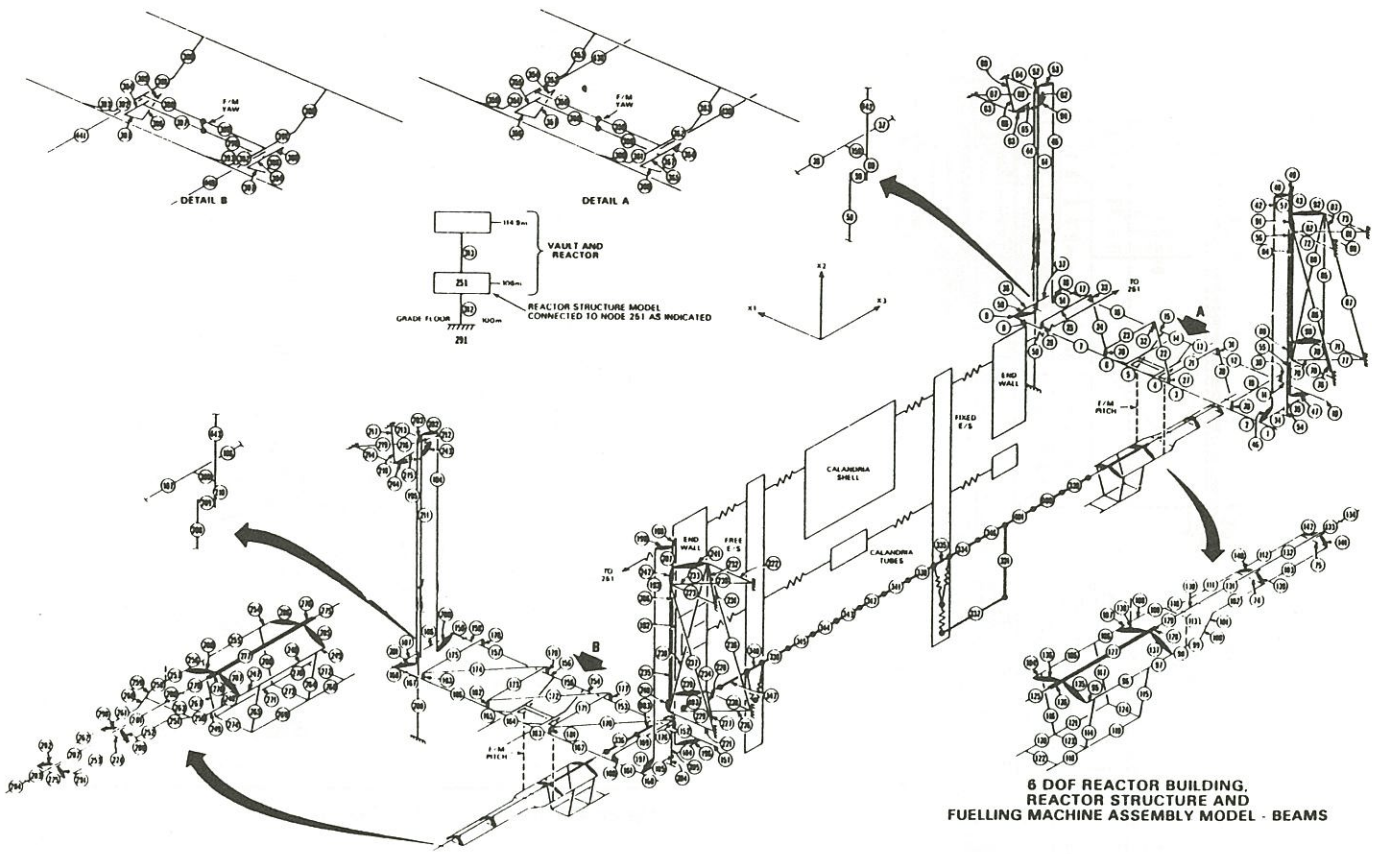

Figure 5b: Fuelling machine dynamic analysis model.

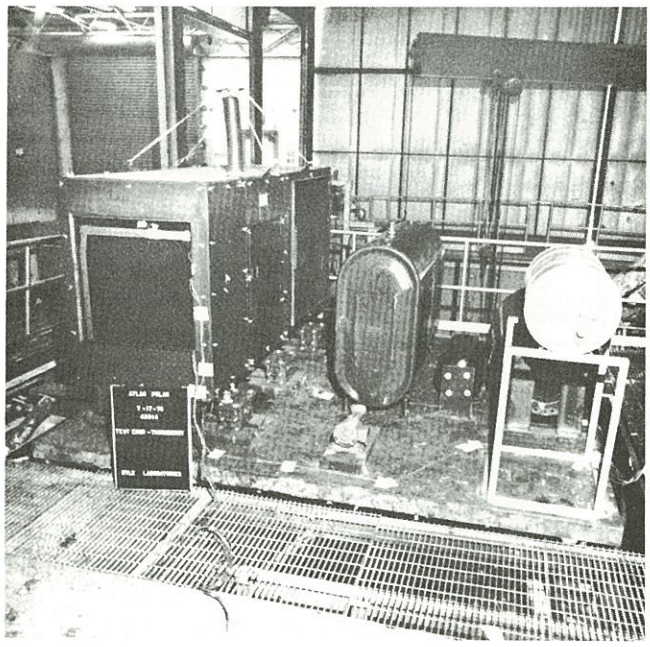

Figure 6: Shake-up test setup EPS diesel generator and accessories.

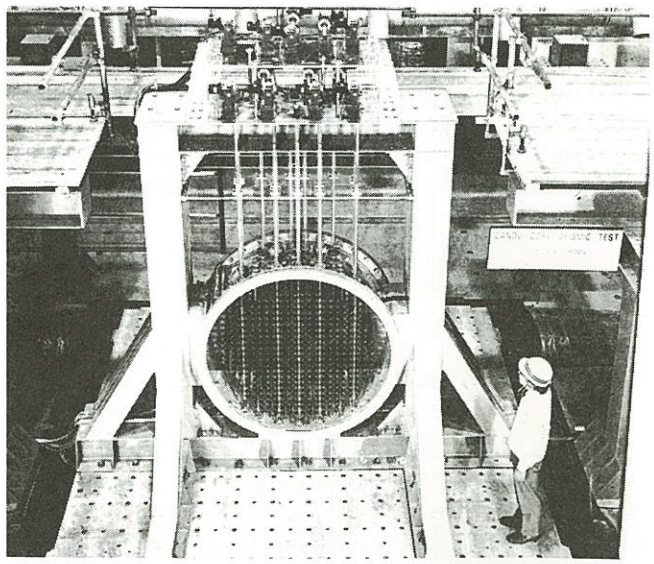

Figure 7a: CANDU core seismic test 1/5 scale model.

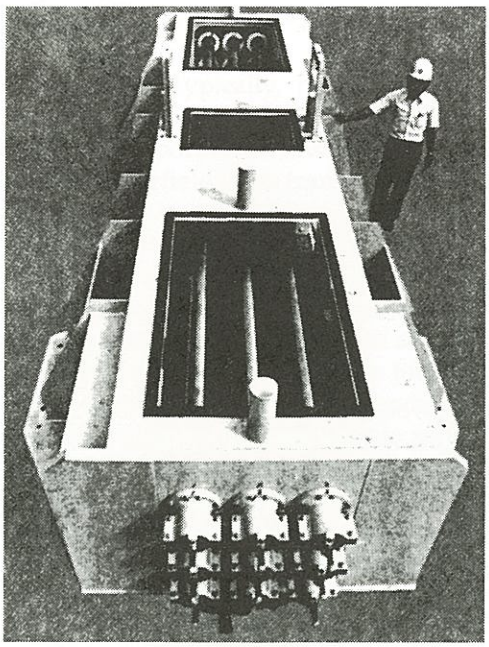

Figure 7b: CANDU core seismic full-scale partial model.

plant's system and equipment are unique in some respects, especially in terms of design conservatism, pre-operational inspection, and avoidance of any need to cater explicitly for an operating basis earthquake. By designing essential structures and systems to at least the earthquake requirements of the National Building Code of Canada – and all areas important to safety to the low-probability DBE – using conservative criteria, CANDU nuclear power plants are capable of safely surviving any earthquake they are likely to experience during their operating lifetime. The CANDU equipment and systems are seismically qualified using state-of-the-art technique and methods.

Acknowledgements

The material presented in this paper is based on various AECL reports and publications. Review comments and suggestions from C.G. Duff and S.K.W. Yu are gratefully acknowledged. Ray Juneau's assistance in preparation of illustrations and figures is also appreciated.

References

1. American Society of Mechanical Engineers boiler and pressure vessel code, section III, division 1, nuclear components, 1983.
2. *Banwatt AS*, et al. CANDU 600 fuelling machine non-linear finite element modelling and model testing. Proceeding of the 3rd International Modal Analysis Conference, Orlando, Florida 1985.
3. *Duff CG, Usmani SA.* Canadian approach to seismic design of CANDU-PHW nuclear power plants. Proceedings of the Conference on Structural Analysis and Design of Nuclear Power Plants, Porto Allegre, Brazil, October 1984.
4. *Duff CG, Heidebrecht AC.* Earthquake fatigue effects on CANDU nuclear power plant equipment. 3rd Canadian Conference on Earthquake Engineering, Montreal, June 1979.
5. *Duff CG, Stevenson JD.* Seismic qualification of nuclear power plants by inspection. 8th World Conference on Earthquake Engineering, San Francisco, California, July 1984.
6. *Kuroda T, Duff CG.* Experimental and analytical studies on the seismic behaviour of CANDU-PHW cores. International Meeting on Thermal Nuclear Reactor Safety, American Nuclear Society, Chicago, September 1982.
7. International Atomic Energy Agency, Vienna. Safety in nuclear power plant siting – a code of practice. No. 50-C-S, and associated safety guides on earthquakes. Vienna, Austria: IAEA, 1978–1979.
8. National Building Code of Canada. National Research Council of Canada, Ottawa, Ontario, Canada, NRCC No. 17303, 1980.
9. National Standards of Canada (Canadian Standards Association, Rexdale, Ontario, Canada). CAN3-N289 Series. Seismic qualification of CANDU nuclear power plants. 1980–81.
10. National Standards of Canada. CAN3-N285 Series. Pressure-retaining systems and components in CANDU nuclear power plants. 1981.
11. National Standards of Canada. CAN3-N287 Series. Requirements for concrete containment structures for CANDU nuclear power plants. 1978–81.
12. *Usmani SA.* Seismic qualification of CANDU-PHW nuclear power plant equipment. Proceedings of International Federation for Theory of Machines and Mechanism (IFTOMM) Symposium, Karlovac, Yugoslavia, October 14–17, 1986.

Multifield Methods for Nuclear Thermalhydraulics Problems

S. Banerjee
Department of Chemical and Nuclear Engineering
University of California
Santa Barbara, CA 93106

Abstract

The multifield model, in which separate sets of conservation equations are written for each phase, or clearly identifiable portion of a phase, is derived by averaging the local instantaneous equations. The closure relationships required to replace information lost in the averaging process are discussed. The mathematical structure of the model is considered and it is shown that application to a variety of problems in which the phases are well separated leads to good predictions of experimental data. For problems in which the phases are more closely coupled, the model is more difficult to apply correctly. However, careful consideration of interfield momentum and heat transfer is shown to give excellent results for some complex problems like density wave propagation in bubbly flows. The model in its present form is shown to be less useful for highly intermittent regimes like slug and churn flows. Data on a reflux condensation situation near the flooding point are discussed to indicate directions in which further work is required.

Résumé

Le modèle multifluides dans lequel des systèmes separés d'équations de conservation sont écrits pour chaque phase, ou pour chaque portion clairement identifiable d'une phase, est demontré en moyennant les équations locales instantanées. Les relations de fermeture necessaires pour replacer les informations perdues au cours de l'opération de moyenne sont discutées. La structure mathématique du modèle est considerée et il est montré que des applications à des problèmes variés dans lesquels les phases sont bien separées conduits a de bonnes predictions des résultats experimentaux. Pour des problèmes où les phases sont plus fortement couplées, il est plus difficile d'appliquer correctement le modèle. Néanmoins, il est demontré que la considération soigneuse du moment interfluides et du transfer de chaleur donne d'excellents résultats pour des problèmes complexes comme la propagation d'ondes de densité en milieu à bulles. Il est demontré que le modèle dans sa présente forme est moins utile pour des régimes d'écoulements fortement intermittents comme les écoulements à poches ou à bouchons. Quelques résultats expérimentaux, concernant une situation de condensation à reflux, sont presentés pour indiquer les directions vers lesquels un travail plus approfondi est nécessaire.

Introduction

The approach to 2-phase flow modelling that is now widely used in computer codes like TRAC, and RELAP5 [see the TRAC PD2 manual 1982, and Ransom *et al.* 1984] is based on averaging of the original local instantaneous conservation equations for mass, momentum, and energy. Averaging may be done in time, space, over an ensemble, or in some combination of these, and details may be found in Panton (1968); Vernier and Delhaye (1968); Delhaye (1970); Drew (1971); Kocamustafaogullari (1971); Ishii (1971); Boure *et al.* (1975); Ishii (1975); Delhaye and Achard (1976); Hughes *et al.* (1976); Yadigaroglu and Lahey (1976); Agee *et al.* (1978); Lyczkowski *et al.* (1978); Nigmatulin (1978, 1979); Banerjee and Chan (1980); and Drew (1983), amongst others. The procedure is to derive an averaged set of conservation equations for each field. A field may be thought of as a clearly identifiable portion of a phase, e.g., annular flow may be modelled with 3 fields – one for the liquid film, one for the droplets, and one for the gas core. Selection of the fields depends on the modeller but should, in the spirit with which the model is derived, in all cases be consistent with the physics of the problem. To illustrate this point further, a vertical slug flow might be described by 4 fields – the first for the large bullet-shaped gas bubbles, the second for the liquid film around these bubbles, the third for the highly dispersed gas bubbles in between the large gas bubbles, and the fourth for the liquid surrounding the dispersed bubbles. This level of sophistication may be required in some cases for highly intermittent flows.

While averaging makes the mathematical solution of 2-phase flow problems tractable, information regard-

Keywords: multifield methods, thermalhydraulics, loss of coolant, two-phase flow analysis

ing local gradients between fields and the distribution of phases is lost. Therefore, closure relationships or 'constitutive equations' are required to replace this information. Typically, one needs relationships for interfield forces, heat transfer, and area. For problems involving vaporization and condensation of one component, interfield mass transfer may be related to heat transfer, but in more general problems interfield mass transfer relationships are also needed.

Since averaging also eliminates information regarding the distribution of fields, distribution coefficients relating products of averages to averages of products are therefore also needed. By judiciously choosing fields that are relatively homogeneous, the requirement for distribution coefficients may be minimized, but is difficult to eliminate entirely for all flow regimes.

The form of the closure relationships has important consequences for the mathematical structure of the problem and solution procedures. For example, the simplest multifield models which account for interfield forces through algebraic drag correlations invariably result in high-wavenumber instabilities that are not physical [see, for example, Drew (1983), and Ramshaw and Trapp (1978)]. Considerable work has been done to resolve this problem. The main reason for the non-physical behaviour now appears to lie in rather subtle aspects of pressure interactions between fields, aspects that were neglected in the early models. Recent work on these interactions leads to excellent prediction of a variety of phenomena, as will be discussed later in the paper.

We will first outline the derivation of the averaged conservation equations, identify the closure relationships needed, and analyze the mathematical structure of the multifield model. We will then illustrate the application of the model to flows in which the fields are loosely coupled, i.e., separated flows, and then flows in which the fields are more closely coupled. Finally, the difficulties with the model for intermittent flows will be discussed.

The Multifield Model

Averaged Conservation Equations

The local instantaneous form of the conservation equations for phase k may be written as

$$\frac{\partial \rho_k \psi_k}{\partial t} + \nabla \cdot \rho_k \psi_k \vec{V}_k + \nabla \cdot \gamma_k - \rho_k \hat{S}_k = 0, \tag{1}$$

where conservation requires

$$\begin{aligned} &\psi_k = 1,\ \gamma_k = 0,\ \hat{S}_k = 0, \quad \text{for mass,} \\ &\psi_k = \vec{V}_k,\ \gamma_k = p_k \bar{\bar{I}} - \bar{\bar{\tau}}_k,\ \hat{S}_k = \vec{F}_k \quad \text{for momentum, and} \\ &\psi_k = E_k,\ \gamma_k = \vec{q}_k - (p_k \bar{\bar{I}} - \bar{\bar{\tau}}_k) \cdot \vec{V}_k,\ \hat{S}_k = \vec{F}_k \cdot \vec{V}_k + Q_k \\ &\qquad\qquad \text{for energy conservation.} \end{aligned} \tag{2}$$

Here $\vec{V}$ is velocity, p is pressure, $\bar{\bar{\tau}}$ is the shear stress tensor, $E = e + \vec{V} \cdot \vec{V}/2$ is the internal plus kinetic energy, ρ is density, $\bar{\bar{I}}$ is the identity tensor, $\vec{F}$ is body force, Q is the body heat source, and $\vec{q}$ is heat flux.

While these equations, together with appropriate boundary and initial conditions, constitute the exact mathematical problem, they cannot even be solved for high Reynolds single-phase flow. Direct simulation using super-computers is becoming possible for some simple single-phase flow situations, but is still far in the future for flows in which interface motion and configuration are an integral part of the problem. Because the mathematical problem is impossible to solve at present, the governing equations are reduced to solvable forms by a variety of procedures. The procedure that is most widely used is to volume average the equations, and then time / ensemble average them. The averaging operations are commutative and the order can be reversed, resulting in the same averaged equations. Volume averaging is done rather than area averaging, to assure that the dependent variables and their first derivatives are continuous [see Banerjee and Chan (1980) for more detail].

The procedure will be illustrated for volume averaging of two-phase flow in a duct. Consider the flow situation in Figure 1, which defines the symbols. In this case, 2 phases are shown, but the derivation is not affected if there were more than 2 phases or fields. To proceed, forms of Gauss' theorem and Liebnitz's rule particular to this geometry will be used. We will use these relationships to interchange derivative and volume integral operations. They are:

Leibnitz's rule

$$\frac{\partial}{\partial t} \int_{V_{k(z,t)}} f(x, y, z, t) dV = \int_{V_k} \frac{\partial f}{\partial t} dV + \int_{a_i} f(\vec{V}_i \cdot \vec{n}_k) dS; \tag{3}$$

Gauss' theorem

$$\int_{V_{k(z,t)}} \nabla \cdot \vec{a} dV = \frac{\partial}{\partial z} \int_{V_k} \vec{n}_z \cdot \vec{a} dV + \int_{a_i} \vec{n}_k \cdot \vec{a}\, dS. \tag{4}$$

Defining

$$\langle f_k \rangle = \frac{1}{V_k} \int_{V_k} f_k\, dV$$

and

$$\langle f_k \rangle_i = \frac{1}{V} \int_{a_i} f_k\, dS$$

and

$$\alpha_k = V_k / V,$$

the volume averaged conservation equations are

$$\frac{\partial}{\partial t} \overline{\alpha_k \langle \rho_k \rangle} + \frac{\partial}{\partial z} \overline{\alpha_k \langle \rho_k u_k \rangle} = -\overline{\langle \dot{m}_k \rangle_i} = -\overline{\rho_k \vec{n}_k \cdot (\vec{V}_i - \vec{V}_k)}; \tag{5}$$

$$\frac{\partial}{\partial t} \overline{\alpha_k \langle \rho_k u_k \rangle} + \frac{\partial}{\partial z} \overline{\alpha_k \langle \rho_k u_k^2 \rangle} + \frac{\partial}{\partial z} \overline{\alpha_k \langle p_k \rangle} + \frac{\partial}{\partial z} \overline{\alpha_k \langle \vec{n}_z (\bar{\bar{\tau}}_k \cdot \vec{n}_z) \rangle} -$$

$$\alpha_k \langle \rho_k \vec{F}_k \rangle = -\frac{1}{V} \int_{a_i} \overline{[\dot{m}_k u_k + \vec{n}_z \cdot \vec{n}_k p_k - \vec{n}_z \cdot (\vec{n}_k \cdot \bar{\bar{\tau}}_k)]}\, dS +$$

$$\frac{1}{V} \int_{a_{kw}} \overline{\vec{n}_z \cdot (\vec{n}_{kw} \cdot \bar{\bar{\tau}}_k)}\, dS; \text{ and} \tag{6}$$

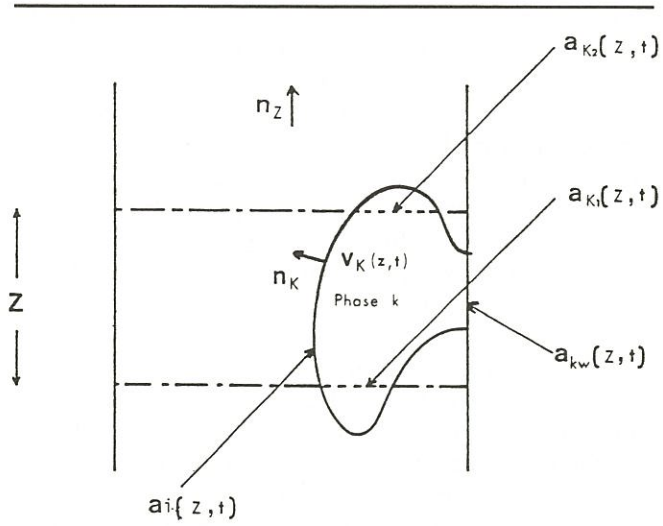

Figure 1 Schematic of two-phase flow field defining the symbols.

$$\frac{\partial}{\partial t}\overline{\alpha_k\langle\rho_k E_k\rangle} + \frac{\partial}{\partial z}\overline{\alpha_k\langle\rho_k u_k E_k\rangle} + \frac{\partial}{\partial z}\overline{\alpha_k\langle\vec{q}_k\cdot\vec{n}_z\rangle} + \frac{\partial}{\partial z}\overline{\alpha_k\langle p_k u_k\rangle} -$$

$$\frac{\partial}{\partial z}\overline{\alpha_k\langle\vec{n}_z\cdot(\bar{\bar{\tau}}_k\cdot\vec{V}_k)\rangle} - \overline{\alpha_k\langle\rho_k(\vec{F}_k\cdot\vec{V}_k + Q_k)\rangle} = -$$

$$\overline{\frac{1}{V}\int_{a_i}[\dot{m}_k E_k + \vec{n}_k\cdot(\vec{q}_k + p_k\vec{V}_k - \bar{\bar{\tau}}_k\cdot\vec{V}_k)]\,dS} -$$

$$\overline{\frac{1}{V}\int_{a_{kw}}\vec{n}_{kw}\cdot q_k\,dS}. \qquad (7)$$

Here $\dot{m}_k$ is the mass transfer out of phase k, and u_k is the velocity in the z direction. The terms involving derivatives of $\bar{\bar{\tau}}$ and $\vec{q}$ on the left hand sides, i.e., axial diffusion of momentum or heat due to molecular effects, are often neglected, since they are very small in most cases. The overbar signs indicate that an ensemble or time averaging operation has been carried out after volume averaging. Double averaging leads to certain desirable properties, which will not be considered further here, but Delhaye and Achard (1978) may be consulted for a definitive discussion.

These equations apply not only to each plane, but to any clearly identified portions of a phase, which is often called a 'field,' provided appropriate relationships are supplied for the quantities on the right-hand side. The central difficulty with such an averaged multifield model arises from all information being lost about the gradients between fields and at the wall. Therefore, closure relationships must be supplied for all the integrals on the right-hand sides, since they cannot be calculated *a priori* from the model. This happens as well in single-phase flow, where the momentum equation is often phrased as

$$\frac{\partial}{\partial t}\overline{\langle\rho u\rangle} + \frac{\partial}{\partial z}\overline{\langle\rho u^2\rangle} + \overline{\frac{\partial\langle p\rangle}{\partial z}} = \overline{\frac{1}{V}\int_{a_{kw}}\vec{n}_z\cdot(\vec{n}_w\cdot\bar{\bar{\tau}})\,dS} = -$$

$$\frac{2f\langle\bar{\rho}\rangle\langle\bar{u}\rangle\langle\bar{u}\rangle}{D}, \qquad (8)$$

with f being the friction factor and D the diameter. Similarly, relationships involving wall-fluid heat transfer coefficients are used to model the last term in (7) in single-phase flow, i.e., the wall heat flux.

In 2-phase flow, however, the empirical basis for such closure relationships is not well established, and an entirely new set for the interfield transfer of mass, momentum, and energy is needed. Therefore, while the 2-phase flow problem is not qualitatively different from the single-phase flow problem, it requires much more information in the form of closure relationships.

A problem also arises with terms on the left-hand side of (5), (6), and (7). In order to have the same number of variables as equations, we need to relate quantities like $\overline{\alpha_k\langle\rho_k u_k^2\rangle}$ to $\overline{\alpha_k}$, $\overline{\langle\rho_k\rangle}$, $\overline{\langle u_k\rangle}^2$. The problem also occurs in single-phase gas dynamics, where $\overline{\langle\rho_k u_k^2\rangle}$ must be related to $\overline{\langle\rho_k\rangle}$, $\overline{\langle u_k\rangle}^2$. To resolve this problem, the assumption is often made that the density and velocity profile is flat across the duct in single-phase flow. While this is reasonably accurate for turbulent flows, it may give substantially wrong answers in some cases, even in single-phase flow – see Bird *et al.* (1960). In 2-phase flow, density variations in the averaging volume are usually negligible; however, substantial variations in phase volume fraction ($\overline{\alpha_k}$) and velocity ($\overline{\langle u_k\rangle}$) may exist. Therefore, distribution effects are important in a wider range of problems.

Jump Conditions

Moving on to what is known about the closure relationships from the formal averaging procedure, all we have are the consistency relationships for interfield transfer. For 2 fields these jump conditions [see Banerjee and Chan (1980)] are

$$\sum_{k=1}^{2}\frac{1}{V}\int_{a_i}\bar{\dot{m}}_k\,dV = 0; \qquad (9)$$

$$\sum_{k=1}^{2}\frac{1}{V}\int_{a_i}\overline{[\dot{m}_k u_k + \vec{n}_z\cdot(n_k p_k) - \vec{n}_z\cdot(\vec{n}_k\cdot\bar{\bar{\tau}}_k)]}\,dS = 0; \text{ and} \qquad (10)$$

$$\sum_{k=1}^{2}\frac{1}{V}\int_{a_i}\overline{\left[\dot{m}_k\left(h_k + \frac{V_k^2}{2}\right) + p_k(\vec{n}_k\cdot\vec{V}_k) + \vec{n}_k\cdot(\vec{q}_k - \bar{\bar{\tau}}_k\cdot\vec{V}_k)\right]}\,dS. \qquad (11)$$

All other information regarding closure relationships has to be obtained from experiments, or from modelling and analysis external to the multifield model. In addition, we have the condition for phase volume fraction that

$$\sum_k \alpha_k = 1. \qquad (12)$$

The Equal Pressure Model

For the rest of the section, we will drop the overbar signs with the understanding that all quantities are ensemble averaged. The simplest multifield model is then obtained by putting the average pressures in each phase equal to each other within the averaging volume, and equal to the interfacial pressure, i.e., $\langle p_k\rangle = \langle p_{ki}\rangle =$

$\langle p \rangle$. In that case, the integral involving pressure on the right-hand side of the momentum equation (6) may be simplified by Gauss' theorem as

$$\frac{1}{V}\int_{a_i} \langle p\rangle \vec{n}_k \cdot \vec{n}_z \, dS = \langle p \rangle \frac{\partial \alpha_k}{dz}, \tag{13}$$

and (6) becomes

$$\frac{\partial \alpha_k \langle \rho_k u_k \rangle}{\partial t} + \frac{\partial \alpha_k \langle \rho_k u_k^2 \rangle}{\partial z} + \alpha_k \frac{\partial \langle p \rangle}{\partial z} - \alpha_k \langle \rho_k F_{kz} \rangle = -$$

$$\frac{1}{V}\int_{a_i} [\dot{m}_k u_k - \vec{n}_z \cdot (\vec{n}_k \cdot \bar{\bar{\tau}}_k)] \, dS + \frac{1}{V}\int_{a_{kw}} \vec{n}_z \cdot (\vec{n}_{kw} \cdot \bar{\bar{\tau}}_k) \, dS. \tag{14}$$

Since the pressure differences between phases are expected to be small over a cross-section, the equal pressure assumption is plausible at first sight. However, more careful consideration indicates gradients of the difference between phase pressures and interface pressures may be comparable to the other terms in the momentum equation. As shown in the next section, the terms involving pressure in the multifield momentum equations have a crucial effect on stability.

Structure and Validity of the Model

Separated Flows

Stratified Flow

Consider an incompressible stratified flow in the flow situation shown in Figure 2. If viscous effects are modelled by algebraic terms involving friction factors, as is conventional in single-phase flow, and we assume no heat or mass transfer, then the characteristics for the equal pressure, quasi-linear set of conservation equations (5) and (14) are wholly real only if

$$-\alpha(1-\alpha)\rho_1\rho_2(u_1 - u_2)^2 \geq 0, \tag{15}$$

where we have assumed $\langle u_k^2 \rangle = \langle u_k \rangle^2 = u_k^2$ (say). This is clearly impossible for 2-phase flow, so the characteristics are always complex and high-frequency instabilities may be expected [as discussed by Drew (1983), Ramshaw and Trapp (1978), and Banerjee and Chan (1980)]. The equal pressure model therefore cannot predict phenomena in stratified flows.

In the actual physical situation, the pressures are not equal. The form of the momentum equation can then be derived by writing

$$p_{ki} = \langle p_k \rangle + \Delta p_{ki} + \Delta p'_{ki}, \tag{16}$$

where

$$\Delta p_{ki} = \langle p_{ki} \rangle - \langle p_k \rangle$$

and

$$\Delta p'_{ki} = p_{ki} - \langle p_{ki} \rangle.$$

Since $\langle p_k \rangle$ and $\langle p_{ki} \rangle$ are constant in the averaging volume, therefore the term

$$\frac{1}{V}\int_{a_i} p_k \vec{n}_k \cdot \vec{n}_z \, dS = [\langle p_k \rangle + \Delta p_{ki}] \frac{\partial \alpha_k}{\partial z} + \frac{1}{V}\int_{a_i} \Delta p'_{ki} \vec{n}_k \cdot \vec{n}_z \, dS. \tag{17}$$

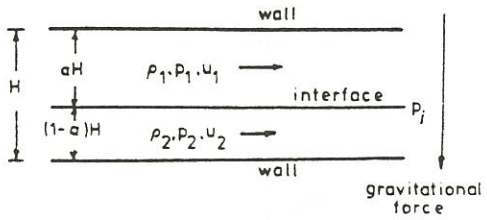

Figure 2 Schematic of stratified flow defining the symbols.

The linear momentum equation then becomes

$$\frac{\partial \alpha_k \langle \rho_k u_k \rangle}{\partial t} + \frac{\partial \alpha_k}{\partial z}\langle \rho_k u_k^2 \rangle + \alpha_k \frac{\partial \langle p_k \rangle}{\partial z} - \Delta p_{ki} \frac{\partial \alpha_k}{\partial z} =$$

$$-\frac{1}{V}\int_{a_i} [\dot{m}_k u_k + \vec{n}_z \cdot \vec{n}_k \Delta p'_{ki} - \vec{n}_k \cdot (\vec{n}_z \cdot \bar{\bar{\tau}}_k)] \, dS$$

$$+\frac{1}{V}\int_{a_i} \vec{n}_z \cdot (\vec{n}_{kw} \cdot \bar{\bar{\tau}}_k) \, dS. \tag{18}$$

To proceed, we now require expressions for Δp_{ki} and $\Delta p'_{ki}$ for the stratified flow situation in Figure 2; the pressure difference between phases may be expressed in the static approximation as

$$p_i - p_1 = \Delta p_{1i} = \rho_1 g \alpha H/2; \tag{19}$$

$$p_i - p_2 = \Delta p_{2i} = -\rho_2 g(1-\alpha)H/2. \tag{20}$$

At the level of this approximation, $\Delta p'_{ki}$ vanishes. Therefore, the right-hand side of the momentum equation is the same as (14), but the left-hand side now contains additional terms that are derivatives of α. Versions of this formulation were proposed by Rousseau and Ferch (1979), and Ardron (1980).

The condition for real characteristics is then

$$(\rho_2 - \rho_1) gH \left[\frac{\alpha}{\rho_1} + \frac{1-\alpha}{\rho_2}\right] \geq (u_1 - u_2)^2. \tag{21}$$

This is exactly the Kelvin-Helmholtz stability criterion for long waves. If the inequality is not satisfied, then interfacial instabilities will grow because the restoring forces due to gravity will not be sufficient to balance the sucking action at the wave crest due to Bernoulli's effect. The criterion in (21) signals a transition to slug flow. (In reality, transition may occur earlier due to non-linear effects; see Ahmed and Banerjee (1985).) Consideration of phase pressure differences, then, captures a real physical effect.

The static approximation in (19) and (20) breaks down for finite amplitude waves. Banerjee (1980) has integrated the transverse momentum equation and shown that higher order terms occur that lead to a Korteweg-DeVries equation for interfacial waves at the next level of approximation.

Inverted Annular Flow

We will consider another example of a separated flow to illustrate the capability of the model to predict rather complex phenomena.

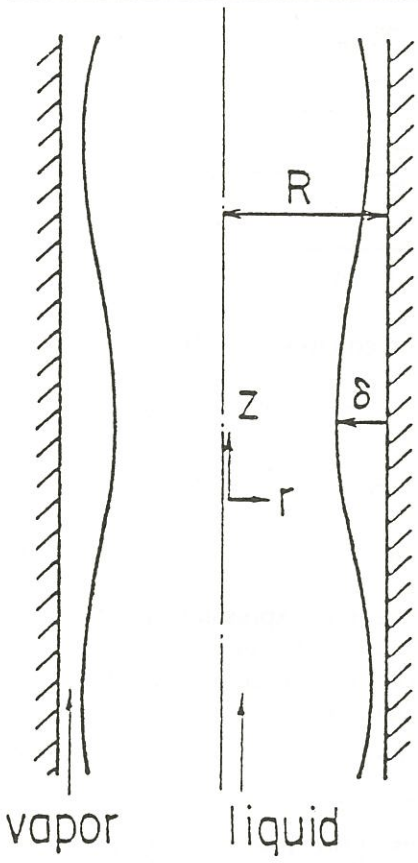

Figure 3 Schematic of inverted annular flow.

Inverted annular flows similar to the schematic in Figure 3 often occur during reflood and rewetting of vertical tubes. The wall may be thought of as being very hot, and a film of vapor is generated that prevents the liquid from wetting the wall. The vapor-liquid interface is wavy, and this enhances heat transfer compared to condensation through a uniform laminar vapor film. To model such a situation, the pressure difference between the phases due to surface tension must be incorporated into the momentum equations. The momentum equation for the liquid then becomes (dropping the averaging signs)

$$\rho_2\alpha_2\frac{\partial u_2}{\partial t}+\rho_2 u_2\alpha_2\frac{\partial u_2}{\partial z}+\alpha_2\frac{\partial p_1}{\partial z}-\frac{\sigma}{2R\sqrt{\alpha_2}}\frac{\partial\alpha_2}{\partial z}-\frac{\sigma R\sqrt{\alpha_2}}{2}\frac{\partial^3\alpha_2}{dz^3}=$$

algebraic terms that do not affect phase speed. (22)

Note that the reference pressure is ρ_1, i.e., the pressure in the vapor; σ is the surface tension; R is the tube radius; and we have assumed distribution coefficients ~1.0.

If a linear stability analysis is performed for the conservation equations, assuming the phases are incompressible, we find the phase speed is real if

$$(u_1-u_2)\le\left[\frac{k^2\sigma R}{2\sqrt{\alpha_2}}-\frac{\sigma}{2R\alpha_2^{3/2}}\left(\frac{\alpha_1}{\rho_1}+\frac{\alpha_2}{\rho_2}\right)\right]^{1/2}, \tag{23}$$

where k is wave number.

Interfacial mass transfer has only a weak effect on this criterion. In particular, the short wavelengths (large k) are stable even at very high velocity differences between phases.

The length of the most unstable waves can be found by seeking the maximum growth factor. Kawaji and Banerjee (1986) show that this wavelength is given by

$$\alpha=\frac{2\pi_2^{1/4}(\sigma R)^{1/2}}{\left[\dfrac{\alpha_2\rho_2\rho_1(u_1-u_2)^2}{\alpha_1\rho_2+\alpha_2\rho_1}+\left[\dfrac{\sigma}{2R\sqrt{\alpha_2}}\right]\right]^{1/2}}. \tag{24}$$

As shown in Figure 4, this result compares extremely well with the experimental data of De Jarlais (1983).

Dispersed Bubbly Flows

While the multifield model may be expected to predict separated flows with accuracy, its application to more closely coupled flows is less obvious. This is because great care has to be taken in considering forces arising out of the pressure variation over interfaces, i.e., the term involving $\Delta p'_{ki}$ on the right-hand side of (18) requires attention.

To illustrate the problem, consider forces on an assemblage of spheres spaced sufficiently far apart that interactions are weak. The situation is shown schematically in Figure 5. Let the continuous phase be incompressible, inviscid, and without circulation. Pauchon and Banerjee (1985) have shown for this case that the governing equations are of the form:

$$\frac{\partial\alpha_1}{\partial t}+u_1\frac{\partial\alpha_1}{\partial z}+\alpha_1\frac{\partial u_1}{\partial z}=0, \tag{25a}$$

$$\frac{\partial\alpha_1}{\partial t}+u_1\frac{\partial\alpha_1}{\partial z}+\alpha_1\frac{\partial u_1}{\partial z}=0, \tag{25b}$$

$$\rho_1\alpha_1\frac{D_1u_1}{Dt}+\alpha_1\frac{\partial p_1}{\partial z}=-\frac{1}{2}\rho_2\alpha_1\left(\frac{D_1u_1}{Dt}-\frac{D_2u_2}{Dt}\right), \text{ and} \tag{25c}$$

$$\rho_2\alpha_2\frac{D_2u_2}{Dt}+\alpha_2\frac{\partial p_2}{\partial z}=\Delta p_{2i}\frac{\partial\alpha_2}{\partial z}+\frac{1}{2}\rho_2\alpha_1\left(\frac{D_1u_1}{Dt}-\frac{D_2u_2}{Dt}\right), \tag{25d}$$

where

$$\Delta p_{2i}=-\frac{1}{4}\rho_2(u_1-u_2)^2 \tag{25e}$$

and $\Delta p_{1i}=0$.

The material derivative $D_k/Dt=\partial/\partial t+u_k\,\partial/\partial z$. The last term on the right-hand side of (25c) and (25d) arises from the accelerations of the continuous and dispersed phases and is sometimes called the 'virtual mass' term. The first term on the right-hand side of (25d) arises from the difference between the average continuous phase pressure and the average interfacial pressure. This difference is straightforward to calculate for spheres and is given in (25e). Clearly, the $\Delta p_{2i}\,\partial\alpha_2/\partial z$ term vanishes if the phase volume fraction gradients vanish; therefore it does not appear for a single sphere in a large averaging volume.

There is still considerable controversy over the form

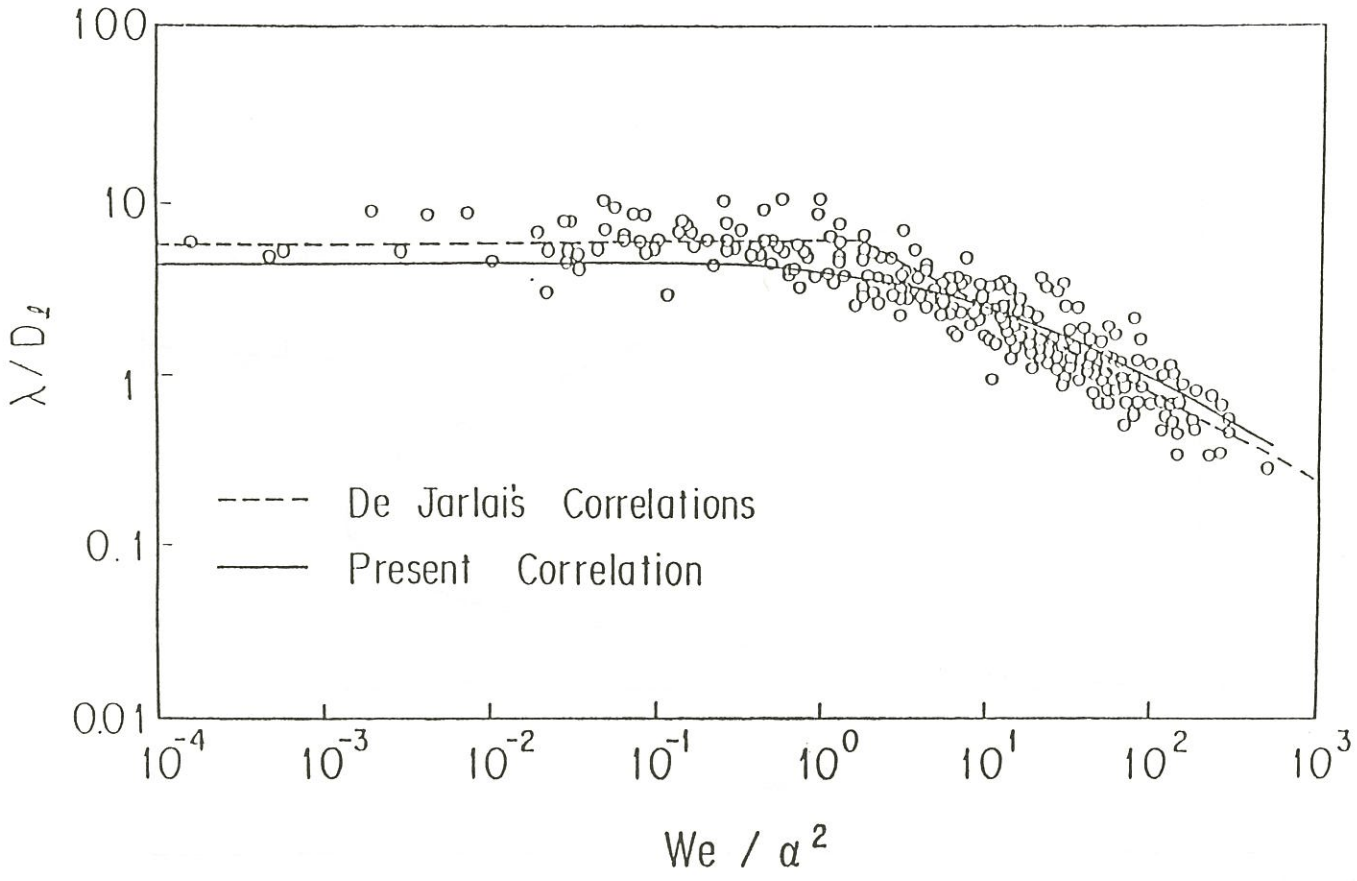

Figure 4 Comparison of predictions with De Jarlais' data.

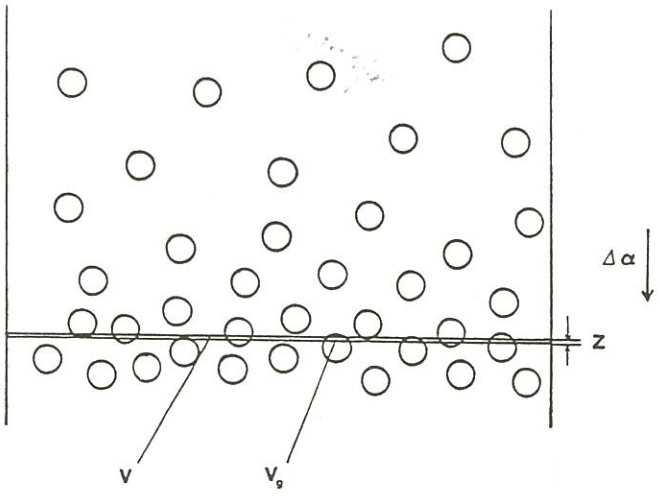

Figure 5 Schematic of bubbly flow showing averaging volume.

of (25c) and (25d). Drew *et al.* (1979) suggest that the acceleration should be 'objective' and the virtual mass term should then contain an additional derivative of the form $(u_1 - u_2)\,\partial/\partial z\,(u_1 - u_2)$. We are not as yet certain whether (25c) and (25d) are correct or Drew *et al.*'s form is correct. In any case, we will proceed to study the stability of the system (25a)–(25e).

Pauchon and Banerjee (1985) have shown that the characteristics for (25) with $\rho_1 \ll \rho_2$ are

$$\lambda^* = \frac{\alpha_2}{2 + 4\alpha_1\alpha_2} + \sqrt{\Delta}/(1 + 2\alpha_1\alpha_2), \tag{26}$$

where

$$\lambda^* = \frac{\lambda - u_2}{u_1 - u_2}$$

and

$$\Delta = \frac{\alpha_2^2}{4} - \alpha_1\alpha_2\left(\frac{1}{2} + \alpha_1\alpha_2\right).$$

These characteristics give the void propagation velocity and are wholly real for

$$\alpha_1 \lesssim 0.26. \tag{27}$$

The model, therefore, predicts a transition to a qualitatively different flow regime when $\alpha_1 > 0.26$. This is approximate because the coefficient for the virtual mass term and Δp_{2i} is based on an assembly of non-interacting spheres of constant radius. As the phase volume fraction increases, interactions increase, and some modification to the criterion may be expected, i.e., the

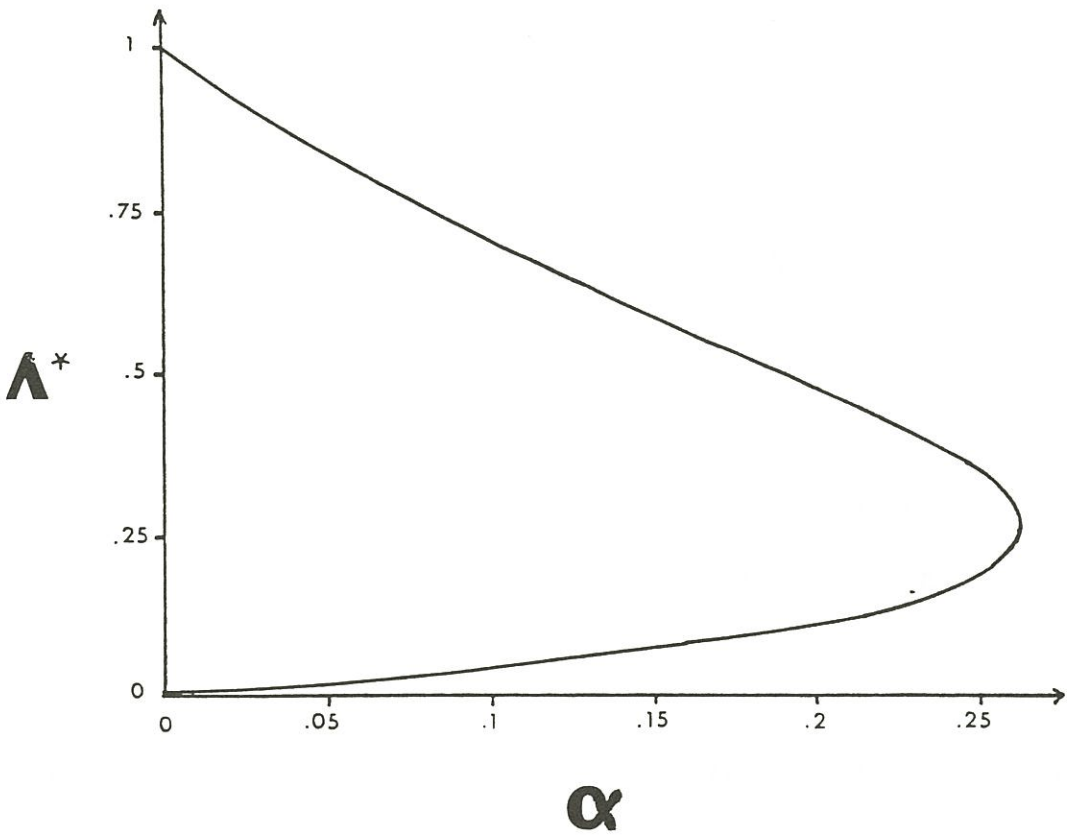

Figure 6 Plot of the non-dimensional characteristic velocity against void fraction.

transition is probably slightly wrong. The solution for λ^* given in (26) is plotted in Figure 6. The void propagation velocities lie between velocities for the continuous and dispersed phase. Therefore, measurement of void propagation (say, by cross-correlation techniques) does not give the velocity of either phase. To determine whether the model is correct, comparisons have been made with the data of Bernier (1981) and Pauchon and Banerjee (1985). Plots of the predictions and experimental data are shown in Figures 7 and 8. It is evident that the agreement is quite excellent even at relatively high gas velocities. This is an indication that the main features of the model are correct even when the phases are closely coupled.

Dispersed Droplet Flow

A similar analysis, as for dispersed bubbly flow, can be performed for droplet flow, but a fifth equation is needed to complete the system of equations, since an additional dependent variable R_d has to be introduced to the system through the pressure difference term. In terms of this added variable, the liquid volume fraction can be expressed as follows:

$$\alpha_l = \frac{4}{3}\pi R_d^3 n,$$

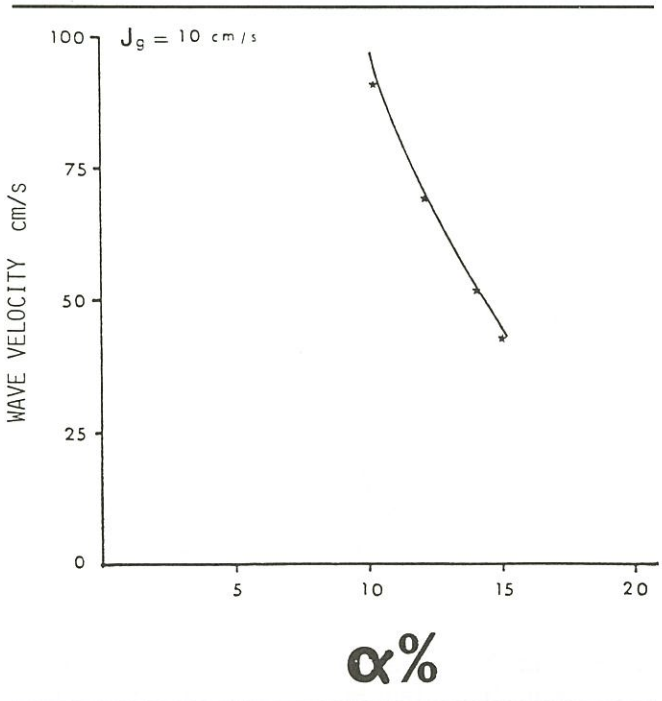

Figure 7 Void propagation velocity-predictions compared with data of Pauchon and Banerjee (1985). The liquid superficial velocity is $0.0884 \leq j_2 \leq 0.765$ m / s.

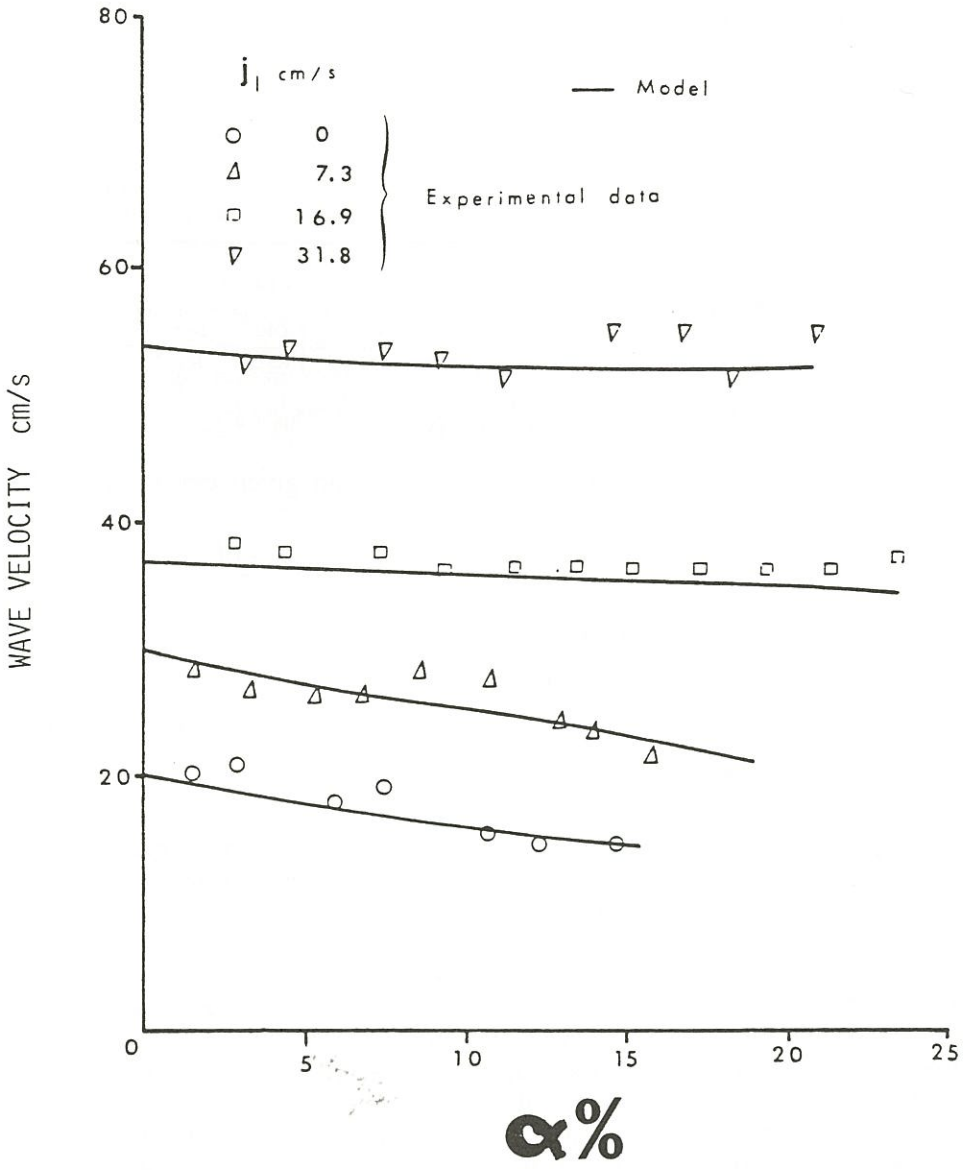

Figure 8 Predictions of void propagation velocity compared with Bernier (1981) data with $0 \leq j_2 \leq 0.318$ m / s.

where n = number density of drops. As the drops travel along the flow channel, both n and R_d change, resulting in net variation of α_l. Note that we subscript with l for liquid, v for vapor, and d for droplet in this section to distinguish the results from the previous one.

In the present analysis, the variables n and R_d are used instead of α_l as the fourth and fifth dependent variables, in addition to U_l, U_c, and P_v. To complete the hydraulic equation system, however, a fifth equation is necessary. For this, we consider a simple problem of the behaviour of a droplet of radius R_d subjected to a gas stream with a relative velocity U_r. For such a droplet, the external pressures at the forward and rear stagnation points ($\tau = 0$ and π, respectively) and at the equator ($\theta = \pi/2$) are given, respectively, by the following equations

$$P_{vi}(\theta = 0 \text{ or } \pi) = P_v + \frac{1}{2}\rho_v U_r^2; \tag{28}$$

$$P_{vi}(\theta = \pi/2) = P_v - \frac{5}{8}\rho_v U_r^2. \tag{29}$$

Due to this external pressure difference, the droplet is expected to be pressed at stagnation points, deforming into an oblate spheroidal shape, which is an ellipsoid formed by rotating an ellipse about its minor axis. Unless the droplet breaks up, these forces tending to deform the droplet are balanced by surface tension, which tends to restore a spherical shape. Photographic observations of liquid drops, either suddenly intro-

duced into an air stream [Haas (1976)] or moving at a steady speed [Ryan (1976)] show clearly that the drops become flattened and spheroidal in shape. Ryan's experiments involving drops of water with surfactant added to reduce surface tension further show that the degree of flattening increases with decreasing surface tension, as expected.

For the present analysis, we assume that the semi-minor and semi-major axes of the spheroid at equilibrium state are equal to a and b, respectively. Furthermore, we assume the potential flow about a sphere is still applicable and can approximate the pressure distribution on the surface of a spheroid. Then, at equilibrium, the following relationship must hold between the dynamic pressure and surface tension at the stagnation points and at the equator, respectively:

$$P_l - P_v - \frac{1}{2}\rho_v U_r^2 = \frac{2\sigma}{R_d} X^2 \tag{30}$$

and

$$P_l - P_v + \frac{5}{8}\rho_v U_r^2 = \frac{\sigma}{R_d}(X^{1/2} + X^{-5/2}), \tag{31}$$

where $X = a/R_d$ (shape factor). Subtracting equation (30) from (31), and rearranging, we obtain the following equation describing the degree of flattening the droplet is subjected to in order to balance the forces originating from the dynamic pressure of the vapor phases:

$$We = \frac{\rho_v U_r 2R_d}{\sigma} = \frac{16}{9}(X^{1/2} + X^{-5/2} - 2X^2). \tag{32}$$

A non-dimensional parameter appearing on the left-hand side of equation (32) is identified to be the Weber number defined in terms of the droplet's mean diameter and relative velocity. As the relative velocity, or Weber number, is increased, the droplet is predicted to become more flattened in shape, as expected from physical intuition. The use of pressure distribution for the potential flow about a sphere rather than a spheroid tends to overestimate the degree of flattening for a given Weber number; however, we adopt the present approach to simplify the analysis. If a more accurate description is desired, an analytical solution for potential flow about an oblate spheroid should be used instead.

To obtain the fifth equation necessary for the stability analysis, we assume that the shape factor remains constant and differentiate equation (32) with respect to z (or t). The following equation is obtained to complete the equation system for stability analysis:

$$\frac{2}{U_r}\frac{dU_r}{dz} + \frac{1}{R_d}\frac{dR_d}{dz} = 0. \tag{33}$$

Performing a similar analysis as described for the inverted annular flow, the following dispersion relation for the droplet flow is obtained

Table 1: Critical Weber Number for Various Density Ratios and Void Fractions

	α_v					
l_l/l_v	*0.3*	*0.5*	*0.7*	*0.9*	*0.95*	*1.0*
10	20.95	10.75	8.96	8.23	8.11	8.0
100	19.22	10.68	8.96	8.23	8.11	8.0
1000	19.22	10.67	8.96	8.23	8.11	8.0

$$\left(\frac{\omega}{k}\right) = \frac{\rho_l U_l + {}_c\rho_v U - 4\sigma/R_d U_r}{\rho_l + \rho_v} = \left[\frac{64\sigma^2}{R_d^2 U_r^2} + \frac{16\sigma}{R_d}(\rho_l - \rho_v) + \rho_v U_r^2\left(\frac{\alpha_l}{\alpha_v}(\rho_l + \rho_v) - 4\rho_l\right)\right]^{1/2} / 2(\rho_l + \rho_v). \tag{34}$$

For stability, the condition given below has to be satisfied:

$$We < \frac{16(\beta - 1) \pm 16[(\beta + 1 - \alpha_l/\alpha_v)(\beta + 1)]}{\beta(5 - 1/\alpha_v) - 1/\alpha_v + 1}, \tag{35}$$

where

$$\beta = \rho_l/\rho_v. \tag{36}$$

We first note that in the limit $\alpha_v = 1.0$, equation (34) simplifies to

$$We < 8. \tag{37}$$

The stability criterion obtained above implies breakup of drops for a given dispersed flow system when the Weber number, defined by equation (32), exceeds a critical value.

For various density ratios and void fractions, the values of the critical Weber number predicted by equation (34) are tabulated in Table 1. The effect of density ratio is small. As void fraction is decreased from unity, the critical Weber number is predicted to increase gradually. The validity of this predicted behaviour is not clear at present due to the lack of experimental data concerning the breakup of drops in a confined flow channel.

An infinitely large critical Weber number is obtained as void fraction decreases to a value of 0.2. In reality, however, dispersed flow usually exists for void fractions greater than about 0.8. At lower values, droplet coalescence, collision, and breakup processes will be important, and the present analysis no longer applicable. It is also noted here that the present analysis is limited to the well-established dispersed flow, for example, in regions well downstream of the inverted annular flow in reflooding of a hot vertical tube. The assumption of potential flow about a sphere has limited validity in the transition region, where the liquid core in inverted annular flow destabilizes and breaks up into slugs, ligaments, and various large and small droplets. In this region, the mechanisms responsible for droplet breakup may be quite different from those relevant to well-developed dispersed flow with high

void fraction, and the situations of droplet breakup in a free gas stream are discussed below.

The breakup of drops of a free gas stream has been investigated in the past, both experimentally and theoretically. For cases where the inertial force and surface tension dominate the viscous effects, the droplet breakup can be specified by a critical Weber number [Hinze (1955)]. Hinze (1948) suggested further that the value of the critical Weber number should depend on the rate of droplet acceleration with respect to the gas stream. Various cases have been investigated in the past, ranging from a drop suddenly exposed to a high-velocity gas stream to that of a drop moving in a gas stream at a terminal speed. For these two extreme cases, Hinze (1955) recommends critical Weber numbers of 13 and 22, respectively.

The experimental data of Haas (1976) for the breakup of mercury drops in air indicate a critical value of 10, while Hanson *et al.* (1963) obtained values ranging from 7 to 17 for the breakup of water and methyl alcohol drops by air blast. On the other hand, the experimental data of Lane (1951) and Ryan (1976), involving a water drop placed in a vertical wind tunnel and held stationary by an upward flow of air, indicate critical values of 10 and 12, respectively. Wallis (1974) suggests that a drop moving in an infinite medium at its terminal speed will break up at a critical Weber number equal to 8, in agreement with equation (37). Kataoka *et al.* (1983) also suggests a critical Weber number of 8–17 for a large drop falling at its terminal speed.

The stability criterion derived from the present analysis is consistent with the available data on droplet breakup in a gas stream. Furthermore, Ryan's data (1976) indicate that the degree of maximum flattening before breakup, defined by the ratio a/b, is nearly constant at a value of 0.4 for drops of varying surface tension, and maximum equivalent spherical diameter between 4.4 mm and 9.1 mm. The limiting value of a/b equal to 0.4 corresponds to the shape factor a/R_d of 0.54 and, from equation (32), the Weber number of 8.4, which is also close to the critical value found in the present stability analysis.

If the ΔP_{vi} term is neglected in the above analysis, then the stability condition expressed by equation (37) is obtained for all void fractions and density ratios. This shows that the ΔP_{vi} term accounting for the nonuniformity of the interfacial pressure distribution tends to enhance the stability of the dispersed flow system, a result consistent with that reported by Pauchon and Banerjee (1986).

Rewetting of Horizontal Channels

The preceding methodology can be applied to the study of rewetting and refilling of a horizontal tube. The details are given in Chan and Banerjee (1981a, b, c).

Consider the flow situation shown in Figure 9. We

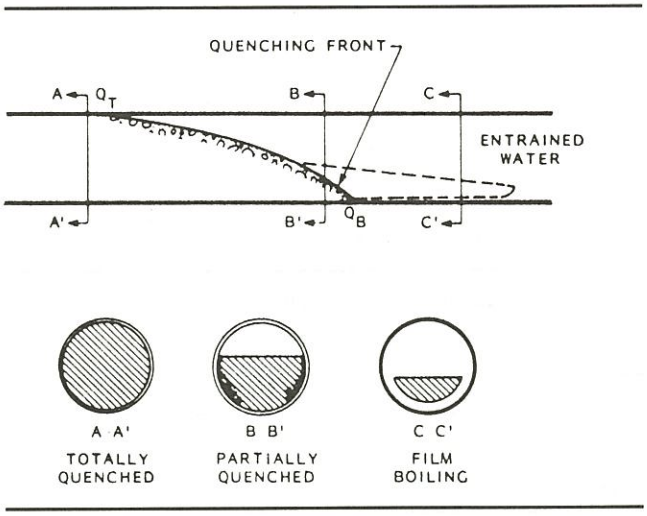

Figure 9 Characteristics of horizontal channel rewetting.

can write sets of conservation equations for the liquid and the vapor, i.e., a 2-field model. This ignores bubbles in the liquid and droplets in the vapor, but appears to be a reasonable assumption for subcooled conditions at the quench front.

The mass and momentum conservation equations may then be phrased as

$$\frac{\partial \bar{U}}{\partial t} + \bar{A}\frac{\partial \bar{U}}{\partial z} = \bar{E}, \tag{38}$$

where

$$U = \begin{bmatrix} h_L \\ U_L \end{bmatrix}, \quad A = \begin{bmatrix} U_L & y_h \\ g & U_L \end{bmatrix}, \quad E = \begin{bmatrix} E_1 \\ E_2 \end{bmatrix},$$

and U_L is the liquid velocity, h_L is the height of liquid in the pipe, g is gravitational acceleration, $y_H = \alpha_L/(\partial\alpha_L/\partial\alpha_L)$, α_L is the fraction of the cross-sectional area occupied by the liquid, and E_1 and E_2 are terms involving wall and interfacial friction, vaporization rate, and gas phase inertia.

Some simplifications have gone into deriving these equations, and these are discussed in more detail in Chan and Banerjee (1981b). The bulk liquid temperature, T_L, is given by the energy balance

$$\frac{\partial(\alpha_L T_L)}{\partial t} + \frac{\partial}{\partial z}(\alpha_L U_L T_L) = \left(\frac{1}{\rho C}\right)\left[k_L \frac{\partial}{\partial z}\left(\alpha \frac{\partial T_L}{\partial z}\right) + (1-\beta)q^{111}\right], \tag{39}$$

where q^{111} is the heat flux per unit volume and depends on the mode of heat transfer; e.g., for refilling and rewetting problems, it may assume different values for the film boiling (or precursor cooling) region, and the wet (boiling or forced convection to liquid) region. Chan and Banerjee (1981c) discuss the applicable relationships in detail.

$(1-\beta)$ is the fraction of energy input that goes into

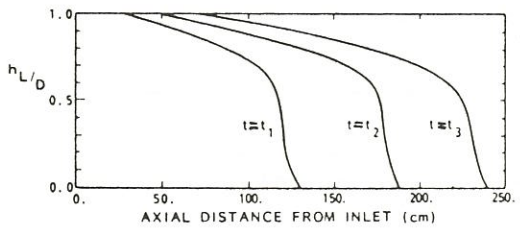

Figure 10 Propagation of refilling front.

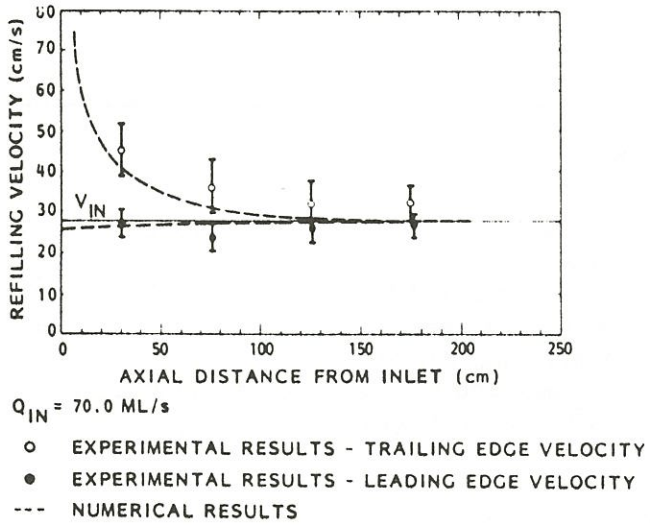

Figure 11 Refilling velocities – Q_{in} = 8–.0 ml / s.

heating the liquid phase. This is not known *a priori*, and it is necessary to make a model for energy partition to heat the liquid and cause vaporization.

The hydraulic equations (38) can be solved to determine whether the relatively simple problem of refilling a horizontal cold tube can be predicted. If the refilling process is started by suddenly opening a valve, then the refilling front propagates with the shape shown in Figure 10. Note that the leading edge propagates faster than the trailing edge. The velocity of the leading edge and trailing edge of the front are compared with experiments in Figure 11. It is clear that the theoretical predictions are in agreement with the experiments, which gives confidence in the 2-field model in (38).

If the tube is hot, so that the refilling front moves faster than the rewetting (or quench) front, as in Figure 10, then a rewetting criterion is necessary for predictions. As discussed previously, a criterion based on temperature is not satisfactory. This is because the rewetting temperature can be very different at different axial and circumferential locations. A model for rewetting has therefore been proposed by Banerjee and Chan (1981c).

The model postulates that film boiling is maintained

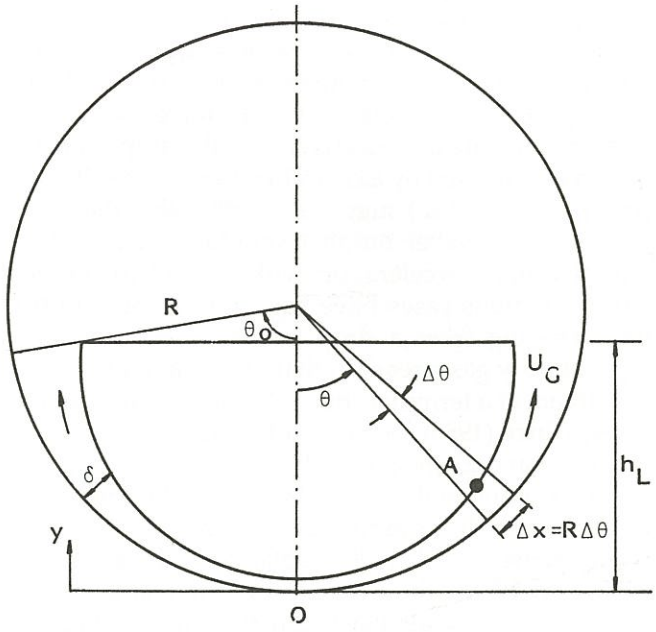

Figure 12 Film boiling model.

because the circumferential vapor flow, as shown in Figure 12, supports the liquid – much like a Hovercraft. However, as the depth of the liquid in the tube increases, the vapor velocity needed to support it also increases. At some depth, the vapor velocity may become sufficient to excite the Kelvin-Helmholtz instability, as discussed earlier. This in itself is only a necessary, but not sufficient, condition for rewetting. The sufficient condition is that the enhancement in local heat transfer due to the instability must be much larger than the conduction heat transfer from the surrounding region. Only then can the cooled regions grow rapidly, leading to rewetting. However, for a thin-walled pipe with low thermal capacitance, conduction in the wall is small. Therefore, for thin-walled pipes, onset of an interfacial instability may lead to rewetting; i.e., is both necessary and sufficient. The onset of the interfacial instability can be related to the depth of liquid through the circumferential velocity. Therefore, the rewetting criteria is phrased in terms of the depth of the liquid.

The model was tested against experimental data, and the results are shown in Figure 13. The two lines are for the first 2 modes of the instability. It is clear that the data fall between the predictions for the modes, and are largely independent of the initial wall temperature.

If this rewetting mechanism is introduced into the 2-field model, i.e., to give q^{111} in (39), then the wall temperatures can be predicted. The theoretical and experimental results are compared in Figure 10. The agreement is good, considering the complexity of the phenomena. In particular, note that the top (say, TET) rewets later than the bottom (TEB) at any location (say,

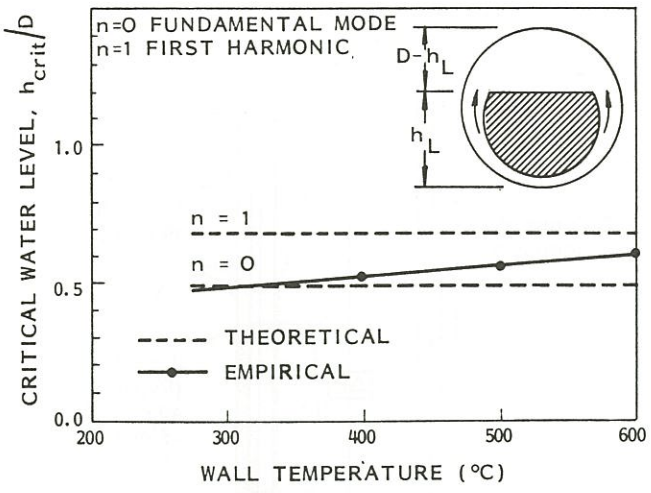

Figure 13 Comparison of theoretical and empirical water level for vapor film instability.

E). Also, the bottom shows much greater precursor cooling due to the liquid tongue and film boiling.

The theoretical rewetting velocities for different injection rates and wall temperatures are compared with

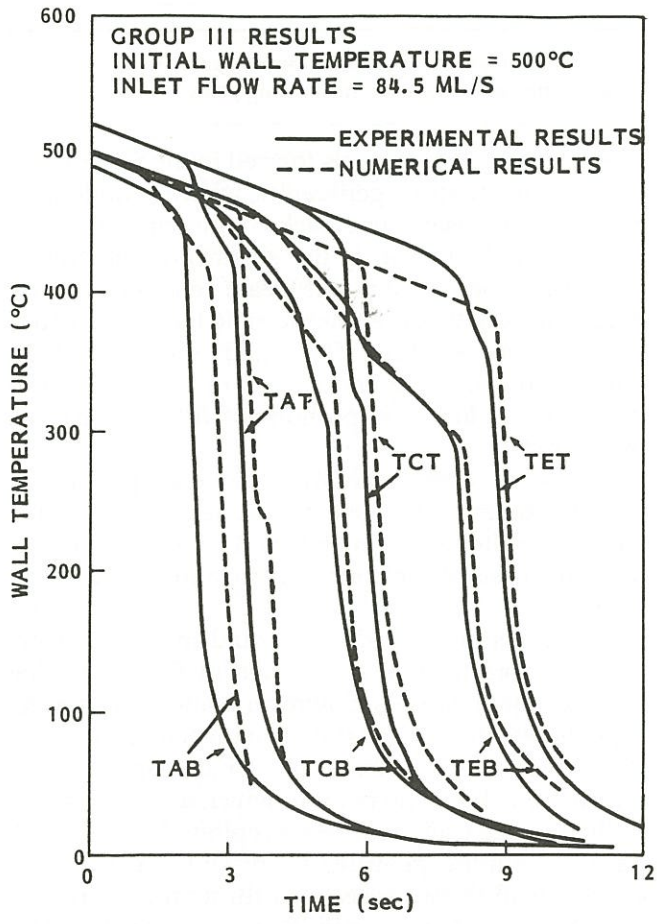

Figure 14 Transient top and bottom wall temperatures – comparison of experimental and numerical results.

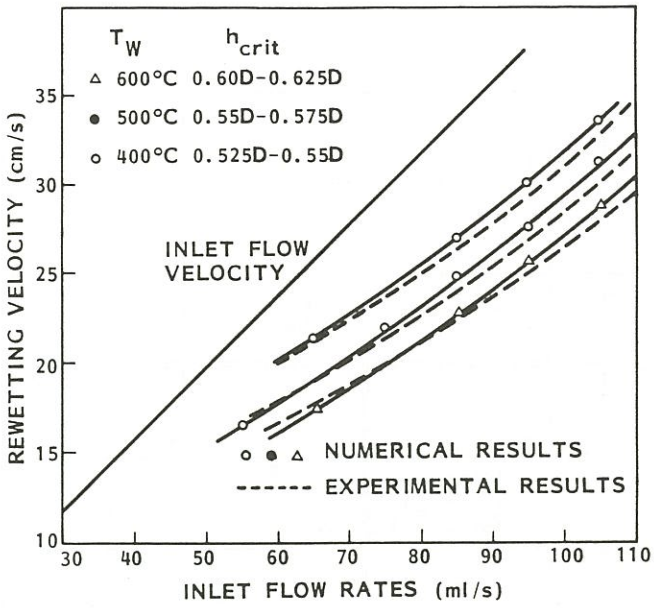

Figure 15 Average rewetting velocity versus inlet flow rate – comparison of experimental and numerical results.

data in Figure 15. Again, it is clear that the agreement is good. Note that the model does not use adjustable parameters to improve the 'fit' and is based on the simple postulate that rewetting coincides with the onset of an interfacial instability, when the wall is thin.

Limitations of the Model

The preceding discussion illustrates that the multifield model can predict a variety of phenomena without adjustment, or 'tuning,' of coefficients. It works well for both separated and closely coupled flows, provided the closure relationships or interactions between fields are developed with care, and attention is paid to the physics of the flow situation.

We turn now to the closure relationships required for forces at the wall and between fields due to viscous effects, i.e., the terms containing τ in (18), and the part of the $\Delta p'_{ki}$ time affected by viscosity – called form drag in Bird *et al.* (1960). For the multifield model these terms are written by analogy with single-phase flow, so the forces are expressed as:

$$\text{total drag (form + friction)} = -\frac{1}{8}\rho_c a_i C_D(\langle\overline{u_c}\rangle - \langle\overline{u_d}\rangle)\,|\,\langle\overline{u_c}\rangle - \langle\overline{u_d}\rangle\,|$$

for submerged objects;

$$\text{frictional drag} = -\frac{1}{2}\rho_c a_i f(\langle\overline{u_c}\rangle - \langle\overline{u_d}\rangle)\,|\,\langle\overline{u_c}\rangle - \langle\overline{u_d}\rangle\,|$$

for separated flows; and

$$\text{wall drag} = -\frac{1}{2}\rho_c a_{kw} f\langle\overline{u_c}\rangle\,|\,\langle\overline{u_c}\rangle\,|\,, \qquad (40)$$

where a_i and a_{kw} are the interfield and wall areas per unit volume, C_D is a drag coefficient, f is friction factor,

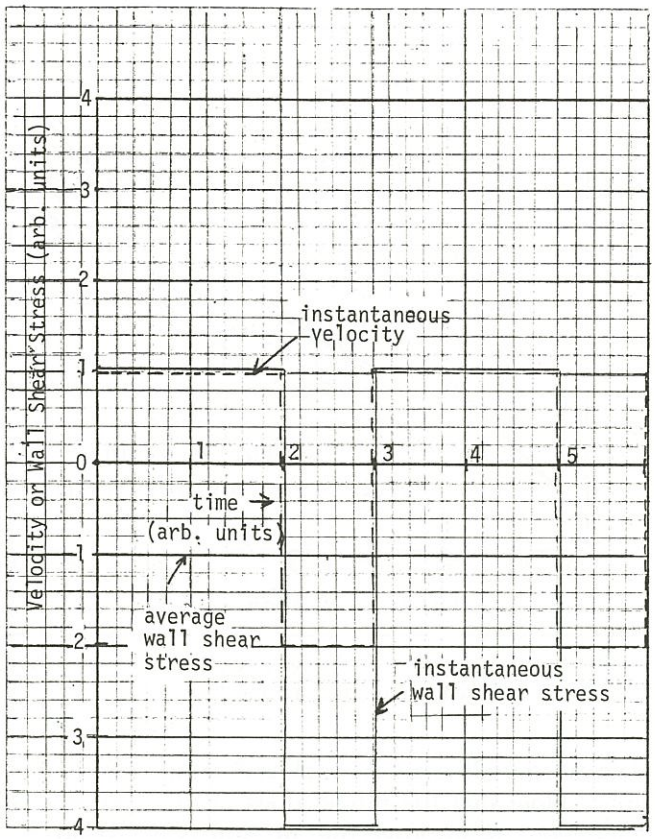

Figure 16 Schematic showing instantaneous velocity with mean velocity = 0, and instantaneous and average wall shear stress. The wall shear stress varies as the square of the velocity.

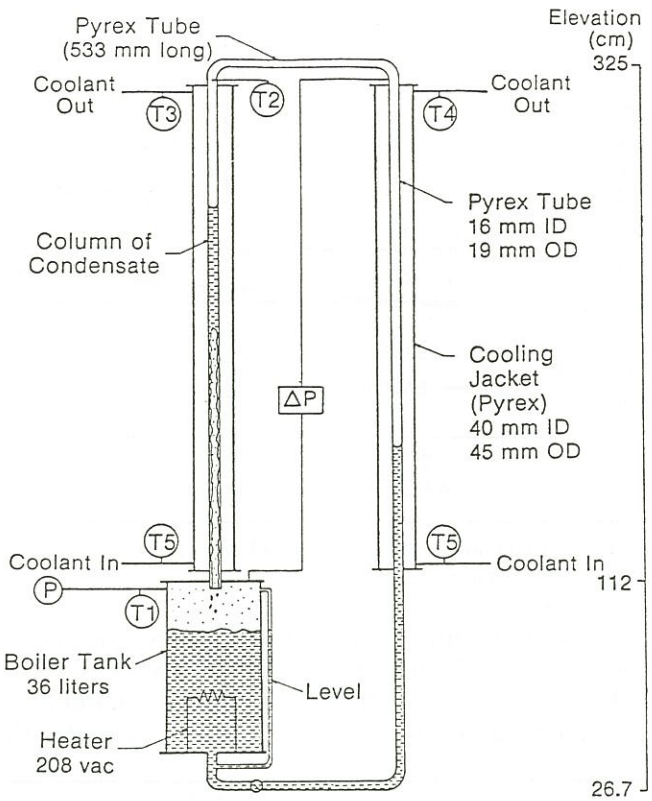

Figure 17 Schematic of experimental apparatus showing fluid distribution during refluxing near the flooding point.

and subscripts c and d denote continuous and dispersed phases, respectively. The absolute value signs are used to take flow reversal into account, so that the force points in the right direction.

For each flow regime, expressions have been developed for the unknowns in (40) [see, for example, Ransom *et al.* (1984); the TRAC-PD2 manual (1982); and Banerjee (1985)].

A difficulty arises, however, when flows are oscillatory. Consider a flow and wall shear stress history shown schematically in Figure 16. Here the time-averaged flow vanishes. However, the time-averaged wall shear stress does not because it is proportional to the sphere of the velocity. Thus expressions like (40) do not predict wall (or interfacial shear stress) in such situations.

To illustrate this, some data on flux condensation is presented. The physical situation for refluxing near the flooding point is shown in Figure 12. Vapor flow is introduced at the bottom of a vertical pipe, flows upwards, and condenses. The liquid, on the average, runs downward countercurrent to the vapor flow.

This situation is of importance in assessing small break accidents in pressurized water reactors. A scenario which has been observed in experiments is shown in Figure 18. Here, steam is formed in the reactor core and flows to the steam generators, where it condenses, and the condensate runs back countercurrent to the steam flow. However, if the steam flow is slightly above the flooding value, the steam generators do not drain completely on the riser side and liquid is held up, as shown in the figure. The liquid head exerts back pressure on the core and causes the liquid level to drop. In certain cases, portions of the core may be uncovered.

It is therefore important to predict the liquid inventory distribution in the system and, particularly, on the riser side of the steam generators. This is impossible to do on the basis of shear stress correlations of the form in (40).

To demonstrate this, data on liquid and vapor velocities and void fraction are plotted in Figure 19. The average liquid flow is downward and the average vapor flow is upward, as shown in the figure. A single-phase region exists above the condensing 2-phase region, i.e., above the point at which α goes to zero.

The average wall shear stress is plotted in Figure 20, together with the quantity $\langle u_2 \rangle | \langle u_2 \rangle |$. It is evident the average wall shear stress goes through a change in sign. The average wall shear stress, if modelled by an expression of the type in (40), would indicate that the flow at the bottom of the condenser is upward, and

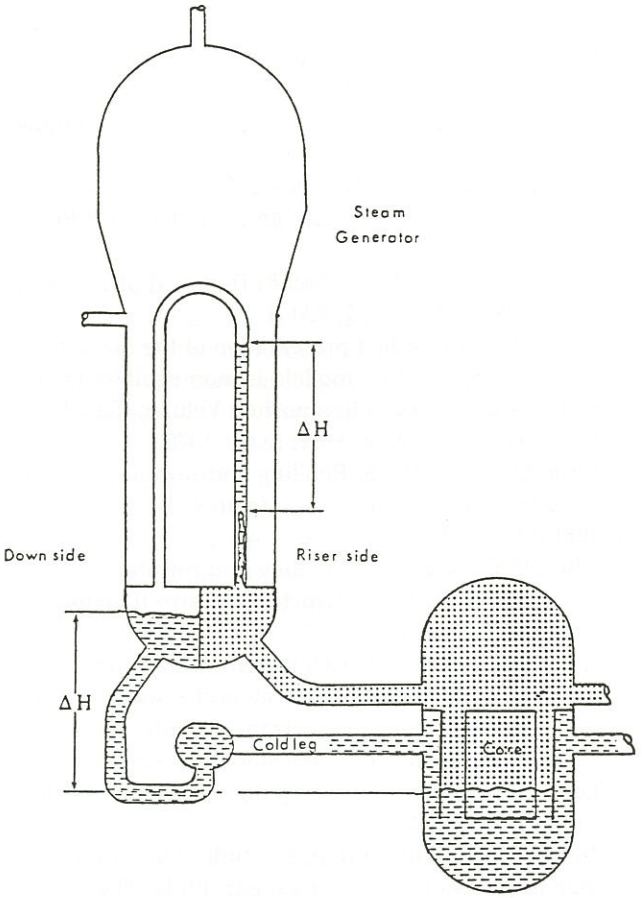

Figure 18 Small break accident scenario with steam generation rate leading to flooding during reflux condensation.

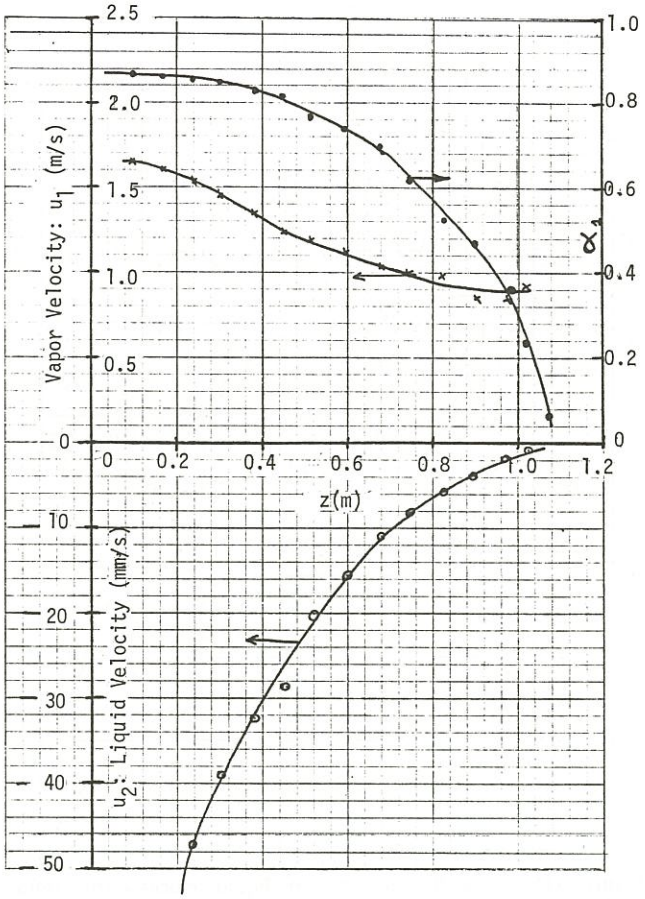

Figure 19 Data on liquid and vapor velocities and void fraction during reflux condensation near the flooding point.

downward at the top. This is at variance with the measurements. The same result is found in all the experiments we have done in this regime [see Nguyen and Banerjee (1985)]. Clearly, something is wrong with the model!

The reasons for this curious behaviour in wall shear stress may be explained qualitatively as follows: Consider the flow to be oscillatory, with large waves travelling upwards at velocities close to that of the vapor, and relatively slow downflow in the liquid film between waves. The shear stress under the waves is high because of the high-velocity upflow, whereas the wall shear stress in the draining film is low. However, as the vapor condenses, its velocity is reduced, and the wave velocity is also reduced. As a consequence, the shear stress at some point goes to zero, because the component due to upflow in the waves is exactly balanced by downflow in the film. Below this point, the wave velocity is high enough to give a negative shear stress, whereas above this point shear stress is positive. The data can be explained more quantitatively if observed values of wave frequency and velocity are used, together with appropriate velocity gradients at the wall in the wave and draining film regions.

The question, however, is to determine whether the multifield model can be modified to incorporate such phenomena. The correlations required for wall and interfacial shear stress in the slug / churn would clearly have to be quite different from (40).

A method to deal with problems of this nature has not yet been developed. One possibility is to divide the liquid flow into 2 fields – a wave or slug field and a film field. The momentum interactions in these fields with the gas / vapor and the wall would be quite different. At present, there appears to be no information which can be obtained from the model about the division of liquid between these fields. Information on disturbance length, amplitude, and frequency is needed to proceed further, and it appears this has to be supplied to the model on the basis of experiments. However, we speculate that careful stability analysis of the model could lead to disturbance frequencies and lengths. Almost certainly this analysis would have to take some non-linear effects into account.

In summary, then, the multifield model successfully captures many subtle phenomena in 2-phase flows, where oscillations are small compared to the mean flow. However, in regimes where the oscillations are

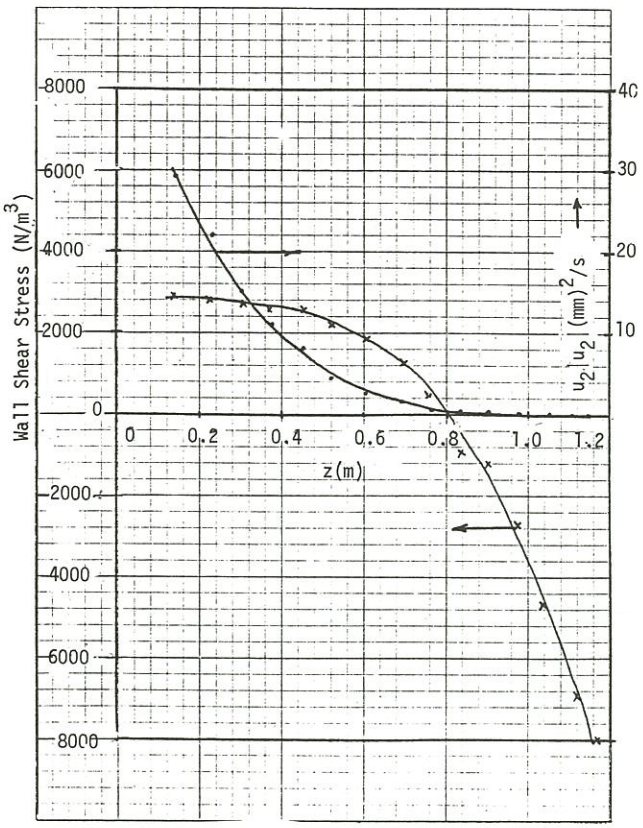

Figure 20 Data on wall shear stress and liquid velocity during reflux condensation showing that the wall shear stress is not proportional to the square of the mean velocity.

much larger, the model is more difficult to apply. The difficulty lies in determining the correct closure relationships. If the present framework for closure relationships is used, then the limitations are clear – experimental measurements on wall and interface momentum interactions cannot be predicted for intermittent flows.

Acknowledgements

This paper was originally presented at the Second International Conference on Simulation Methods in Nuclear Engineering, Montreal, 14–16 October 1986.

References

1. *Agee LJ, Banerjee S, Duffey RB, Hughes ED.* Some aspects of two fluid models and their numerical solutions. Second OECD Specialists Meeting on Transient Two Phase Flow 1978; 1: 27–58.
2. *Ahmed R, Banerjee S.* Finite amplitude waves in stratified two-phase flow: transition to slug flow. AIChE J 1985; 31: 1480–7.
3. *Ardron KH.* One-dimensional two-fluid equations for horizontal stratified two-phase flow. Int J Multiphase Flow 1980; 6: 295–304.
4. *Banerjee S, Chan AMC.* Separated flow model. I. Analysis of the averaged and local instantaneous formulations. Int J Multiphase Flow 1980; 6: 1–24.
5. *Banerjee S.* Separated flow models. II. Higher order dispersion effects in the averaged formulation. Int J Multiphase Flow 1980; 6: 241–8.
6. *Banerjee S.* Closure relationships and constitutive equations. Lecture presented at Two-Phase Flow Short Course, ETH-Zurich, March 1985.
7. *Bernier RJ.* Unsteady two-phase flow instrumentation and measurement. Cal Tech, Engr Appl Sci Div, Report No. E200.4, 1981.
8. *Bird RB, Stewart WE, Lightfoot E.* Transport phenomena. John Wiley, 1960: 191–2, 220–1.
9. *Boure JA.* On a unified presentation of the non-equilibrium two phase flow models in non-equilibrium two phase flows. *In*: ASME Symposium Volume, Eds. Lahey RT, Jr, Wallis GB. New York: ASME, 1975.
10. *Chan AMC, Banerjee S.* Refilling and rewetting of a hot horizontal tube. Part I. Experiments. J Heat Transfer 1981a; 103: 281–6.
11. *Chan AMC, Banerjee S.* Refilling and rewetting of a hot horizontal tube. Part II. Structure of a two-fluid model. J Heat Transfer 1981b; 103: 287–92.
12. *Chan AMC, Banerjee S.* Refilling and rewetting of a hot horizontal tube. Part III. Application of a two-fluid model to analyze rewetting. J Heat Transfer 1981c; 103: 653–9.
13. *De Jarlais G.* An experimental study of inverted annular flow hydrodynamics utilizing an adiabatic simulation. NUREG / CR-3339, 1983.
14. *Delhaye DA.* Contribution à l'étude des écoulements diphasiques eau-air et eau-vapeur. Ph.D. Thesis, University of Grenoble, 1970.
15. *Delhaye JM, Achard JL.* On the averaging operators introduced in two phase flow modeling. Proc CSNI Specialists Meeting in Transient Two Phase Flow. Eds. Banerjee S, Weaver KR. Toronto, Aug. 3–4, 1976.
16. *Drew DA.* Average field equations for two-phase media. Studies in Applied Mathematics 1971; 1.
17. *Drew DA, Cheng L, Lahey RT, Jr.* Analysis of virtual mass effects in two phase flow. Int J Multiphase Flow 1979; 5: 233–42.
18. *Drew DA, Lahey RT, Jr.* Application of general constitutive principles to the derivation of multidimensional two phase flow equations. Int J Multiphase Flow 1979; 5: 243–64.
19. *Drew DA.* Mathematical modelling of two phase flow. Ann Rev Fluid Mech 1983; 15: 261–91.
20. *Haas FC.* Stability of droplets suddenly exposed to a high velocity gas stream. AIChE J 1976; 10: 920–4.
21. *Hanson AR, Domich EG, Adams HS.* Shock tube investigation of the breakup of drops by air blasts. Physics of Fluids 1963; 6: 1070–80.
22. *Hinze JO.* Critical speeds and sites of liquid globules. Appl Sci Res 1948; A1: 273–88.
23. *Hinze JO.* Fundamentals of the hydrodynamic mechanism of splitting in dispersion process. AIChE J 1953; 1: 289–95.
24. *Hughes ED, Lyczkowski RW, McFadden Niederauer GF.* An evaluation of state of the art two velocity two phase flow

models and their applicability to nuclear reactor transient analysis. EPRI Report NP143, 1976; 1, 2, 3.
25. *Ishii M.* Thermally induced flow instabilities in two-phase mixtures in thermal equilibrium. Ph.D. Thesis, Georgia Institute of Technology, 1971.
26. *Ishii M.* Thermo-fluid dynamic theory of two phase flow. Paris: Byrolles, 1975.
27. *Kataoka I, Ishii M, Mishima K.* Generation and size distribution of droplets in annular two-phase flow. ASME J Fluids Engr 1983; 105: 230–8.
28. *Kawaji M, Banerjee S.* Application of a two-field model to reflooding of a hot vertical tube. I. Model structure and interfacial phenomena. J Heat Transfer 1987; 109: 204–11.
29. *Kocamutafaogullari G.* Thermo-fluid dynamics of separated two-phase flow. Ph.D. Thesis, Georgia Institute of Technology, 1971.
30. *Lahey RT, Jr, Cheng L, Drew D, Flaherty J.* The effect of virtual mass on the numerical stability of accelerating two phase flow. Int J Multiphase Flow 1980; 6: 281–94.
31. *Lane WR.* Shatter of drops in streams of air. Ind Eng Chem 1951; 43: 1312–7.
32. *Lyckowski RW.* Theoretical bases of the drift flux field equations and vapor drift velocity. Proc 6th Int Heat Transfer Conf Washington: Hemisphere Press, 1978; 1: 339–44.
33. *Nguyen Q, Banerjee S.* Interfacial heat and momentum transfer for condensation in vertical tubes. Paper presented at AIChE annual meeting, Chicago, 1985.
34. *Nigmatulin RI.* Averaging in mathematical modeling of heterogeneous and dispersed mixtures. Paper presented at International Center for Heat and Mass Transfer Symposium, Yugoslavia, 1978.
35. *Nigmatulin RI.* Spatial averaging in the mechanics of heterogeneous and dispersed systems. Int J Multiphase Flow 1979; 5: 353–85.
36. *Panton RJ.* Flow properties for the continuum viewpoint of a nonequilibrium gas particle mixture. J Fluid Mech 1978; 31: 273–303.
37. *Pauchon C, Banerjee S.* Interphase momentum interaction effects in the averaged multifield model. I. Void propagation in bubbly flows. Int J Multiphase Flow 1986; 12: 559–73.
38. *Ramshaw JD, Trapp JA.* Characteristics, stability, and short wavelength phenomena in two phase flow equation systems. Nuc Sci and Engineering 1978; 66: 93–102.
39. *Ransom VH,* et al. RELAP5/MOD2 code manual. Vol. I. Code structure, system models and solution methods. EGG-SAAM-6377, 1984.
40. *Rousseau JC, Ferch RL.* A note on two-phase separated flow models. Int J Multiphase Flow 1979; 5: 489–93.
41. *Ryan RT.* The behavior of large, low-surface-tension water drops falling at terminal velocity in air. J Appl Meteor 1976; 15: 157–65.
42. *Sleicher CA.* Maximum stable drop size in turbulent flows. AIChE J 1967; 8: 471–7.
43. TRAC-PD2, an advanced best estimate computer program for PWR loss of coolant accident analysis. Los Alamos National Lab. Rept. LA-8709-MS (NUREG/CR-2054), 1981.
44. *Vernier P, Delhaye JM.* General two phase flow equation applied to the thermo-hydrodynamics of boiling water nuclear reactors. Energie Primaire 1968; 4.
45. *Wallis GB.* The terminal speed of single drops or bubbles in an infinite medium. Int J Multiphase Flow 1974; 1: 491–511.
46. *Yadigaroglu G, Lahey RT.* On the various forms of the conservation equations in two phase flow. Int J Multiphase Flow 1976; 2: 477–94.

CATHENA Simulation of Thermosiphoning in a Pressurized-Water Test Facility

J.P. Mallory
Wardrop Engineering Consultants
77 Main Street
Winnipeg, Manitoba R3C 3H1
P.J. Ingham
Atomic Energy of Canada Limited
Whiteshell Nuclear Research Establishment
Pinawa, Manitoba R0E 1L0

Abstract

Under some postulated accident conditions, decay heat is removed from a reactor core by 2-phase natural circulation or 'thermosiphoning' of the primary coolant. To assess the ability of the computer code CATHENA (Canadian Algorithm for THermalhydraulics Network Analysis, formerly ATHENA) to predict such events, simulations were performed of thermosiphoning tests conducted in the RD-14 facility at the Whiteshell Nuclear Research Establishment. Predictions for 3 test conditions are presented. Generally, the predicted behaviour agrees with the observed results. Non-oscillating 2-phase thermosiphoning, and the onset of oscillatory flow, are well predicted. Channel heater temperature behaviour is also well predicted. In some instances, the predicted oscillating period tends to be longer than that observed in the experiment, and the predicted amplitude larger than the experimental results. It is speculated that the simplified heat transfer boundary conditions, used to represent the steam generators secondary side, are mainly responsible for these discrepancies.

Résumé

Dans certaines conditions d'accidents hypothétiques, la chaleur de désintégration est évacuée du coeur d'un réacteur par la circulation naturelle à deux phases ou 'processus de thermosiphon' du caloporteur primaire. Pour évaluer la capacité du programme de calcul CATHENA (Canadian Algorithm for THErmalhydraulics Network Analysis, appelé avant ATHENA) de prédire de tels évènements, on a simulé des essais de circulation naturelle (processus de thermosiphon) effectués dans l'installation RD-14 de l'Établissement de recherches nucléaires de Whiteshell. On présente les prédictions pour trois conditions d'essais. En général, le comportement prédit correspond aux résultats observés. La prédiction de la circulation naturelle à deux phases (processus de thermosiphon) non oscillante et du début de l'écoulement oscillatoir est bonne. La prédiction du comportement thermique des réchauffeurs de canaux est bonne également. Dans certains cas, la période d'oscillation tend à être plus longue que celle observée lors des essais et l'amplitude prédite plus grande que les résultats d'essais. On suppose que les conditions aux limites simplifiées de transfert de chaleur, qui servent à représenter le circuit secondaire des générateurs de vapeur, sont les causes principales de ces différences.

Introduction

The computer code CATHENA has been developed primarily to analyze postulated loss-of-coolant accidents (LOCA) scenarios for CANDU™ nuclear reactors. Under some conditions, decay heat removal from the core is by single or 2-phase thermosiphoning. It is important to determine that decay heat can be adequately removed in this situation.

Tests were conducted in the RD-14 facility to examine the thermosiphoning flow behaviour as a function of the initial primary fluid inventory. These experiments provide data which can be used to assess the predictive capability of various thermalhydraulic codes.

In this paper, results are presented for 3 of the test conditions examined. The test facility, the experiments, and the code are described briefly. The experiments and the CATHENA simulations are discussed in more detail.

Experiments

Facility Description

Figure 1 shows a simplified flow diagram of the RD-14 thermalhydraulic test facility. The emergency coolant injection system and the blowdown lines were not used in these experiments. The facility is a

Keywords: after-heat removal, natural convection, computerized simulation.

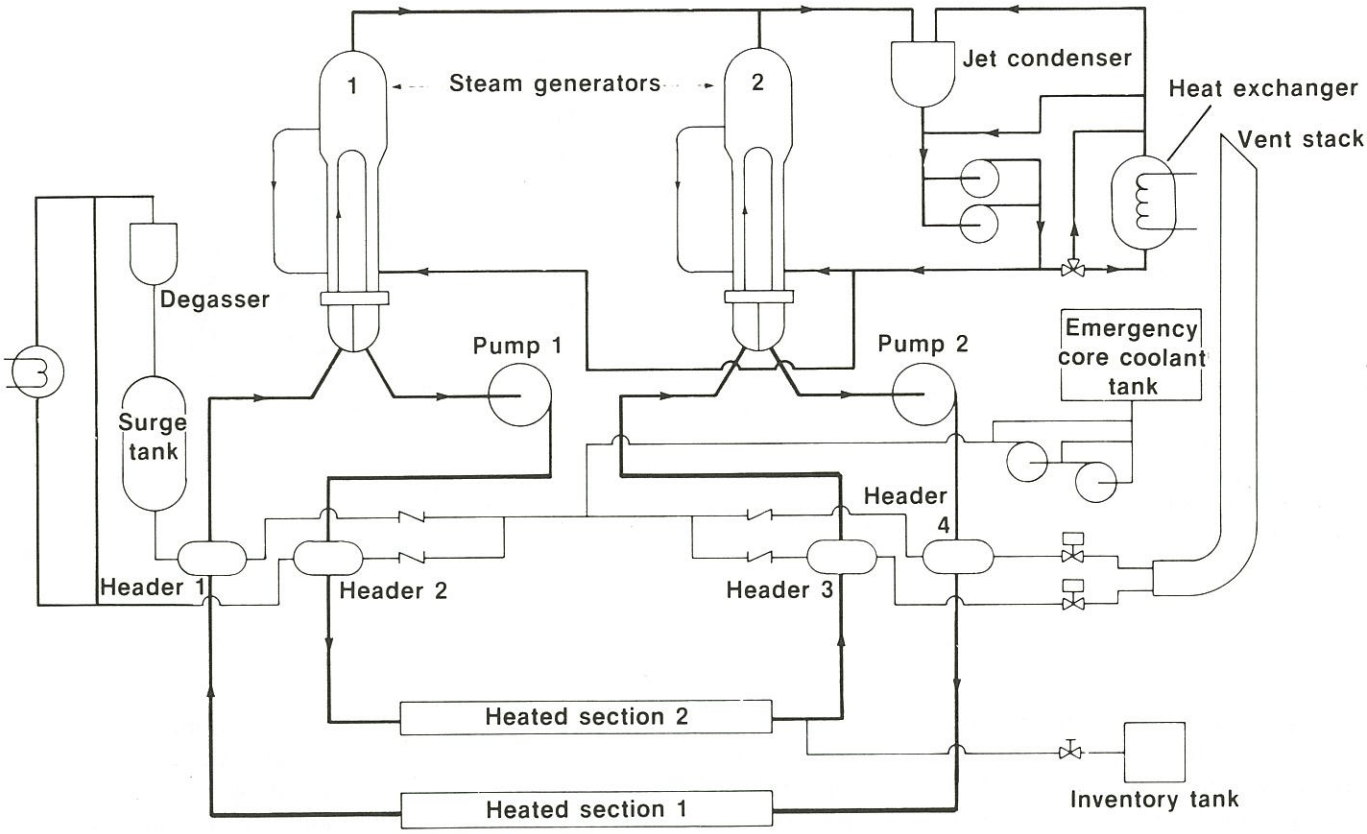

Figure 1 Schematic diagram of the RD-14 facility.

pressurized-water loop (10 MPa nominal) with the basic 'figure-of-eight' geometry of a CANDU™ reactor. It has two 6-metre-long, 5.5 MW horizontal channels, connected to end-fitting simulators representing 2 passes through a reactor core. Each channel contains 37 electrically heated fuel-element simulators of almost the same heat capacity as reactor fuel. Heat is removed from the primary circuit through 2 recirculating U-tube-type steam generators with internal pre-heaters and external downcomers. Primary fluid circulation is provided by 2 high-head centrifugal pumps, which generate channel flowrates similar to a single reactor channel.

The heated channels, steam generators, pumps, and headers are arranged to obtain a 1:1 vertical scale of a typical CANDU reactor. The steam generators are also scaled approximately 1:1 with those of a typical CANDU steam generator in terms of tube diameter, mass, and heat flux, to achieve reactor-like conditions within them. The facility is designed to produce the same fluid mass flux, transit time, pressure, and enthalpy conditions in the primary system as those in a typical reactor under both forced and natural circulation. Major loop parameters of RD-14 and a typical reactor are shown in Table 1.

Primary side pressure is controlled by a surge tank equipped with an electrical heater. Secondary side pressure is controlled by a jet condenser in which steam is condensed by contact with cold water. The cooled condensate is returned to the steam generator as feedwater.

Fluid removed from the primary circuit, for these thermosiphoning tests, is cooled and stored in an inventory tank. Level monitoring of the inventory tank provides a record of the quantity of primary fluid removed.

Loop instrumentation consists of multi-beam gamma-ray densitometers for fluid density measurements, differential and gauge pressure transducers, thermocouples, and resistance temperature detectors. Volumetric flowrates are measured using turbine flow meters.

Experimental Procedure

Before each experiment, the RD-14 facility was evacuated, filled with distilled water, degassed, and final instrument calibrations were completed. The loop was then brought to conditions of stable, single-phase, natural circulation of the primary fluid at the preselected heated section power, and primary and secondary pressures. After the pressurizer was isolated and approximately 10 seconds of steady state data collected, the experiment was begun. Two-phase conditions were induced by controlled, intermittent draining of

Table 1: Comparison of Characteristics of RD-14 with Those of a Typical CANDU Reactor

Characteristic	*RD-14*	*Typical CANDU reactor*
Operating Pressure (MPa)	10	10
Loop volume (m^3)	0.9514	57.0
Loop piping I.D. (m)	0.074	varies
Heated sections	indirect heated 37-rod bundles	nuclear fuel 37-element bundle
Length (m)	6	12 × 0.5
Rod diameter (m)	0.0131	0.0131
Flow tube diameter (m)	0.1034	0.1034
Power (kW / channel)	5500	5410
Pumps:	single-stage	single-stage
Impeller diameter (m)	0.381	0.813
Rated flow (kg / s)	24	24 (max / channel)
Rated head (m)	224	215
Specific speed	565	2000
Steam generators	recirculating U-tube	recirculating U-tube
Number of tubes	44	37 / channel
Tube diameter I.D. (m)	0.01363	0.01475
Secondary heat-transfer area (m^2)	41	32.9 / channel
Heated section-to-boiler top elevation difference (m)	21.9	21.9

primary fluid from the outlet of heated section 2 into an inventory tank. A typical draining sequence can be seen in Figure 5. In the first 5 draining operations, approximately 2% of the initial loop inventory of 0.9514 m^3 (excluding pressurizer volume) was removed. In each of the subsequent draining operations, 10% was removed. In the experiments described in this paper, intermittent draining was continued until the heater element sheath temperatures reached 600°C.

Two different secondary side pressures were chosen. The higher pressure, 4.6 MPa, is representative of reactor secondary pressure following a postulated loss-of-class-IV power event. The lower pressure, 0.2 MPa, is representative of a postulated loss-of-primary-coolant, design-basis earthquake or main steam-line break event. At each secondary side pressure, a high- and a low-power test was conducted. Two of the tests were checked for repeatability, with good results. Table 2 contains a summary of the test conditions. A more detailed discussion of the experimental results is available [Krishnan 1987].

CATHENA Simulations

Code Description

CATHENA is a 1-dimensional thermalhydraulics computer code developed at WNRE, primarily to analyze postulated loss-of-coolant accident scenarios for CANDU nuclear reactors. The code uses a non-equilibrium, 2-fluid thermalhydraulic model to describe fluid flow. Conservation equations for mass, momentum, and energy are solved for each phase (liquid and vapour). Interphase transfer of mass, momentum, and energy is handled by a set of flow-regime-dependent constitutive relations. As well, flow-regime-dependent constitutive relations for wall shear specify momentum transfer between the fluid and the pipe surfaces.

The numerical solution method used is a staggered-mesh, semi-implicit, finite-difference method that is not transit-time-limited [Hanna *et al.* 1985]. Conservation of mass is achieved using a truncation error correction technique similar to that used in RELAP5 / MOD2 [Ransom 1983]. Mass conservation is particularly important in predicting 2-phase thermosiphoning because of its sensitivity to small changes in mass inventory. As well, the length of the transients makes them vulnerable to the accumulation of small errors, to a point where the solution is adversely affected.

Heat transfer from metal surfaces is handled by a complex wall heat transfer package. A set of flow-regime-dependent constitutive relations specify energy transfer between the fluid and the pipe wall and / or fuel element surfaces. Heat transfer by conduction within the piping and fuel is modelled in the radial direction and can be modelled in the circumferential direction as well. Radiative heat transfer and the zirconium-steam reaction can also be included. Built

Table 2: Summary of Test Conditions

Heated section power (kW)	*Secondary pressure (MPa)*	*Initial primary pressure (MPa)*	*Total inventory drained*	
			(L)	*% Loop volume*
160 4.6	7.1	291	30	
80 4.6	7.1	271	30	
60 0.2	5.1	486	50	
160 0.2	5.1	583	60	

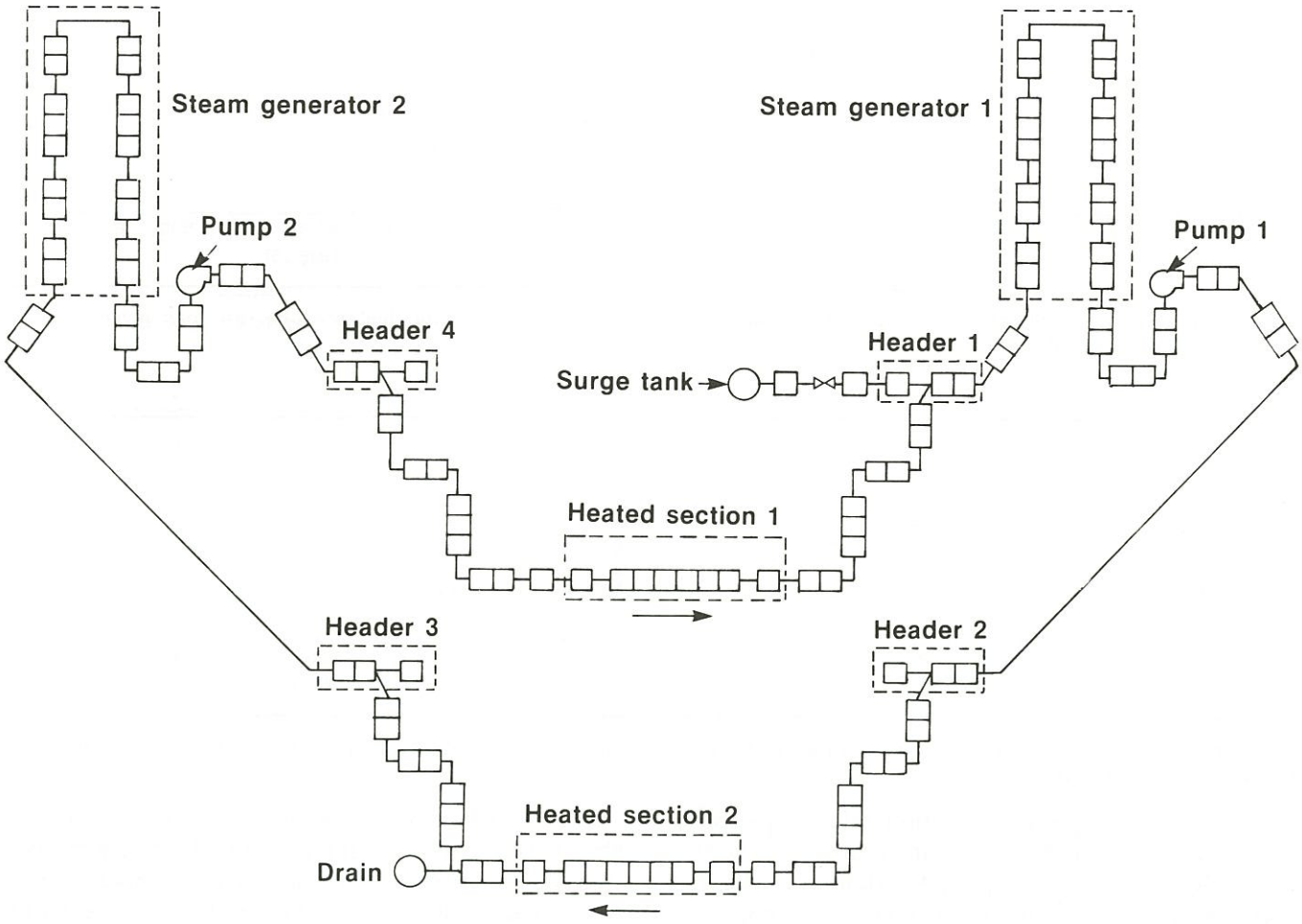

Figure 2 RD-14 primary side nodalization.

into this package is the ability to calculate heat transfer from individual groups of pins in a fuel bundle subjected to stratified flow. Under these conditions, the top pins in a bundle are exposed to steam while the bottom pins are exposed to liquid.

Component models which describe the behaviour of pumps, valves, steam separators, and discharge through breaks are available to complete the idealizations of reactor systems. A more complete description of the CATHENA code is available [Richards *et al.* 1985].

Nodalization

The nodalization used for these simulations is shown in Figure 2. A total of 130 nodes and 130 links were used to model the RD-14 facility. Modelling of the steam generators presented 2 problems which have been rectified. First, it was not clear what type of recirculation mode occurred within the steam generator secondary side. Normal full-power operation has fluid flow up the shell, with steam carried out of the top and liquid returning to the bottom of the shell via the downcomer. However, no recirculation via the external downcomer occurred, resulting in a 'kettle-like' operation of the steam generators in the tests described here. Rising 2-phase flow near the centre of the steam generators, and falling single-phase flow near the outer shell, was the probable mode of recirculation. This would have resulted in the outer tubes being exposed mainly to single-phase liquid and the inner tubes seeing a 2-phase mixture. To simplify the simulation it was assumed that all steam generator tubes experienced the same secondary side conditions of 2-phase boiling. An estimate of the heat transfer coefficient on the outer tube surfaces was made, based on detailed CATHENA steam generator simulations. All secondary side temperatures, except those in the preheater section of the steam generator, were assumed to be constant, and were set to the saturation temperature corresponding to the experimental secondary side pressure.

Second, 2 of the experiments showed evidence of unsteady feedwater flow in steam generator 2, which resulted in periodic drops in the primary fluid temperature exiting the steam generator, (see Figures 3 and 4). Since the predictions proved to be quite sensitive to these temperature drops, the boundary condition

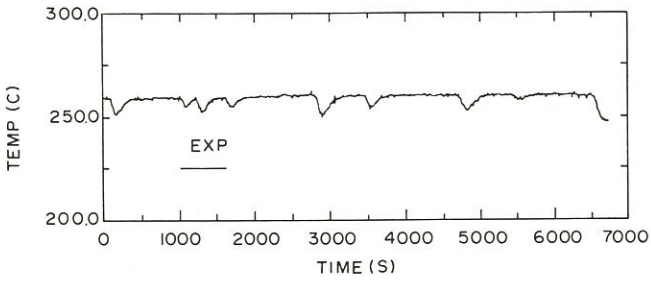

Figure 3 High-power, high-pressure case steam generator 2 – primary system outlet fluid temperature.

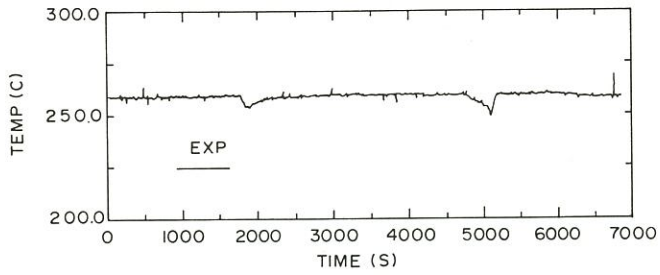

Figure 4 Low-power, high-pressure case steam generator 2 – primary system outlet fluid temperature.

temperature in the preheater section only was periodically adjusted to match the experimental observations.

Heat losses from the loop pipework to the environment were included in the analysis. Draining was simulated by an imposed intermittent flow of liquid from the outlet of heated section 2 into a boundary reservoir.

Results

The first 3 test conditions shown in Table 2 were simulated using CATHENA and are presented here. The primary loop inventory history of each test is shown at the beginning of each series of plotted results. Each fall in the level indicates a draining operation. A brief characterization of each experiment is followed by a comparison of the predicted and experimental parameters.

High-Power, High-Pressure Test

Figures 5 to 11, inclusive, show the simulation and experimental results for the high-power (160 kw / pass) and high-pressure (4.6 MPa) test. Generally this case is characterized by stable non-oscillating forward flow. Some small oscillations are evident for a brief period around 6,000 seconds. Near the end of the test, at loop inventories of about 70%, sufficient void penetrates the steam generators to cause reduced primary flow and stratification in the heated channels. The exposed top heater pins quickly heat up and trip the power on high temperature, terminating the experiment.

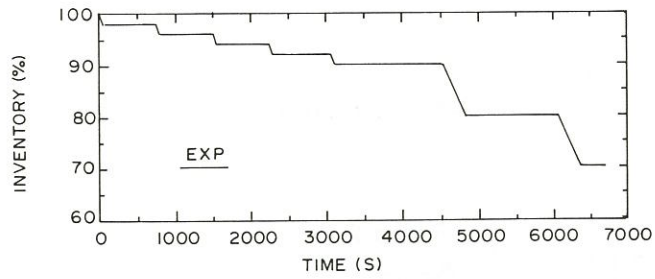

Figure 5 High-power, high-pressure case loop inventory (full 951.4 L).

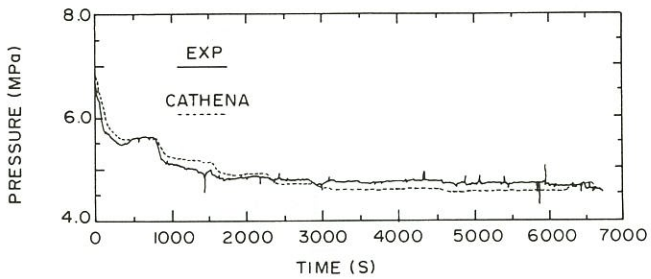

Figure 6 High-power, high-pressure case header 1 pressure.

The primary side pressure history at header 1 is shown in Figure 6. Generally, good agreement between the CATHENA simulation and the experimental results was achieved. A slight overestimation early in the transient is probably a result of small discrepancies in the initial fluid temperatures. The slight underestimation in pressure after 3,000 seconds is thought to result from overestimating the heat removal rate from the steam generators.

Figure 7 shows the volumetric flow at the inlet to test section 2. Only a slight underestimate in flow is seen until around 2,300 seconds. The prediction overestimates the primary flow beginning around 3,000 seconds. Up to this time, each draining operation has resulted in decreased system pressure and increased void. The increased void results in a higher driving

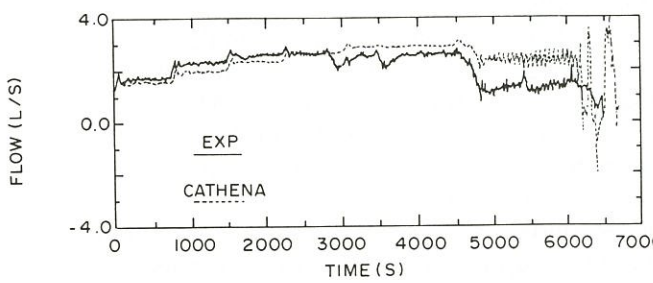

Figure 7 High-power, high-pressure case heated section 2 inlet flow.

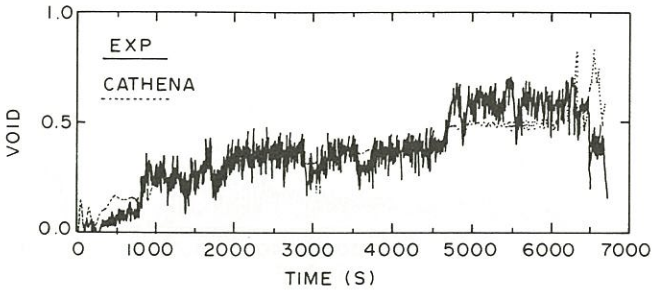

Figure 8 High-power, high-pressure case heated section 1 outlet void.

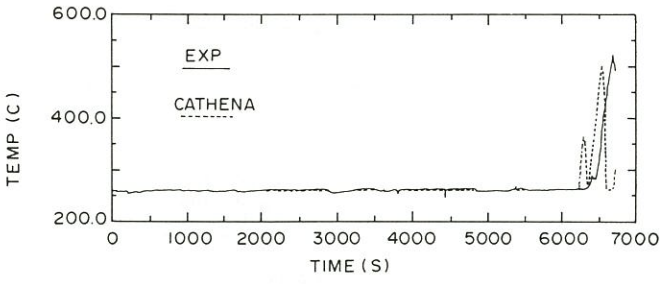

Figure 9 High-power, high-pressure case heated section 1 inlet – upper sheath temperature.

head, and therefore higher flowrates. Also, up to this time the void condensed completely in the riser side of the steam generator tubes. After 3,000 seconds, void was able to reach the top of the tubes and collect in the cold-leg side, thereby retarding the flow. An overestimate in the steam generator heat removal rate, mentioned previously, caused a delay in the timing of void carry over, resulting in the predicted flows being higher than the measured flows.

Oscillations in the CATHENA simulation started at 4,800 seconds. Small-amplitude oscillations commenced in the experiment at about 6,000 seconds.

Figure 8 shows the void fraction at the outlet of heated section 1. The predicted results agree well with the measured values until about 4,500 seconds, with only a slight overestimate in void in the first 900

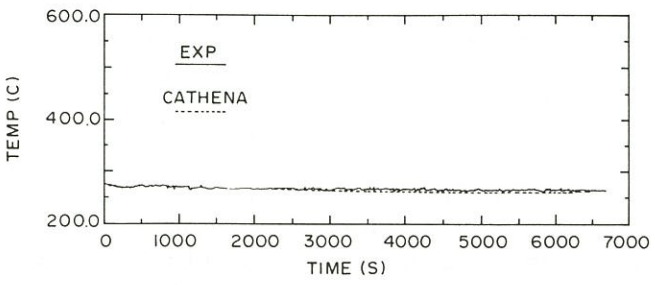

Figure 10 High-power, high-pressure case heated section 1 middle – lower sheath temperature.

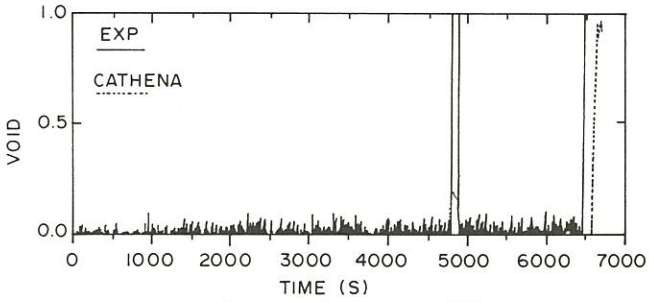

Figure 11 High-power, high-pressure case steam generator 1 outlet void.

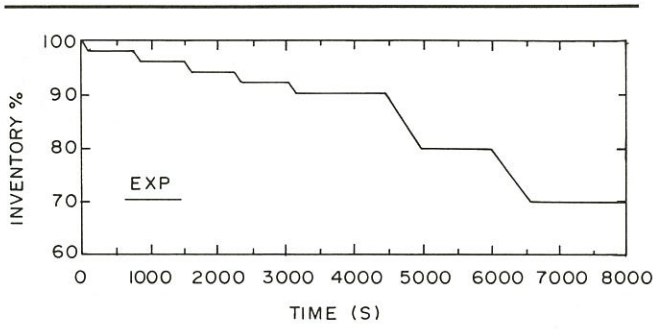

Figure 12 Low-power, high-pressure case loop inventory (full 954.1 L).

seconds. The CATHENA prediction underestimates the void after 4,500 seconds as a result of the high flows predicted in Figure 7.

Figures 9 and 10 show the heater pin sheath temperatures of the uppermost pin at channel 1 inlet, and a lower pin near the middle of channel 1, respectively. The effects of flow stratification were correctly captured in the CATHENA simulation. The code correctly predicted dryout of the top heater pin with no dryout of the lower pin. However, timing of dryout was slightly premature.

The void fraction history shown in Figure 11 is taken at the inclined outlet of steam generator 1. As previously mentioned, around 3,000 seconds void is able to penetrate the steam generators past the top of the tubes and begin collecting in the cold-leg side. The draining operation beginning at 4,500 seconds causes additional steam to be generated, 'flashing' in the piping between the heated section outlets and the steam generator. Unable to condense all of the entering vapour, the steam generator becomes flooded with steam, and in so doing retards the flow (see Figure 7). Figure 11 indicates that the steam generator first becomes steam-filled at 4,800 seconds. After the draining operation stops at about 4,800 seconds the system begins to stabilize and re-establish a more steady flow. The void returns to a low value, indicating that the steam-liquid interface has moved back up into the

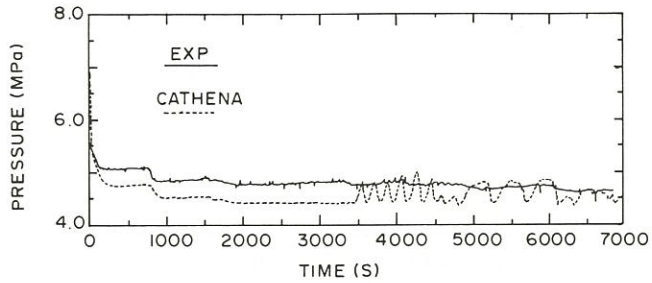

Figure 13 Low-power, high-pressure case header 1 pressure.

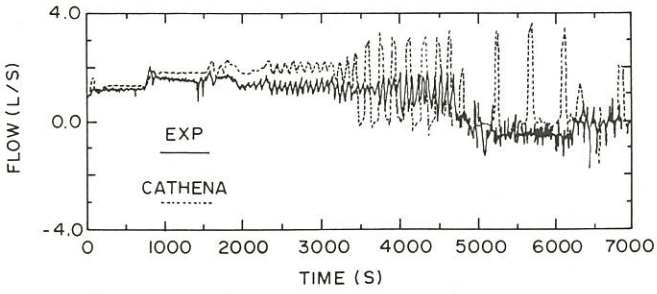

Figure 14 Low-power, high-pressure case heated section 2 inlet flow.

steam generator cold-leg side. CATHENA correctly predicted the occurrence of void at this time, but in insufficient quantities, again a result of high heat removal rates in the steam generator. The void spike after 6,400 seconds was predicted late in the simulation.

Low-Power, High-Pressure Test

Figures 12 through 18, inclusive, show the simulation and experimental results for the low-power (80 kw/pass) and high-pressure (4.6 MPa) case. This test, like the previous one, starts out in a stable non-oscillatory forward flow mode. Around 2,000 seconds, and at 94% loop inventory, small regular oscillations begin to appear and grow in amplitude as more primary fluid is drained. The flow oscillations occur in both halves of the loop and are almost in phase with one another. At about 4,600 seconds, and approximately 90% loop inventory, flow stagnation and fuel temperature excursions first occur. At 5,000 seconds, and at 80% loop inventory, a small less well defined oscillating negative flow develops which results in periodic dryout of the upper fuel elements. After 6,000 seconds, and at 70% loop inventory, the flow oscillates about a zero mean, the channel flow stratifies, and high pin temperature trip terminates the experiment.

The primary side pressure trace, Figure 13, shows the predicted pressure to be low up to 3,500 seconds. Since similar secondary side boundary conditions were used for this case as used in the high-pressure

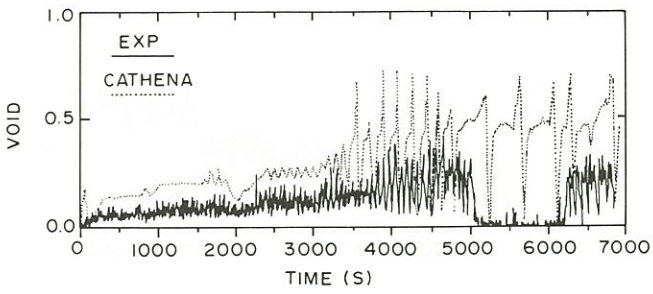

Figure 15 Low-power, high-pressure case heated section 1 outlet void.

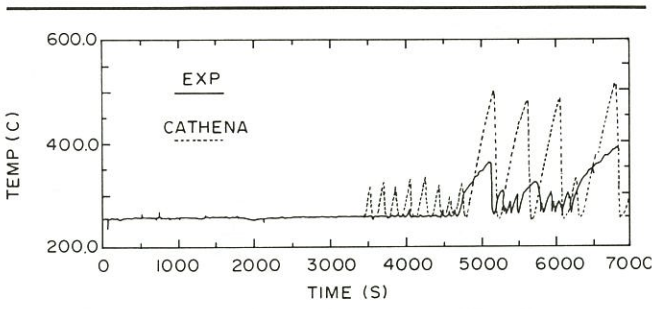

Figure 16 Low-power, high-pressure case heated section 1 inlet – upper sheath temperature.

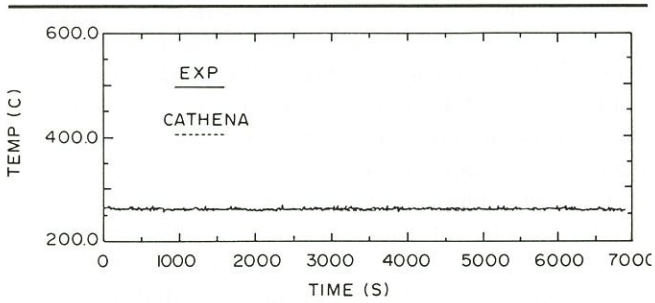

Figure 17 Low-power, high-pressure case heated section 1 middle – lower sheath temperature.

high-power case, excessive predicted heat removal in the steam generators is suspected. The effect is more pronounced because of the lower input power used in this experiment. After 3,500 seconds, pressure spikes are incorrectly predicted. They result from excessively large predicted flowrates and heater pin temperature oscillations.

Figure 14 shows the predicted flow to be high up to 3,200 seconds. The assumed high predicted heat removal rate from the steam generators results in a lower predicted system pressure, seen in Figure 13, and a higher predicted test section outlet void, seen in Figure 15, than occurred in the experiment. The increased void creates a higher driving head, and therefore higher flow rates, than those observed. The

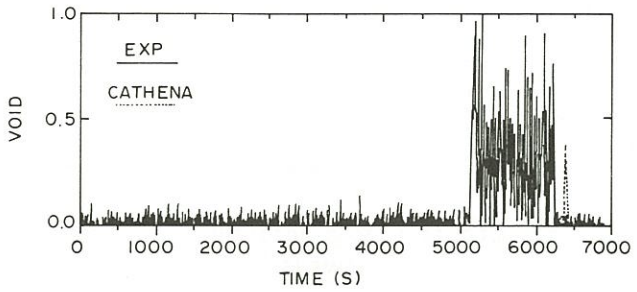

Figure 18 Low-power, high-pressure case steam generator 1 outlet void.

onset, amplitude, and period of the oscillations are, however, well predicted. After 3,200 seconds the predicted oscillations become much larger and longer in period than in the experiment. The reason for this discrepancy is thought to lie in the predicted higher voids, which cause a transition from bubbly flow to annular flow in the vertical pipe sections. This allows quicker movement of vapour to the steam generators where it accumulates and slows the flow. The resulting annular flow that develps in the steam generator tubes also reduces the condensation rate, thereby increasing the period of oscillation. It does this through a reduction in the vapour-to-liquid interface area. The relatively steady reverse flow, observed in the experiment between 5,000 and 6,000 seconds, was not predicted by CATHENA. The near stagnant conditions predicted were probably a result of the overestimation in void. The results of the draining operation after 6,000 seconds, which causes the flow to stagnate in the experiment, support this.

Shown in Figure 15 is the void fraction at the outlet of heated section 1. Generally, it shows higher outlet void than that observed in the experiment. As explained previously, the suspected high heat removal rate in the steam generators, which causes low system pressure to be predicted, is responsible. The single-phase liquid conditions seen in the experiment between 5,000 and 6,200 seconds result from the small reverse flow seen in Figure 14. The code predicted near stagnant conditions with occasional large brief positive flows, and, as a result, overestimates the amount of void present. After 6,200 seconds, the observed flow returns to near stagnant conditions and a sharp increase in void occurs.

The predicted heater pin sheath temperature shown in Figure 16 has numerous spikes beginning around 3,500 seconds. Intermittent dryout of the top heater pins is evident in the experiment around 4,000 seconds, but the temperature spikes tend to be much much smaller in amplitude. Again, this is caused by the large predicted flow oscillations that produce periods of flow stagnation in the channel. Dryout of the lower heater pin was correctly predicted not to occur (Figure 17).

Figure 18 shows the steam generator outlet void. In the experiment, the appearance of void at this location is a result of the flow reversal observed after 5,000 seconds. The void remains until 6,200 seconds because the small, steady, reverse flow persists until that time. Later, the void disappears as flow stagnation occurs. CATHENA predicted near-stagnant conditions, with periodic positive flow surges starting around 5,000 seconds, and therefore did not predict the appearance of void at this location. The spike predicted at 6,400 seconds resulted from void carried through the steam generator tubes by a positive surge in flow around 6,300 seconds (see Figure 14). Previous flow surges at 5,200, 5,600, and 6,100 seconds flooded the steam generators with steam, but during the periods of stagnant flow between surges the steam generators were able to condense the steam. The surge in flow at 6,300 seconds follows shortly after the surge at 6,100 seconds, and the steam generator was not able to recover sufficiently from the previous flow surge.

Low-Power, Low-Pressure Test

Figures 19 through 25, inclusive, show the simulation and experimental results for the low-power (60 kw / pass) and low-pressure (0.2 MPa) test. In this test an intermittent flow pattern develops early at about 98% of loop inventory. Large, nearly in-phase flow surges

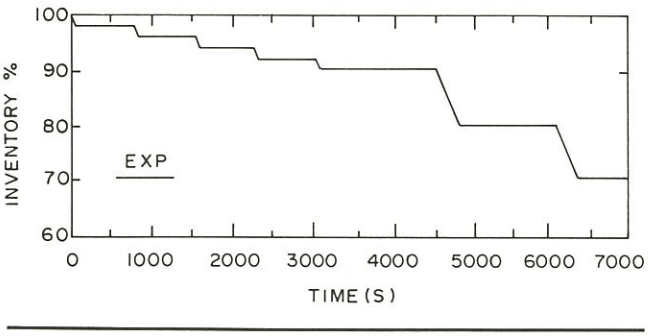

Figure 19 Low-power, low-pressure case loop inventory (full 954.1 L).

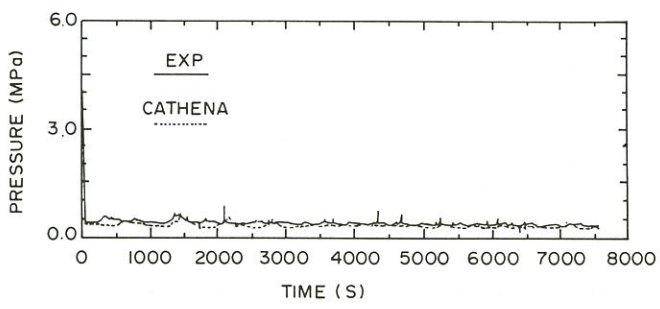

Figure 20 Low-power, low-pressure case header 1 pressure.

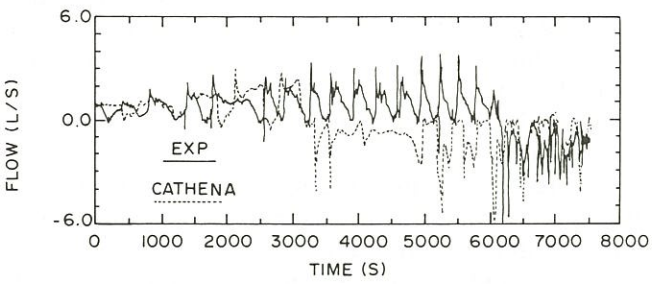

Figure 21 Low-power, low-pressure case heated section 2 inlet flow.

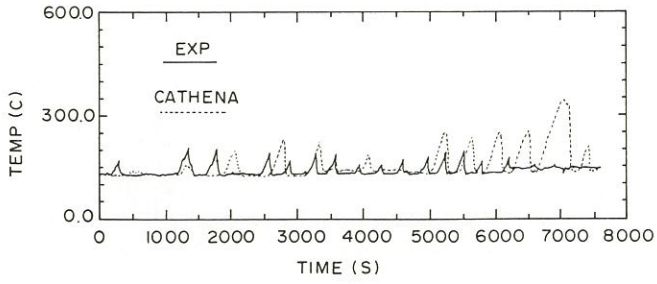

Figure 23 Low-power, low-pressure case heated section 1 inlet – upper sheath temperature.

from near-stagnant conditions were observed in both halves of the primary circuit. This allowed periodic dryout of the upper fuel elements. With each successive draining operation, the period of the oscillations shortened. At loop inventories of about 70% the mean flow direction reversed, and less well defined negative flow oscillations developed. Finally, at 50% of primary loop inventory, flow stagnation occurs, resulting in a power supply trip on high heater pin temperature and termination of the experiment.

The predicted primary pressure shown in Figure 20 shows good agreement with the experimental pressure. Only a small underestimation of the pressure and some discrepancies in timing of the pressure oscillations are seen in the CATHENA simulation.

Figure 21 shows the predicted flow oscillations, up to 3,400 seconds, have the correct general shape and amplitude but a longer period. In addition, the flow reversal observed in the experiment after 6,000 seconds is prematurely predicted to occur at about 3,400 seconds. Since these cases are very sensitive to the amount and distribution of void, especially in the vertical pipe legs, it is important to predict correctly condensation within the steam generators. Large primary side oscillations can be expected to induce void and flow oscillations in the secondary side which affect the heat removal rate from the primary side. The simple modelling of the secondary side used in these simulations is again suspected of being inadequate in this case.

Shown in Figure 22 is the void fraction at the outlet of heated section 1. The oscillations up to 3,400 seconds tend to have much longer periods than those observed in the experiment, as a result of the longer period flow oscillations predicted by CATHENA. During the time period from 3,400 to 5,000 seconds the predicted reverse flow removes any void from this location. Once periodic stagnant flow is again predicted, starting after 5,000 seconds, spikes in void reappear. After 6,000 seconds the flow reverses in the experiment and is maintained with only brief periods of stagnant flow. As a result, no spikes in void appear. The prediction shows void spikes because the flow is predicted to stagnate for much longer periods of time.

The sheath temperature of the upper heater pin, Figure 23, shows that the predicted oscillations, before the predicted flow reversal at 3,400 seconds, have the correct amplitude but a longer period than in the experiment. After 5,000 seconds large temperature excursions due to the long periods of stagnated flow are predicted. Unlike in the previous two test cases, the lower pin location, plotted in Figure 24, approaches dryout conditions. This is predicted well by CATHENA.

The steam generator outlet void fraction plot, Figure 25, shows that the arrival of void, at 3,600 seconds in

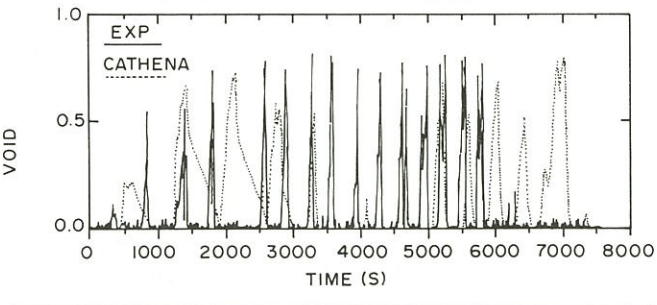

Figure 22 Low-power, low-pressure case heated section 1 outlet void.

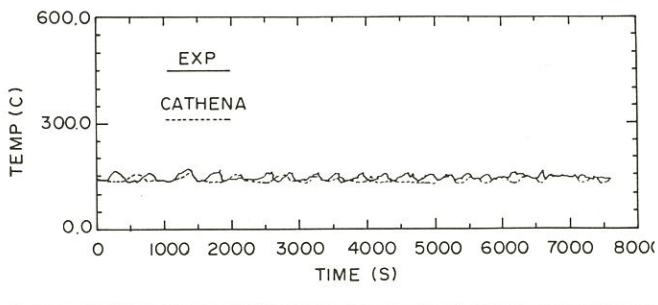

Figure 24 Low-power, low-pressure case heated section 1 middle – lower sheath temperature.

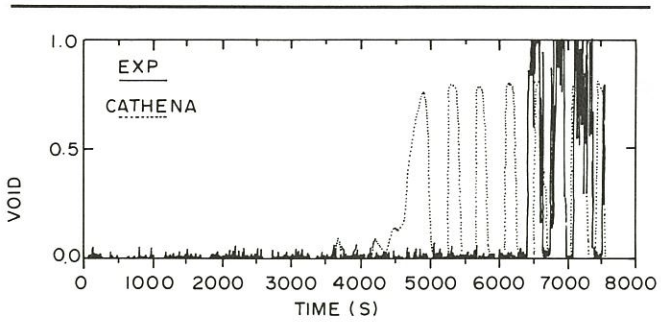

Figure 25 Low-power, low-pressure case steam generator 1 outlet void.

the simulation, occurred shortly after a negative flow was predicted. The experiment also shows the arrival of void after a negative flow developed, but not until 6,400 seconds.

Conclusions

The CATHENA code has been used to predict thermosiphoning tests conducted in the RD-14 thermalhydraulic test facility. In the tests simulated, the code has correctly predicted the occurrence of non-oscillating and oscillating 2-phase thermosiphoning flow behaviour.

Non-oscillating 2-phase thermosiphoning flow and the timing of the onset of oscillations are well predicted. The use of constant boundary conditions for the steam generator secondary side is adequate for these conditions.

Oscillating 2-phase thermosiphoning flow is not as well predicted. The predicted period tends to be longer and the amplitude exaggerated. For this type of flow, constant boundary conditions for the steam generator secondary side may not be adequate. Where the period of oscillation is long and the oscillation amplitude large, the interaction between the primary and secondary side appears to be important.

In all cases, the differing behaviour of the upper and lower pins was captured in the predictions. In the presence of stratified flow upper elements became exposed to steam and experienced temperature excursions, while the lower elements remained cooled by single-phase liquid.

Acknowledgements

The experiments presented in this paper were funded by the CANDU Owners Group (COG).

This paper is a revised and expanded version of a paper originally presented at the Second International Conference on Simulation Methods in Nuclear Engineering, Montreal, 14–16 October 1986.

Notes and References

1. *Hanna BN*, et al. One-step semi-implicit method for solving the transient two-fluid equations that is non-courant limited. 11th National Heat Transfer Conference, Denver, 1985.
2. *Krishnan VS, Gulshani P* Thermosiphoning behaviour of a pressurized-water facility with CANDU PHTS geometry. Presented at the 2nd International Topical Meeting on Nuclear Power Plant Thermalhydraulics and Operations, Tokyo, 1986.
3. *Ransom VH.* RELAP / MOD2: for PWR transient analysis. In: CNS / ANS International Conference on Numerical Methods in Nuclear Engineering. Montreal, 1983: 40–60.
4. *Richards DJ*, et al. ATHENA: a two-fluid code for CANDU LOCA analysis. Presented at the Third International Topical Meeting on Reactior Thermalhydraulics, Newport, Rhode Island, 1985.

Use of Quantitative Indicators of Nuclear Safety in Ontario Hydro

R.T. Popple and S.B. Harvey

Abstract

The measurement of reactor safety performance from a public risk standpoint is rapidly becoming an area of wide interest, both in the public mind and within the industry. This paper outlines the quantified operational risk assessment methodology that has been in use in the Ontario Hydro nuclear-electric program since the early 1960's. It enables an assessment of risk arising from operation to be compared with Ontario Hydro standards and those set by the Federal regulator of the nuclear industry in Canada, the Atomic Energy Control Board. Although the methodology is a main part of the public safety thrust used by Ontario Hydro to achieve acceptable levels of risk, it is not the only part, and other complementary areas are discussed in the paper.

Introduction

Nuclear generation is now the major option for production of electricity in the province of Ontario because hydraulic resources have been developed almost to the economical limit and fossil fuels are expensive.

Ontario Hydro is a publicly-owned Corporation that supplies the electrical needs of the province of Ontario, which contains the industrial heartland of the country and a population of about eight million people. The present Ontario Hydro in-service nuclear capacity is 9,711 MWe, or 9,969 MWee (Table 1).

Public safety is achieved through a defence-in-depth approach to radioactivity containment that allows for occasional operator mistakes and design oversights. Ontario Hydro nuclear-electric stations have 4 overlapping work program thrusts, to protect the barriers to radioactivity release (ceramic fuel, fuel sheathing, heat transport pressure boundary, containment structures, and exclusion zone). These 4 thrusts, which form the basis of its operational safety management program, are:

- ensure that systems which are normally in service (process systems) are reliable;
- ensure that poised safety systems are reliable;
- ensure that equipment and procedural faults are detected, assessed, and promptly corrected, including re-design when necessary; and
- provide in-depth training to operating staff.

The operational safety management program used by Ontario Hydro has been under continuous improvement over the past 25 years as modelling, fault classification, testing, and data manipulation methods have evolved; such development is expected to continue.

The achievement of high levels of public safety and the ability to demonstrate that achievement requires the following:

1 a knowledge of the areas critical to safety;
2 a set of standards or targets which define acceptable performance;
3 a program to monitor performance, respond to problems, and to report the results;
4 an experience review program to establish a) trends, b) the degree of compliance with standards, and c) root causes where performance is unacceptable or deteriorating; and
5 a means of assessing the impact of proposed changes to hardware or operating procedures and of implementing changes consistent with the accepted standards.

Risk Quantification

The key indicator of effectiveness of a public safety management program is quantified risk. It is expressed as the frequency of a postulated event multiplied by its consequence:

$$\text{RISK}_{(\text{EVENT})} = \text{FREQUENCY}_{(\text{EVENT})} \times \text{CONSEQUENCE}_{(\text{EVENT})}. \quad (1)$$

The total risk resulting from station operation is the sum of the events risks

$$\text{RISK}_{(\text{TOTAL})} = \sum_{\text{EVENTS}} \text{RISK}_{(\text{EVENT})} \quad (2)$$

A risk management program could be based on risk from individual postulated events or on total plant risk, or, as is used in Ontario Hydro, both.

Keywords: risk assessment, nuclear safety, public risk, safety systems, safety management, nuclear regulation.

Table 1: Ontario Hydro In-Service CANDU-PHW[2] Nuclear Capacity, 31 December 1986

Station	*Unit*	*Net capacity MWe*	*Net capacity MWee*
NPD NGS	Single	22	22
Pickering NGS-A	1	515	515
	2	515	515
	3	515	515
	4	515	515
Pickering NGS-B	5	516	516
	6	516	516
	7	516	516
	8	516	516
Bruce NGS-A	1	759	770[1]
	2	769	848
	3	759	848
	4	769	848
Bruce NGS-B	5	835	835
	6	837	837
	7	837	837
Total: 5 Stations	16 units	9,711	9,969

In addition to the 9,711 MWe of CANDU-PHW nuclear capacity in service with Ontario Hydro at the end of 1986, a further 4,361 MWe of capacity was under construction.

[1]Incudes electrical equivalent of process steam (only applicable to Bruce NGS-A).

[2]CANadian Deuterium Uranium reactors, heavy-water moderated, use natural uranium fuel, and Pressurized Heavy Water coolant.

The risk to the public from the operation of a nuclear generating station arises from both conventional and radiological hazards resulting from station operation. The conventional risk is not discussed here.

The predominant radiological risk from nuclear station operation results from the potential for premature death due to a radiological dose (measured in rem). The consequence of a given event is therefore measured in rem / event. When this consequence is combined with the expected frequency (events / annum) of the event in question, a measure of risk is obtained.

$$\text{Frequency (events / annum)} \times \text{Consequence (rem / event)} = \text{Risk (rem / annum)}.$$

Risk measured in 'rem / annum' can be directly correlated with a more conventional measure in 'fatalities / annum' (see below, Safety System Unavailability, and Integrated Public Risk).

Systems in a nuclear-electric unit can be broadly separated into process systems and poised safety systems. Process systems are those required to generate electricity; the heat transport systems and reactor power control systems are the most significant from a potential radioactivity release standpoint. Safety systems are poised to shut down the reactor, provide additional fuel cooling if needed, and contain any radioactivity released; they do not play a role in power production.

Ontario Hydro has used the concept of process systems and safety systems in developing its operational risk model. The groups of events which contribute to risk are:

- chronic radiological emissions;
- process system failure with subsequent successful safety system operation (termed single failure);
- process system failure with subsequent failure of a safety system (termed dual failure); and
- process system failure with subsequent failure of more than one safety system (including failures caused by external events).

In Ontario Hydro, separate targets have been developed for chronic and acute risks. Since chronic emissions are directly measurable, a predictive model is not required to enable comparison of results with targets. The Ontario Hydro operational risk management model, therefore, need only consider acute risk. Based on Equation (2):

$$\text{RISK}_{(\text{ACUTE TOTAL})} = \Sigma\,\text{RISK}_{\text{SINGLE FAILURE}} + \Sigma\,\text{RISK}_{\text{DUAL FAILURE}} + \Sigma\,\text{RISK}_{\text{MULTIPLE FAILURE}}. \quad (3)$$

At present, the risk due to multiple failures is not being assessed at operating stations. This is based on a design and licensing requirement that multiple safety system failures should not result from a process system upset; therefore, if any such failure mechanisms are detected, they are eliminated. Design verification activities and an ongoing review of the potential impact of observed faults (locally and world-wide) are intended to eliminate multiple faults. Even if some multiple failure mechanisms remain, their contribution to total risk is expected to be small relative to other terms.

Identification of Critical Safety Areas

The operational risk model described is a means of producing a risk indicator from an existing understanding of overall risk contributors. It is, however, unable to predict actual risk because:

- while it is a design and operating philosophy to maintain independence of safety systems, and of process systems with safety systems, a comprehensive detailed analysis has not been done on operating stations;
- the frequency of process upsets is not based on detailed analysis;
- the analysis of consequences is often highly conservative; and
- the analysis of safety system unavailability assumes, conservatively, that the system provides no benefit.

Ontario Hydro is currently looking at fully integrated event tree / fault tree risk models, i.e., Probabilistic Risk Assessments (PRA) as a means of obtaining a more comprehensive understanding of risk contributors. This improved understanding of risk will be factored

into the operational risk model and is expected to improve its validity and usefulness. Even without a comprehensive PRA, operational experience is expected to yield improvements to our understanding of risk as new events trigger re-assessments.

Ontario Hydro Targets

Ontario Hydro has established targets which, if met, will achieve both the regulatory requirements and the internal public safety risk objective.

Single Failure Frequency

From a public safety perspective the standard for frequency of accidents which have the potential to release radioactive material without safety system action is a maximum of 1 accident per unit in 3 years. Economic considerations would dictate that a target should be much more restrictive than 1 / 3 years.

Safety System Unavailability

Safety system unavailability is defined as the fraction of time that a safety system cannot act as required. An unavailability target of 1×10^{-3} a / a is set to ensure compliance with the regulatory Siting Guide dual accident frequency as follows:

Accident Frequency × Safety System Unavailability ≤ Dual Failure Frequency, (Siting Guide) or

$$\frac{1}{3\,\text{yr}} \times 1 \times 10^{-3} \frac{\text{yr}}{\text{yr}} \leq \frac{1}{3{,}000\,\text{yr}}.$$

The unavailability target is applied to each 'special' safety system individually (i.e., shutdown system; shutdown system no. 2, where installed; emergency coolant injection system; containment system). Targets are also developed for other poised safety-related systems based on the overall importance of the system.

Integrated Public Risk

Ontario Hydro has developed a radiological risk standard based on the principle that:

'The risk to an individual member of the public, from the operation of a nuclear generating station, should be negligible when compared with the everyday risk to which that member of the public is exposed.'

The average risk to the public in Canada for all accidents is approximately 600 premature deaths per annum for every million persons (i.e., 600×10^{-6} fatalities / a). If we define negligible to be less than 1%, the standard would be 6 premature deaths per annum for every million persons (i.e., 6×10^{-6} f / a). Considering a given individual member of the public, his / her risk of death each year would then be 6 chances in one million. The Ontario Hydro standard has been set even more conservatively at 1 chance in a million of a given individual (the most exposed one) suffering a premature death in a one-year period due to releases of radioactive material (i.e., 1×10^{-6} f / a).

This risk standard of 10^{-6} fatalities per annum is converted to a radiological risk standard in rem per annum by using a statistical medical relationship correlating whole-body exposure to a premature death probability:

1 rem whole body = 10^{-4} premature death probability.

Since 1 rem Equivalent Whole-Body (EQWB) dose is defined so as to be equivalent in terms of cancer induction to 1 rem whole-body dose.

1 rem EQWB = 10^{-4} premature death probability.

The Ontario Hydro risk standard can thus be expressed as:

$$\text{Risk Standard} = 10^{-6} \frac{\text{fatalities}}{\text{annum}} \times \frac{1 \text{ rem EQWB}}{10^{-4} \text{ fatalities}},$$

or Risk Standard = 10^{-2} EQWB dose (rem) / annum

Monitoring, Response, and Reporting

Active Systems

Failures in systems which are directly involved in power production are immediately detectable. A test program is not required. The safety management program focuses on ensuring that, in the short term, operator response to a failure will minimize public risk, and in the longer term, lessons learned from the failure are acted upon.

Short-Term Operator Response

The operator is given guidance regarding the optimum response to a process system failure in the following ways:

- operating procedures specify step-by-step response for events which are anticipated to occur frequently, or where an optimum response can be established with confidence;
- operating procedures specify general response criteria for events which have not otherwise been addressed in detail; and
- operators are trained to recognize and respond to key plant parameters, regardless of the cause of the event.

Reporting

Operators prepare a 'Significant Event Report' (SER) for any serious process system upset. These SERS record the first hand observations of the upset. Based on a subsequent thorough analysis of the event, process system faults are then categorized using the following:

Type A a failure that would have caused significant fuel failures or radiological hazards in the absence of Special Safety System action

Type B a failure which did not require Special Safety System action to prevent significant fuel failures or a radiological hazard, but was due to fortuitous factors

rather than specific design or control provisions

Type C a failure that tended to raise fuel temperature but could not cause significant fuel failures or radiological hazards even in the absence of Special Safety System action

Type D a failure which would have tended to raise fuel temperature in the absence of Special Safety System action if fortuitous factors had been different

Type E a failure that had no effect on fuel temperature, or lowered it

Poised Systems

Poised systems are those which normally monitor process variables and are triggered when an upset occurs (e.g., shutdown system, emergency coolant injection system). A test program is required to detect system failure, and hence to provide confidence that the system would work if needed.

Test Program

It is necessary to determine which functions or components must be tested, and the test frequency. Reliability analysis is used for these purposes.
The system test frequencies are based on:

- the system unavailability target;
- the failure rates of components using either generic or plant-specific data, as available; and
- the degree of difficulty or the risk of spurious operation in doing the test.

For record and analysis purposes, faults of poised systems that are typically detected on the basis of defined testing program, are classified as follows:

A *Type 1* fault significantly reduced the effectiveness of the system, such that it would have been of little or no benefit if the worst possible process system failure had occurred.
A *Type 2* fault reduced the effectiveness of the system, such that it would have failed to satisfy the design intent. However, the system would still have operated and significant benefit would have been gained from its operation.
A *Type 3* fault reduced the level of redundancy that is built into the system. The effectiveness of the system was not significantly reduced and the design intent could still be satisfied.
A *Type 4* fault reduced the effectiveness of the system, or a single component, such that it was outside normal operating limits. However, the design intent could still be satisfied.
A *Type 5* fault had no negative effect on the system.

Type 4 and 5 faults are maintained in the data base to ensure auditability of the classifications (eg, a Type 4 which should be a Type 3) and to allow reclassification if design changes are considered.

Special Safety System Reporting Indices

Conversion of observed system performance into unavailability estimates can be done in many ways. Ontario Hydro uses 4 indices because no single index can provide total insight into system performance given the statistical limitations of finite data. These indices are:

1 *system inoperability*
2 *observed system unavailability*
3 *derived system unavailability*
4 *expected system unavailability*

System Inoperability

System inoperability is the fraction of time during the past year that a system is fully incapable of providing protection for the events with which it is designed to cope. This index is determined directly from observation. It does not include marginal failures to meet the design intent of the system, and is therefore a non-conservative measure of system performance. However, when used in conjunction with *observed system unavailability* (see below), it is useful in distinguishing between major system faults, which definitely impact on public risk, and faults which may, in reality, represent only an erosion of the conservative assumptions used in the plant safety analysis.

Observed System Unavailability

(Also known as *actual past unavailability*)
Observed system unavailability is the time fraction that the overall system was known to be *not fully available* during the past year. Again, this index is determined directly by observation. This index includes any faults which result in *system inoperability* with all other faults (or combination of faults) which resulted in the system not being capable of fully meeting the design intent. Hence, it is a conservative measure of system performance. While this index provides a conservative measure of the actual system performance, it is susceptible to large statistical fluctuations from year to year, which makes decision making difficult if based on this parameter alone. It also provides little information on component or subsystem performance.

Derived System Unavailability

(Also known as *derived past unavailability*)
Derived system unavailability is a calculated index which uses a reliability model (generally a simple functional block model) to combine the results of the testing program obtained over a 1-year period. All unsafe faults which occurred over the past year are included, and subsystem / component unavailabilities are calculated using an estimate of average future fault durations. This index is sensitive to short-term changes in system performance, and provides more information than *observed system unavailability* on the contribution of individual component / subsystem failures to overall system performance. It also provides an indication of the statistical significance of the value of the *observed system unavailability* in a particular year. If *observed*

Table 2: Summary of Risk Indicators vs Experience

		*Average observed lifetime performance***			
	Target	*PNGS-A*	*PNGS-B*	*BNGS-A*	*BNGS-B*
Unit years in-service		55	5	32	2
Single failure rate	1 / 3 f / a	0.2	0	0	0
Shutdown system 1					
Unavailability*	1 a / a***	0.27	0	0.97	0
Inoperability*		0.017	0	0	0
Shutdown system 2					
Unavailability*	1 a / a	N / A	0.007	2.15	0.009
Inoperability*		N / A	0	0	0
Emergency coolant injection system					
Unavailability*	1 a / a***	89.0	0.04	30.5	1.19
Inoperability*		1.0	0.04	0.003	0
Containment system					
Unavailability*	1 a / a***	30	0.07	1.97	0.83
Inoperability*		0	0	0	0
Acute risk indicator	10^{-2} rem (EQWB) / a	2.4×10^{-3}		1.6×10^{-3}	1.6×10^{-4}

*All unavailability and inoperability targets / results are to be multiplied by 10^{-3}.
**Calculated from in-service date to end 1985.
***Target is 3×10^{-3} for Pickering A.

system unavailability is significantly higher than *derived system unavailability*, this indicates that faults on redundant components overlapped to a greater extent than expected, or that fault durations were much longer than we would reasonably expect in the future. Conversely, if *observed unavailability* is much less than *derived*, this can be taken to indicate a fortuitous situation which should not be expected to continue in the long term.

Expected System Unavailability
(Also known as *predicted future unavailability*)
Expected system unavailability is a calculated index which uses the same reliability model as *derived system unavailability* to combine all relevant subsystem (or component) experience obtained to date on the system of interest. Where few or no failures have been observed, a 50% confidence chi-squared estimate of failure rate is used to provide an estimate of subsystem (or component) performance. After a few years, this index provides a statistically valid upper limit estimate of long-term average system performance. As it uses all relevant experience, it does eventually become relatively insensitive to sudden changes in the performance of equipment, but such changes are detected by other means (e.g., *derived system unavailability*).
There is one point which should be emphasized in looking at actual experience: although the second, third and fourth indices contain the word 'unavailability,' this does *not* denote the time that the system is totally incapable. They quantify the effects of faults which reduce the redundancy or capability of the system, even though the system may still provide adequate protection for most events. These parameters are, in reality, conservatively defined indices which combine experience in a predetermined manner. The achievement of target using these indices indicates excellent system performance; but because of the conservatism inherent in this approach, failure to meet target does not necessarily imply unacceptable risk.

Results of the Safety Management Program
Table 2 shows the lifetime average of the key risk management indices as compared to their targets for a spectrum of mature and immature in-service stations as of end of 1985. Table 2 is intended to be illustrative only. In any given year, or on a particular system, targets may be exceeded, but the overall risk indicator has always been achieved by a considerable margin. Design or operational changes have been made, or are being made, in all cases where a system target is consistently not met. The operational risk indices have shown where such changes are needed.

The following summarizes Ontario Hydro's experience to the end of 1985:

1 There has not been a failure which resulted in a release of radioactivity causing a measurable radioactivity dose to a member of the public in over 100 reactor-years of in-service operation.

The failure rate of process systems exceeded target at Pickering NGS-A in the initial years of station operation but design changes were successful in reducing the failure rate to well below target.

System unavailability and inoperability targets have generally been met, in many cases with wide margins. Although the overall risk from Pickering operations is

significantly better than target (40 times), the Pickering emergency coolant injection system performance has been well above target (30 times), warrants reliability improvement, and design changes are in progress. Similarly, design changes have been made to improve the unavailability of the Bruce-A emergency coolant injection system.

The Pickering NGS-A containment system average performance is well over target. The vast majority of this unavailability is due to a single penetration which had degraded and remained undetected for over 1 year. A comprehensive test program has been instituted to avoid a recurrence and there have been no similar undetected holes in containment either at Pickering or at other stations, which benefitted from a knowledge of the failure mode. No design changes were warranted.

All of the Pickering experience has been incorporated in the design and operating practices of subsequent stations; this is reflected in the observed good performance of these stations and in our expectation of good future performance at Pickering NGS-A.

2 A quantitative and systematic operational safety management program can demonstrate achievement of acceptable public safety while allowing for design, equipment, and operator failures. It can further provide a prioritization of unavailability contributors that can be systematically attacked and eliminated where justifiable.

3 The approach is effective but not perfect and is undergoing continuous improvement.

4 Past achievement cannot justify complacency, and a continued program of vigilance and improvement is in place.

Safe, Permanent Disposal of Nuclear Fuel Waste

W.T. Hancox
Atomic Energy of Canada Limited
Whiteshell Nuclear Research Establishment
Pinawa, Manitoba R0E 1L0

Abstract

This paper describes the Canadian concept for safe, permanent disposal of nuclear fuel waste deep in plutonic rock of the Canadian Shield. The ability of the disposal concept to isolate the wastes is then discussed in the light of laboratory and field research results. The methodlogy developed to characterize the hydrogeology of a plutonic rock mass is outlined and results obtained from its application to a field site are described. Also highlighted are the Canadian field research areas and the Underground Research Laboratory.

Résumé

Dans la présente communication, on décrit le concept canadien d'évacuation sûre, permanente, des déchets de combustible nucléaire à grande profondeur dans la roche plutonique du bouclier canadien. Ensuite on examine la capacité du concept d'évacuation d'isoler les déchets à la lumière des résultats de recherche en laboratoire et sur le terrain. On donne un aperçu de la méthodologie développée pour caractériser l'hydrogéologie d'une masse rocheuse plutonique ainsi que le détail des résultats obtenus en l'appliquant à une zone de recherches sur le terrain. En outre, on met en lumière les zones de recherches sur le terrain au Canada et le Laboratoire de Recherches Souterrain.

Introduction

Nuclear fuel wastes have been managed safely in Canada since the mid-1940's, when the first wastes were produced: first, at the Chalk River Nuclear Laboratories and, more recently, at each of the nuclear-electric generating stations. The waste producers recognized from the beginning that permanent disposal would be necessary as the final management step.

In the mid-1970's, Energy, Mines and Resources Canada initiated a study, led by Professor F.K. Hare of the University of Toronto, to identify disposal methods suitable for implementation in Canada. The study concluded [Aitken *et al.* 1977]:

1 Underground disposal in geologic formations was the most promising option within Canada and igneous rocks were the preferred geologic medium.
2 The repository should be regarded as a central, nationa facility and should be located in Ontario.

Surface disposal was rejected because it would leave to future generations the duty to keep watch on the wastes, and would be more vulnerable to man-made hazards. It was accepted that if something should go wrong with a deep geological disposal site, it would be difficult to rectify; nevertheless, if done correctly, such disposals could be forgotten by future societies.

Based on the recommendations of the Hare Study, the Governments of Canada and Ontario, in 1978, launched the Nuclear Fuel Waste Management Program. AECL was given the responsibility for assessing the concept of disposal of nuclear fuel wastes deep in plutonic rock of the Canadian Shield, and for developing and demonstrating the associated technologies [Boulton 1978]. It was recognized that the physical and chemical processes that might lead to release of radioactive materials and to their transport back to the surface would evolve over thousands of years. Therefore, it would not be possible to provide a direct physical demonstration of the concept's safety. The approach adopted was to base the demonstration of safety on long-term predictions using mathematical models that represent the various components of the disposal system, including the waste material and the plutonic rock mass. The research program was designed to provide a thorough understanding of the underlying physical and chemical processes, to develop appropriate models, and to validate them against carefully integrated laboratory and field experiments.

The research program is now well advanced and a comprehensive understanding of the waste isolation

Keywords: geologic disposal nuclear fuel waste.

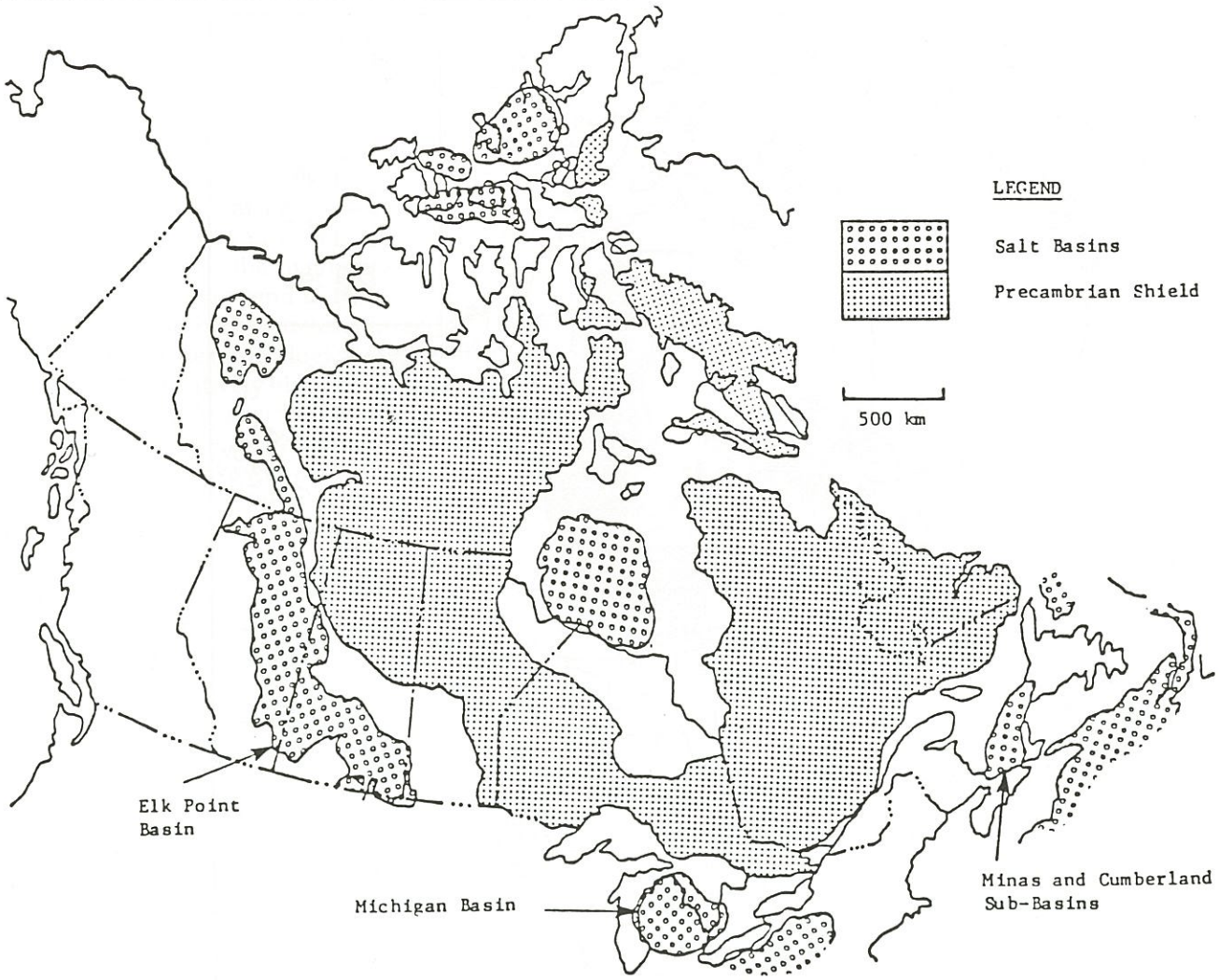

Figure 1 Some geological formations in Canada of potential interest for nuclear fuel waste disposal.

capability of the concept has evolved [Hancox 1986]. In the light of this understanding, a review follows of the rationale for the choice of plutonic rock as the disposal medium. Next, the nature of nuclear fuel waste, the concept for its isolation, and our current understanding of physical and chemical processes that ensure isolation, are outlined. Then, field research areas are highlighted that have contributed to our understanding of groundwater flow systems and geochemical processes, and to the development of our methodology for characterizing the hydrogeology of candidate disposal sites. Finally, the Underground Research Laboratory is described.

Geologic Medium

The concept of using a multi-barrier system involving a geologic medium in combination with engineered systems has gained strong technical support as the most feasible method for nuclear fuel waste disposal [OECD 1986]. There are a variety of potentially suitable geologic media, such as plutonic rock, bedded salt, and volcanic tuff, all of which can, under the right conditions, provide an acceptably safe site for a disposal vault. Where countries are studying more than one geologic medium, the rationale is to ensure that there are a number of locations, with a wide geographic distribution, available for selecting an acceptable site. Some countries have already selected the geologic medium that makes most sense for them: for example, salt in Germany, clay in Belgium, and plutonic rock in Canada and Sweden.

The defining criteria for appropriate geologic media include:

1 many potential sites in the geographic region of interest;
2 geologic stability for hundreds of thousands of years, and freedom from economically attractive concentrations of minerals, making future subsurface exploration unlikely;
3 groundwater transport times of hundreds of thousands of years from deep in the rock mass to the surface; and
4 geologic and hydrogeologic characteristics that can be readily determined using available technology, and that lend themselves to mathematical description.

Figure 1 shows geologic formations in Canada with

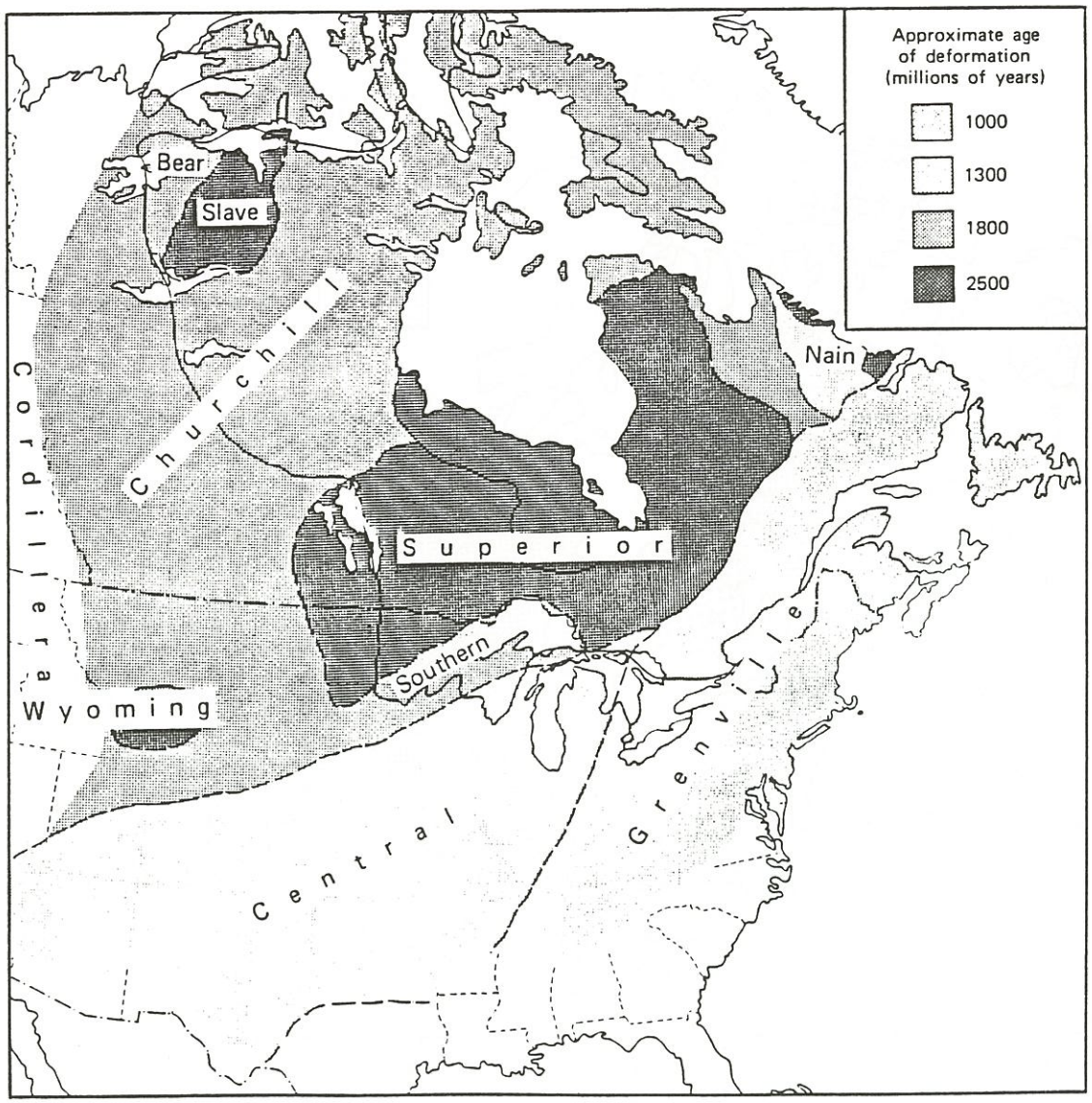

Figure 2 Structural Provinces of the Canadian Shield. (From *Stern CW, Carroll RL, Clark TH.* Geological evolution of North America. 3rd. ed., John Wiley & Sons, 1979.)

attributes of potential interest for nuclear fuel waste disposal [Mayman *et al.* 1976], salt basins, and the Precambrian Shield. Most of the salt basins are located outside the provinces with established nuclear power programs, and most coincide with petroleum and potash production activities. As a result, selection of salt as a disposal medium would severely limit both the geographic location of a site and the number of potential sites.

Figure 2 shows the structural provinces of the Precambrian Shield. In contrast to the relatively limited geographic distribution of salt, plutonic rocks of the Superior structural province of the Precambrian Shield are predominant over much of the province of Ontario, where the majority of Canada's nuclear power plants are located. Further, plutonic rocks of the other structural provinces extend beneath sedimentary rocks over much of North America. Selection of plutonic rock as a disposal medium provides a wide range of potential geographic locations and a large number of potential sites.

The Canadian Shield has been relatively stable for at least 600 million years, and most of the Shield has not had major orogenic activity for 2.5 billion years. Therefore, it is not a large extrapolation to infer that the region will remain stable for the required lifetime of a disposal vault. Also, regional topographic gradients in the Shield are low, about 1 m / km. As a result, the natural driving force for groundwater flow deep in the rock should be weak. Further, field investigations indicate that there are large plutonic rock masses with extremely low porosity and permeability. These would

serve to limit access of groundwater to the waste, thereby slowing its deterioration and inhibiting movement of radionuclides through the rock. Also, minerals in plutonic rock are known to react with many of the radionuclides in nuclear fuel waste, further retarding their movement.

The broad classification of plutonic rock includes all rocks crystallized from a molten state deep within the earth's crust. Large individual intrusives, known as plutons, have been the main focus of our research, because these bodies tend to be of relatively uniform composition and high structural integrity. These plutons fall within the mineralogical spectrum that ranges from granites, relatively high in quartz and feldspar, to gabbros, relatively enriched in minerals containing magnesium and iron. Therefore, we decided to study both granitic and gabbroic plutons. However, it should be emphasized that our field research has not been confined to plutons, but has included the metamorphic rocks into which they have intruded.

To determine the acceptability of a disposal concept, the following are required:

1 criteria that define what is acceptably safe;
2 methodology to evaluate proposed disposal systems against the safety criteria;
3 technology to site and build a disposal vault that satisfies the safety criteria;
4 confidence that an acceptable site can be found.

The criteria that define an acceptably safe disposal system are the responsibility of regulatory and environmental agencies. The basic criteria to be adopted in Canada for the long-term management of radioactive wastes have recently been issued by the Atomic Energy Control Board [Atomic Energy Control Board 1984 and 1986]. These criteria are independent of the geologic medium chosen.

The methodology to assess the performance of a proposed disposal system against the basic safety criteria is being developed and validated as part of our research program, and consists of an integrated program of laboratory and field analysis, engineering design, and mathematical modelling. Although some details are specific to plutonic rock, the methodology itself can be adapted to any geologic medium.

The technology to site and construct a disposal system is the most dependent on the geologic medium. In our program, technology has been developed to:

1 determine geological and hydrogeological characteristics of plutonic rock masses to depths up to 1000 m;
2 determine the thermal-mechanical response of a rock mass to the excavation of a disposal vault and to the heat produced by emplaced fuel waste, with particular emphasis on how these changes might affect groundwater flow and radionuclide migration; and
3 obtain geotechnical information required to support the engineering design of the disposal system.

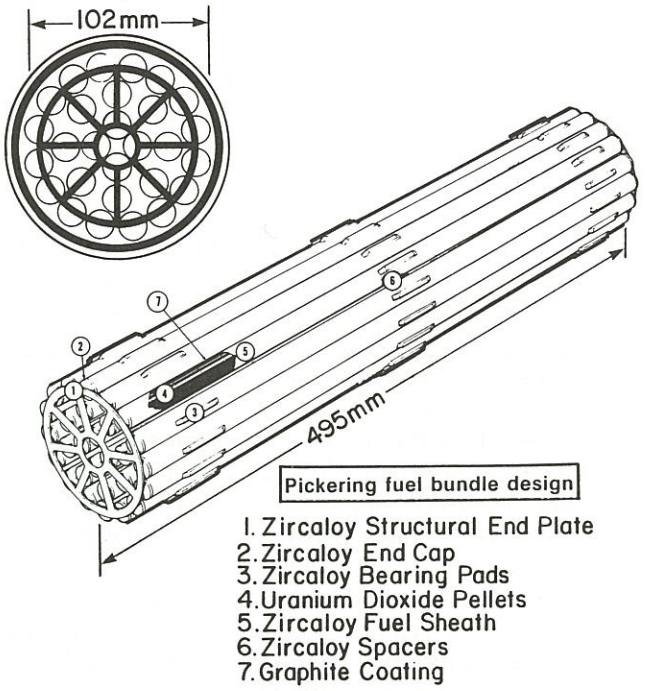

Figure 3 A typical CANDU fuel bundle assembly.

This technology can be generally applied to plutonic rock, whether it is exposed at the surface or lies beneath a layer of sedimentary rock. The major impact of thick overburden or sedimentary cover is additional cost associated with extra hydrogeological testing and monitoring in boreholes drilled and instrumented in the overburden. These are required to relate the groundwater flow system in the sediments to that in the underlying rock mass.

Nature of Nuclear Fuel Waste

A typical CANDU fuel bundle is shown in Figure 3. The uranium dioxide fuel is in the form of ceramic pellets that are sealed inside zirconium alloy tubes, which are assembled into a bundle. When first removed from the reactor, used-fuel bundles are intensely radioactive (1.5 million Ci at discharge). After 1 year of cooling, the intensity of the radiation has decreased by a factor of 100 (15,000 Ci), and the heat generation rate has decreased to 60 W. In 10 years, the radiation intensity has decreased by a factor of 1,000 (1,500 Ci) and the heat generation rate to 4 W.

Table 1 compares the composition of a typical used CANDU fuel bundle, after cooling for one-half year, with that of an unirradiated fuel bundle. The hazard from penetrating gamma radiation is negligible after about 500 years. However, some of the long-lived radionuclides, such as iodine-129 (16 million year half-life), cesium-135 (2.3 million year half-life), technetium-99 (210,000 year half-life) and plutonium-239 (24,500 year half-life) remain toxic for hundreds of

Table 1: CANDU Fuel Bundle Composition (g)

Constituent	*New*	*Used**
Uranium-238	18,865	18,725
Uranium-235	134	44
Other Uranium Isotopes	1	15
Plutonium		71
Other Actinides		1
Iodine		1
Cesium		11
Technetium		4
Other Fission Products		128
	19,000	19,000

*Assuming a burnup of 650 GJ / kg and a cooling time of 0.5 years.

thousands of years, and are the most important radionuclides from a radiological view point. Their potential hazard is similar to that of many non-radioactive toxic wastes. The long-lived radionuclides can do harm only if they are ingested or inhaled.

The plutonium in used fuel is not, strictly speaking, a waste material; it could be recovered by reprocessing and recycled to produce more energy. If the used fuel were reprocessed, the resulting liquid waste would be converted to a highly insoluble glass or glass-ceramic form.

Sodium aluminosilicate glasses have been developed as potential matrices to contain calcined fission product wastes derived from the PUREX process. The resulting waste form has been found to be superior to that based on borosilicate glass and, over a wide range of composition, has a low leach rate in saline groundwaters characteristic of the Canadian Shield [Tait and Mandolesi 1983]. However, aluminosilicate glasses have higher viscosities than borosilicate glasses, which makes their melting and pouring impractical using conventional Joule-heated melters.

Glass-ceramics, based on the natural mineral sphene, have been shown to give further improvements in leach resistance [Hayward 1986]. In this composite material, the sphene is present as a crystalline phase within a continous matrix of durable aluminosilicate glass. The sphene contains a significant fraction of the fission product ions in solid solution, and has been found to be highly resistant to dissolution in many geochemical environments. The composite material can be produced using established glass-making technology: casting from temperatures between 1,250 C and 1,350 C, and controlled recrystallization by reheating to between 900 C and 1,050 C.

Disposal Concept

Either used-fuel bundles or immobilized reprocessing waste would be sealed in corrosion-resistant containers. Figure 4 shows a conceptual design for a thin-walled, particulate-filled container, containing 72 CANDU fuel bundles. Prototype containers of this design, with a 4-mm thick titanium alloy outer shell,

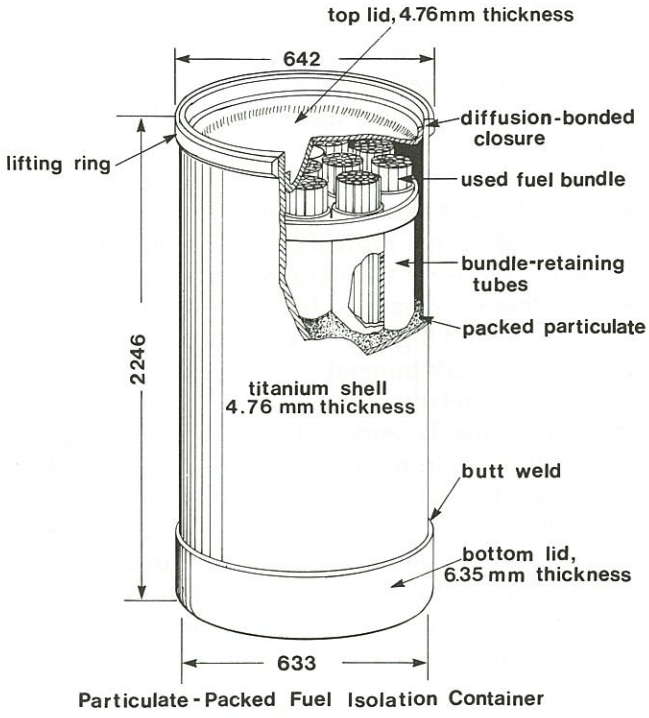

Figure 4 Conceptual design for a thin-walled, particulate-filled container for used CANDU fuel.

have withstood external pressures up to 10 MPa at 150 C, meeting the primary structural requirements for disposal in a vault at a depth of 1,000 m (Teper 1985). Titanium alloys have been found to have sufficient corrosion resistance to provide leak-tightness for at least 500 years, the time during which the hazard is greatest [McKay 1984]. Corrosion experiments indicate that copper would also be an acceptable material for the outer shell.

The disposal vault, shown in Figure 5, would resemble a conventional mine in hard rock, although the quality of the excavation would be superior to that normally required in a conventional mine. A 2-km square network of disposal rooms and access tunnels would be sufficient to dispose of about 190,000 Mg of used CANDU fuel (10 million bundles). It would take about 40 years to fill the vault. Note that the committed 15,500 MW Canadian nuclear-electric generating system, if operated to the year 2,050, would produce about 120,000 Mg of used fuel.

The waste containers would be lowered through a vertical shaft to rooms excavated in the rock mass, 500 m to 1000 m beneath the surface, and placed in holes bored into the floor of the rooms. Prior to receiving the waste containers, the holes would be filled with a mixture of sodium-bentonite clay and sand, mechanically compacted and then rebored to provide a central hole. The clay-sand buffer acts as a diffusion barrier to the movement of groundwater, inhibiting the transport of radionuclides away from the container

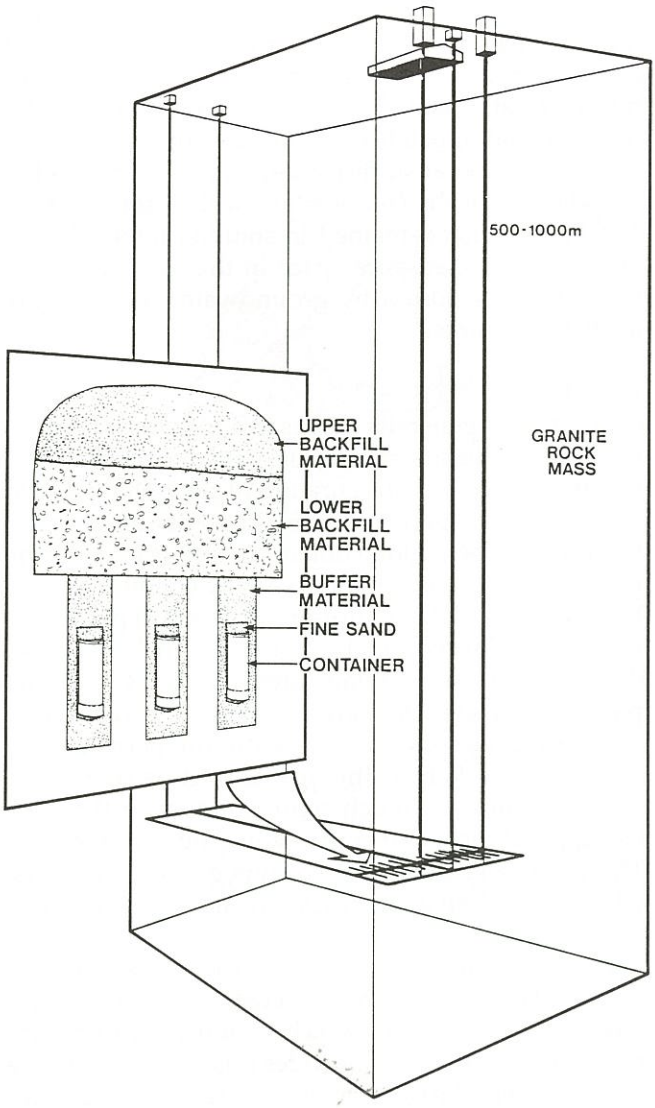

Figure 5 The Canadian concept for a nuclear fuel waste disposal vault.

[Cheung and Chan 1985]. The clearance space between the container and the buffer would be filled with sand.

When filled with waste containers, each room would be backfilled and sealed. The backfilling would be done in 2 stages: first, the lower portion of the room would be filled with a mixture of clay and crushed granite, which would then be mechanically compacted; second, the remaining space would be filled, probably pneumatically, with a mixture of granite aggregate and bentonite-clay. To close the vault, the access tunnels would be backfilled in a manner similar to the disposal rooms, and the access and ventilation shafts would be fitted with a series of bentonite-clay / contrete seals, separated by a backfill mixture of compacted clay and crushed granite.

Post-Closure Behaviour

Vault

After vault closure, as the backfilling materials are saturated with groundwater from the surrounding rock, the bentonite-clay would swell to complete the sealing of containers and disposal rooms. Complete saturation of the buffer and backfill materials is expected to take a few hundred years. Experiments show that the backfilling materials would be as impermeable to groundwater as the surrounding rock.

Heat transferred from the waste containers would gradually raise the temperature of the buffer and backfill materials, and the surrounding rock. Thirty years after a disposal room is closed, the container shell temperature would reach a maximum of about 100 C. About 200 years after closure, the shell temperature would decrease to about 80 C, and then remain at this temperature for another 1,300 years, before decreasing very slowly to the ambient temperature of 15 C. The temperature of the buffer and backfill materials would follow that of the containers, reaching a maximum average temperature of 85 C after about 50 years.

At the depth proposed for a disposal vault, the groundwater is expected to be highly saline, containing high calcium and sodium chloride concentrations [Fritz and Frappe 1982]. The salinity decreases with decreasing depth, and carbonate-rich groundwaters are typically found at shallower depths. Thus, the composition of the groundwater that saturates the vault will depend on its source, and this will in turn depend on the hydraulic conductivity of the rock mass around the vault.

Initially, the groundwater would react with the backfill and buffer materials [Vandergraaf 1987]. The more soluble ions would be leached from the crushed rock, leading to an increase in the pH of the groundwater because of the substitution of alkali metal ions on the surface of the crushed rock by hydrogen ions from the groundwater. The ionic strength of the groundwater may increase slightly. Also, air trapped during backfilling could oxidize ferrous-iron-containing minerals and any organic material present, leading eventually to reducing conditions.

Radiolysis of the groundwater near the waste containers would produce hydroxide and oxide radicals. The oxide radicals would in turn react with ferrous-iron-containing minerals, thus competing with entrapped oxygen, and increasing the time to reach reducing conditions. It should be noted that the chemical reaction rates would be extremely slow and might take thousands of years to reach equilibrium.

After interacting with the groundwater for several hundred years, some container shells would corrode sufficiently to allow the groundwater to come into contact with the used fuel. The rate at which radionuclides could be released is shown in Figure 6

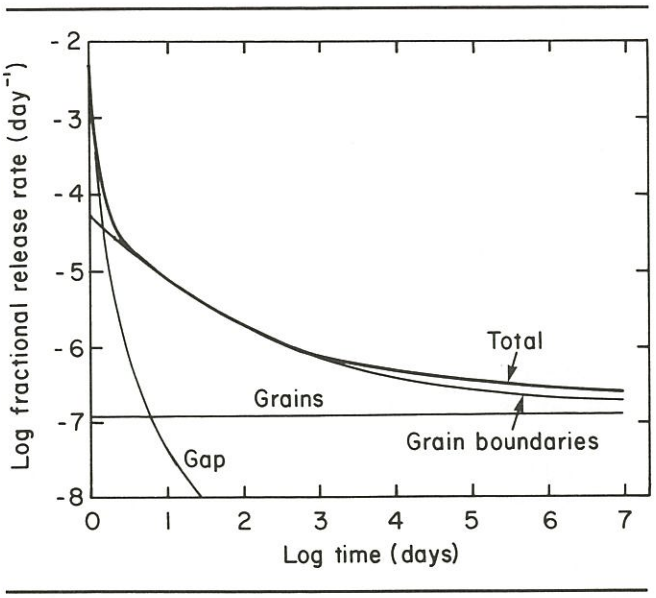

Figure 6 Release of radionuclides from CANDU fuel.

[Garisto *et al.*, to be published]. There are 3 principal release mechanisms:

1 *A rapid release of a fraction (about 2%) of the iodine and cesium when the fuel sheath is breached.* This instant release occurs from spaces between the fuel pellets and sheath, to which volatile fission products migrate during irradiation.
2 *Slow release of the remaining inventory of iodine and cesium by preferential dissolution at the grain boundaries.* The rate of release depends on the irradiation history, which affects the fuel microstructure. In fuels that have been irradiated at high power, the porosity at the grain boundaries is interconnected, allowing water to percolate through the fuel and contained fission productions to escape. In fuel irradiated at low power, there are few interconnected pores, and the release of fission gases is then mainly controlled by dissolution of the uranium dioxide grains and grain boundaries.
3 *Extremely slow release of the remaining fission products and actinides trapped within the uranium dioxide grains by congruent dissolution.* The rate of dissolution is determined by the groundwater redox conditions, lower releases occurring under reducing conditions.

The behaviour of the radionuclides in the vault would depend strongly on the groundwater composition, the temperature, and the minerology in the vault. Cesium and iodine are highly soluble. However, cesium sorbs strongly onto clay materials and phyllosilicates by an ion exchange mechanism, if the ionic strength of the groundwater is low. Iodine does not sorb on natural minerals. Technetium, which is multivalent, has a complex behaviour: under oxidizing conditions it forms poorly sorbing anionic species; however, under reducing conditions it is only slightly soluble and will be present in groundwater only at very low concentrations. The actinides also have multivalent oxidation states. In their reduced state, they also tend to be only slightly soluble; in their higher oxidation states they are more soluble, and tend to form complexes with anionic species such as chloride and carbonate. Thus, a certain fraction of the released radionuclides would be precipitated or sorbed on mineral surfaces, depending on the radionuclide and on the composition of the groundwater. The fraction that remained in solution might diffuse into the connected pore space in the rock matrix, or might be transported by groundwater through any fracture networks.

Rock Mass

Groundwater generally moves in a rock mass because of a three-dimensional potential field that provides the driving force. The configuration of the potential field depends on the particular forces (gravity or temperature) within the region containing the rock mass, the geometry of the region and the flow conditions at its boundaries, and the nature and variation of properties that control flow within the region. Our field research, described in more detail later, indicates that the plutonic intrusives of interest can be conceptualized as relatively large rock volumes with low permeability, separated by relatively thin planar fracture zones. The fracture zones are much more conductive than the background rock, and control the groundwater flow. The flow is primarily driven by topographic gradients, which in the Canadian Shield are small on a regional scale.

The rate of movement of dissolved and suspended radionuclides would be affected by sorption and mechanical dispersion, which would tend to reduce the velocity of the radionuclides relative to that of the groundwater. The surfaces of fractures are coated with alteration minerals. Radionuclide ions in solution, such as cesium, plutonium, and technetium, can participate in exchange reactions with these alteration minerals, resulting in a reduction of the radionuclide concentrations in solution. Also, the heat generated by the waste will set up a temperature gradient, and thermal cycling of groundwater may occur. Minerals that go into solution in the vault, which is higher in temperature than the surrounding rock, may precipitate when the groundwater is cooled by the rock mass. The precipitation of alteration minerals will tend to decrease the fracture aperture, and some fractures may seal.

Mechanical dispersion is a mixing phenomenon. It causes a convective front of radionuclides moving through the rock matrix to spread laterally and longitudinally, and thus to dilute. Diffusion, mass flow caused by a concentration gradient, is a secondary component of the dispersion mechanism that also contributes to dilution. It is significant only when convective transport is very slow. Nonsorbing radio-

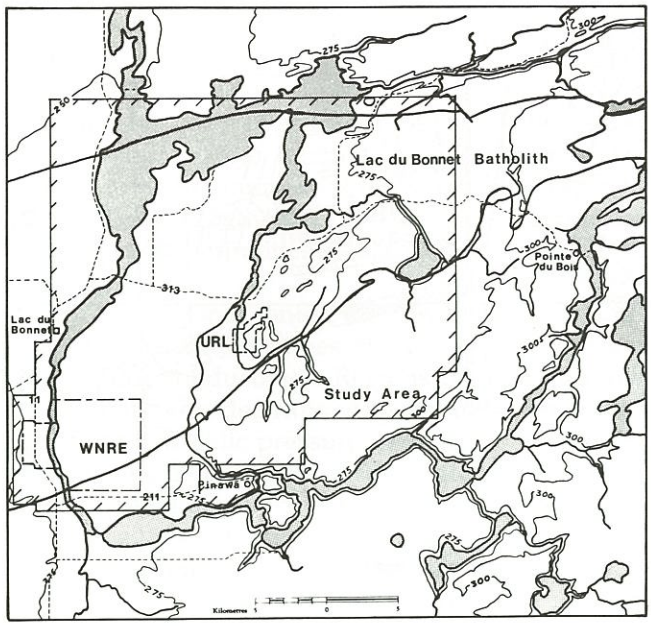

Figure 7 Location of the Whiteshell Research Area.

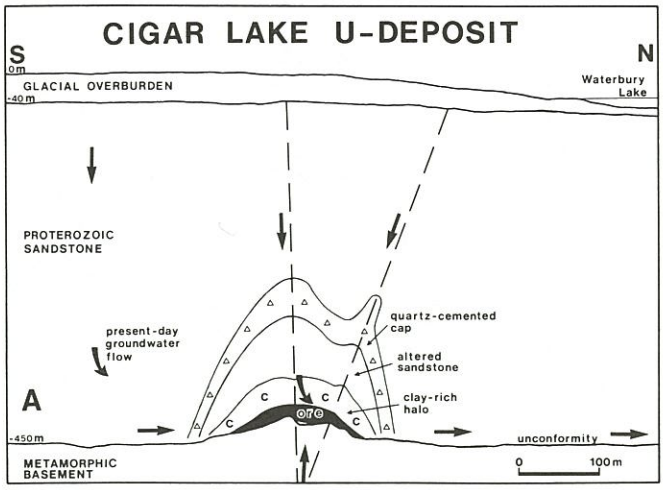

Figure 8 Cigar Lake Uranium Deposit: a natural analogue for some aspects of disposal vault geochemistry.

nuclides, such as iodine, diffuse readily through the connected pore space of the rock matrix. Also, if sorption is depressed, by an increase in the ionic strength of the groundwater, diffusion of even trace concentrations of cesium has been shown to take place over distances of 100 mm in periods as short as 6 months.

Field Research Areas

Field research areas have been established at 3 locations in the Precambrian Canadian Sheild: in the Atikokan and East Bull Lake regions of northern Ontario, and in the Whiteshell region of southeastern Manitoba. Since 1978, these research areas have been extensively characterized from a geotechnical perspective and monitoring of the groundwater flow system in each area is continuing via instrumented networks of boreholes. Field work on a smaller scale is also continuing at AECL's Chalk River site.

The Whiteshell research area (see Figure 7) is now the main focus of our field studies. This region contains the Whiteshell Nuclear Research Establishment and AECL's Underground Research Laboratory (URL), and provides a unique opportunity to validate site characterization methodologies at the scale now thought necessary to characterize a candidate disposal site. The region is situated on the Lac du Bonnet Batholith, a large granite pluton similar to many found in the Canadian Shield. There is a moderate topographic slope across the region of about 50 m from the southeast to the northwest. The Winnipeg River provides stable hydrological boundaries: along the east side of the region the river is controlled at about 273 m, along the south at about 273 m, and along the west at about 254 m.

Cigar Lake

The Cigar Lake uranium deposit is located in northern Saskatchewan and is the focus of a study aimed at gaining insight into long-term geochemical processes [Cramer 1986]. The ore body has survived for 1.3 billion years in a relatively open groundwater system and has no direct chemical or physical signature at the surface.

The deposit is situated at a depth of 430 m, at the interface between the host sandstone formation and the underlying basement rock of the Archean Shield. The ore body is lens-shaped (2,000 m long, 100 m across, and 20 m thick at mid-length), and is capped by a 5-m- to 30-m-thick clay-rich halo. An iron oxide / hydroxide-rich zone forms the contact between the high-grade ore and the clay-rich halo. The average ore-grade is 14% U_3O_8, with local concentrations as high as 60%.

Figure 8 shows a cross section of the deposit in the north-south direction, which coincides with the direction of groundwater flow now. Near the ore body, groundwater flows along a zone of relatively high hydraulic conductivity between the sandstone and the basement rock. The ore body is situated at the intersection of the interface with a number of near-vertical fractures. The local alteration of the sandstone and the uranium mineralization is attributed to hot, reducing water discharged from the basement rock into the sandstone through these fracture conduits. The most plausible mechanism for the formation of the deposit is precipitation of dissolved uranium from local groundwaters, caused by interaction with the hot, reducing water discharged from the basement rock. Alteration of the sandstone is characterized by changes in its

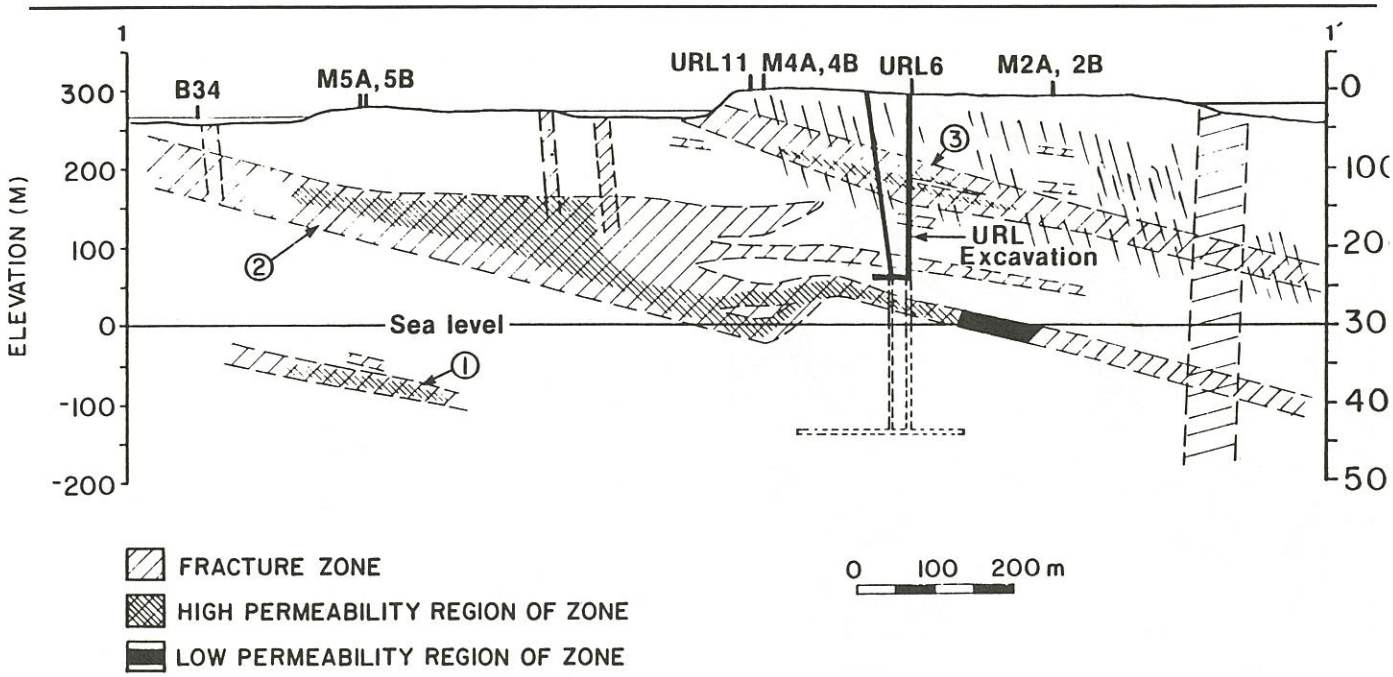

Figure 9 Cross section showing fracture zones in the rock mass containing the URL.

colour and by the clay content. Quartz, in solution, migrated down the thermal gradient and precipitated in the cooler, less altered sandstone to form the quartz outer layer of the cap.

The composition of the ore body is relatively simple: a high concentration of uranium, very small concentrations of other actinides and lanthanides, and extremely small concentrations of radionuclides formed by uranium decay and by natural fission of uranium. The higher uranium concentrations within the quartz cap are consistent with the hydrothermal process that resulted in the formation of the cap and the ore body. There has been no enrichment of uranium on secondary minerals found on open surfaces of fractures in the sandstone further away from the quartz-cap.

The geochemical questions of particular interest are: How did the ore body survive for so long in such an open system saturated with groundwater? What transport and fixation mechanisms influenced the migration of radionuclides in the host rock? Answers to these questions are the focus of our ongoing investigation at Cigar Lake, and will provide insight into the processes expected to control radionuclide movement in a disposal vault.

Hydrogeology

A detailed understanding of the hydrogeology of a candidate rock mass is essential to assess its acceptability. Our methodology for gaining this understanding is derived from a structured process which integrates the various geoscience disciplines. First, the geological features of the rock mass that control the groundwater flow, and the associated physical, chemical, and hydrological characteristics, are determined from field investigations. Then, these geological features and their characteristics are interpreted to establish a conceptual model of the groundwater flow system. Next, based on the conceptual model, a detailed 3-dimensional mathematical model of the flow system is used to predict changes caused by natural and artificial perturbations of the rock mass and flow system. Finally, comparisons are made between predicted and measured responses, to test the conceptual and mathematical models, and to refine them so that, together, they provide a realistic representation of the actual groundwater flow system. As an illustration, a description follows of the methodology as it was applied to the characterization of the site for the URL [Davison 1985].

Over 100 boreholes were drilled into the shallow overburden deposits and into the underlying granite to depths up to 1,100 m. Fractures were characterized in the boreholes, using a number of techniques: by detailed core-logging methods, by in-hole television camera equipment, and by a variety of standard and innovative borehole geophysical logging techniques. Hydraulic conductivity measurements were made at selected intervals in individual boreholes. In addition, interference tests were done, in which water was either injected or withdrawn from one borehole, while groundwater pressures were measured in isolated intervals in neighboring boreholes. These tests provided an understanding of the hydraulic conductivity of the portion of the rock mass between the boreholes.

Analysis of the information obtained from the field investigation identified 3 major fracture zones, shown in Figure 9, dipping at about 20 degrees to the horizontal. The upper and lower zones are relatively uniform and have thicknesses of a few metres. In contrast, the middle fracture zone has a complex geometry, with a number of off-branching limbs. At the surface of the batholith, the fracture zones coincide with major discontinuities identified during geological mapping.

The fracture zones control the movement of groundwater and, within the zones, there is a wide variation in hydraulic conductivity. Regions of high and low conductivity were determined by continuous monitoring of the hydraulic pressure in isolated intervals in the network of boreholes during interference tests. Outside the fracture zones, the rock is relatively unfractured, except for sets of near-vertical fractures that extend from the surface to depths from 100 m to 300 m. These vertical fractures are oriented roughly parallel to the direction of the maximum principal stress.

To describe this conceptual model mathematically, a finite-element computer model, called MOTIF, has been developed [Guvanasen 1985]. It represents the relatively unfractured background rock by an equivalent porous medium, composed of 3-dimensional continuum elements. The high-conductivity zones are represented by special planar elements, which are embedded in the background porous medium. The flow within these planes is dominant along their axes. The 3-dimensional flow field within this assembly of blocks and planar elements is described by porous medium flow equations.

To test these models, the response of the groundwater flow system to the excavation of the URL shaft was predicted at 171 isolated intervals in the network of boreholes used to characterize the rock mass [Guvanasen *et al.* 1985]. These predictions were then compared to the measured responses as the excavation proceeded [Davison 1986].

Figure 10 shows the measured and predicted rate of groundwater flow into the shaft during excavation. The first inflow occurred when several water-bearing near-vertical fractures intersected the shaft walls. The rate of inflow increased as the excavation passed through the upper fracture zone. Notice that the inflows predicted by the MOTIF computer model are generally greater by a factor of three. The predicted maximum inflow occurred as the upper fracture zone was penetrated. At the time the prediction was made, the presence of the vertical fractures was unknown. Subsequently, the predicted rate of inflow gradually declined to a constant value, consistent with the measured inflow.

Figure 11 shows a comparison between measured and predicted histories of hydraulic head at one of the

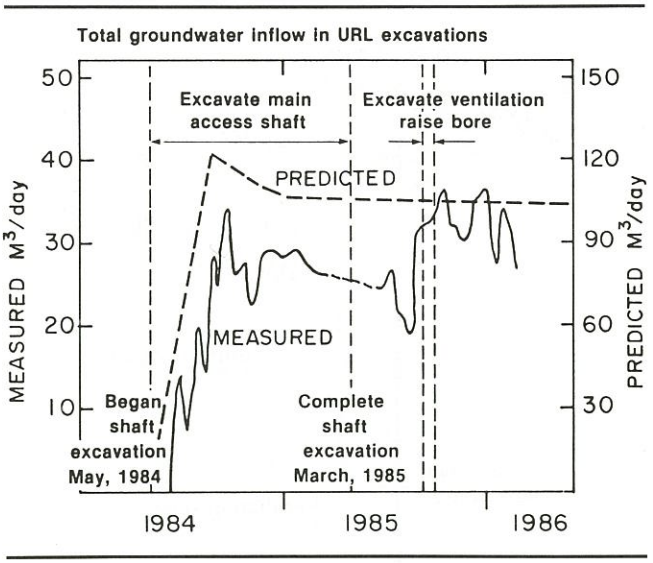

Figure 10 Comparison of predicted and measured groundwater inflow into the URL shaft.

monitoring locations in the upper fracture zone. The onset of the sharp drop in hydraulic head corresponds to the onset of inflow to the shaft. The agreement between prediction and experiment is generally good. The deviations during the period March 1985 to April 1986 are attributed to seasonal variations in recharge, which were not included in the mathematical model. This agreement is typical of that attained at all monitoring locations used in the comparisons, and gives us confidence that the methodology is sound.

The area involved in the investigation described above is much smaller than would be required to characterize a candidate disposal site. So we ask: Can the methodology be transferred to the regional scale, where distances between recharge and discharge can be as much as 10 km to 20 km?

To answer this question we have begun an investigation of the entire Whiteshell research area to a depth of at least 1,000 m. The scope of the field investigations includes: conducting additional detailed geological

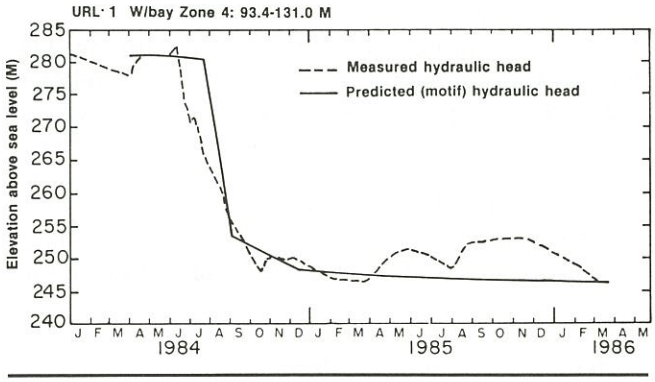

Figure 11 Comparison of predicted and measured hydraulic head of borehole URL-1 in the upper fracture zone.

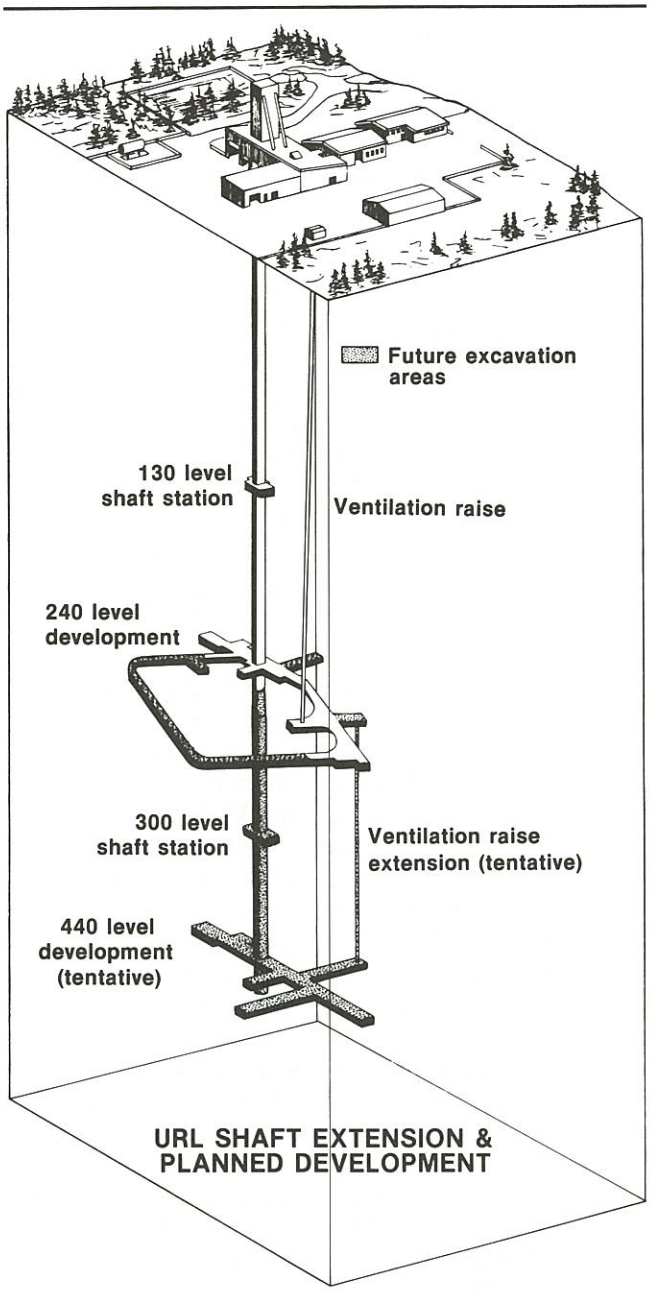

Figure 12 Schematic of the Underground Research Laboratory.

and geophysical surveys in the region; drilling, logging, and instrumenting a network of deep boreholes; and monitoring the groundwater chemistry and hydraulic head fluctuations in the network of boreholes. The areas of particular interest are: the boundary of the batholith; major surface features that are possibly structural discontinuities, such as faults or fracture zones; and the subsurface geological structure and groundwater head distribution.

Underground Research Laboratory

Construction of the URL is now at an advanced stage. It is being constructed in a part of the Whiteshell research area which had not been previously disturbed. The excellent outcrop in the area facilitated the geological characterization of the site. The location of the access shaft and underground laboratory rooms was based on knowledge of the underlying geological structure and groundwater flow system derived from extensive geological and hydrogeological characterization, beginning in 1979. The characterization of the granite rock mass and the excavation of the shafts and rooms contributed directly to the development of a comprehensive methodology to characterize disposal sites and to evaluate their isolation potential. To date, work at the URL has provided unique information on the response of the rock mass and its groundwater flow system. Construction of the URL has also allowed us to test excavation techniques that could be used to construct a disposal vault, particularly drilling and blasting procedures that minimize damage to the rock near excavation surfaces.

The present state of underground development at the URL is shown in Figure 12. The excavations include a 3 m by 4 m rectangular access shaft and a 2-m-diameter ventilation shaft, both 250 m deep, and laboratory rooms excavated at a depth of 240 m. Preparations are underway to extend the access shaft to a depth of 455 m as part of an agreement with the U.S. Department of Energy. The shaft extension will pass through a highly permeable fracture zone just below the 255-depth, and work is underway to characterize and grout this zone prior to beginning the excavation. Excavation of the shaft extension will take place in the period June 1987 to September 1988, and its geotechnical characterization is expected to be completed by September 1989. The rock mass around the shaft at the 455-m level will also be characterized to select sites for experiments. Included will be experiments to study how the rock mass responds to heating, how contaminants and groundwater move through the rock mass, and how various sealing methods perform.

Conclusion

The understanding of basic physical and chemical processes derived from the laboratory and field investigations highlighted above has been incorporated into a mathematical model that describes the complete disposal system for assessments of long-term safety. This model of the disposal system links individual mathematical models for the vault, rock mass, and surface environment to provide an estimate of the range of possible effects to individuals at some future time from an implementation of the disposal technology. This methodology has been developed to conform with the basic safety criteria, and we are confident that it will provide an accurate assessment of the disposal concept's safety.

An innovative methodology for characterizing the

hydrogeology of a plutonic rock mass has been successfully applied and validated in the field to a depth of 400 m. This methodology is now being applied at a regional scale comparable to that required to characterize a candidate disposal site. Based on our experience to date, we are confident that the process by which detailed *in situ* measurements are used (to develop a conceptual model of the hydrogeology of a site which is then idealized into a three-dimensional description) is generally valid.

Our field investigations in the Canadian Shield, supported by assessments of conceptual disposal vault designs, give us confidence that there are a large number of locations which, after detailed examination, will provide disposal sites that meet the basic safety criteria.

Acknowledgements

This paper was originally presented at the Canadian Engineering Centennial Conference, Montreal, 18–22 May 1987.

Notes and References

1. *Aitken JM, Harrison JM, Hare FK.* The management of Canada's nuclear wastes. Energy, Mines and Resources Canada Report, EP-77-6, August 1977.
2. *Atomic Energy Control Board.* Criteria for concept assessment: geological consideration in siting a repository for underground disposal of high-level radioactive waste. Proposed Regulatory Guide, Consultative Document, c-72, 1984.
3. *Atomic Energy Control Board.* Regulatory objectives, requirements and guidelines for the disposal of radioactive wastes. Proposed Regulatory Policy Statement, Consultative c-104, 1986.
4. *Boulton J,* (Ed. management of radioactive fuel wastes: the Canadian disposal program. Atomic Energy of Canada Limited Report, AECL-6314, October 1978.
5. *Cheung SCH, Chan T.* Parameter sensitivity analysis of near-field radionuclide transport in buffer material and rock for an underground nuclear fuel waste vault. Proc Int Symposium on Applied Simulation and Modelling, Montreal. Calgary: Acta Press, 1985: 281.
6. *Cramer JJ.* A natural analog for a fuel waste disposal vault. Proceedings of the Second International Conference on Radioactive Waste Management, Winnipeg. Canadian Nuclear Society, September 1986.
7. *Davison CC.* Hydrogeological characterization of the URL site. Atomic Energy of Canada Limited Technical Record, TR-299, 1985: 231–52.
8. *Davison CC.* URL drawdown experiment and comparisons with model predictions. Atomic Energy of Canada Limited Technical Record, TR-375, 1986.
9. *Fritz P, Frape SK.* Saline groundwaters in the Canadian Shield – first overview. Chemical Geology 1982; 36: 179–90.
10. *Garisto NC, Garisto F, Harvey KB, Johnson LH.* Source terms for the assessment of nuclear fuel waste disposal in Canada. Proc Waste Management, Tucson, 1986. pp. 397–402.
11. *Guvanasen V.* Development of a finite-element code and its application to geoscience research. Atomic Energy of Canada Limited Technical Record, TR-299, 1985: 554–66.
12. *Guvanasen V, Reid JAK, Nakka BW.* Predictions of hydrogeological perturbations due to the construction of the underground research laboratory. Atomic Energy of Canada Limited Technical Record, TR-344, 1985.
13. *Hancox WT.* Progress in the Canadian nuclear fuel waste management program. Proceedings of the Second International Conference on Radioactive Waste Management, Winnipeg. Canadian Nuclear Society, September 1986.
14. *Hayward PJ.* Review of progress in the development of sphene-based glass-ceramics. *In*: Scientific Basis for Nuclear Waste Management 9, Ed. Werme LO. New York and Amsterdam: Elsevier – North Holland, 1986: 355–63.
15. *Mayman SA, Barnes RW, Gale JE, Sanford BV.* The Canadian program for storage and disposal of spent fuel and high-level wastes. Proceedings of the IAEA Symposium on the Management of Radioactive Wastes from the Nuclear Fuel Cycle, Vienna, March 1976.
16. *McKay P.* Crevice corrosion of Ti-(0.8%)Ni-(0.3%)Mo alloy in chloride environments at elevated temperatures. Proc of the Ninth Int Metal Cong 1984; 3: 288.
17. *OECD Nuclear Energy Agency.* Nuclear spent fuel management: experience and options. Paris, 1986.
18. *Tait JC, Mandolesi DL.* The chemical durability of alkali aluminosilicate glasses. Atomic Energy of Canada Limited Report, AECL-7803, 1983.
19. *Teper B.* Feasibility assessment of the particulate-packed, thin-walled container. Atomic Energy of Canada Limited Technical Record, TR-350, 1985; 1:21.
20. *Vandergraaf TT.* High-level nuclear waste management: a geochemical perspective. To be presented at the CSCE Centennial Symposium on Management of Waste Contamination in Groundwater, Montreal, May 1987.

The Projected Environmental Impacts of Transportation of Radioactive Material to the First United States Repository Site – An Overview

J.W. Cashwell, K.S. Neuhauser and P.C. Reardon
Sandia National Laboratories
Albuquerque, NM
G.W. McNair
Pacific North West Laboratory
Richland, Washington

Abstract

The relative national environmental impacts of transporting spent fuel and other nuclear wastes to each of 9 candidate repository sites in the United States were analyzed for the 26-year period of repository operation. Two scenarios were examined for each repository: 1) shipment of 5-year-old spent fuel and Defence High-Level Waste (DHLW) directly from their points of origin to a repository (reference case); 2) shipment of 5-year-old spent fuel to a Monitored Retrievable Storage (MRS) facility and shipment (by dedicated rail) of 10-year-old consolidated spent fuel from the MRS to a repository. Transport by either all truck or all rail from the points of origin were analyzed as bounding cases. The computational system used to analyze these impacts included the WASTES II logistics code and the RADTRAN III risk analysis code. The radiological risks for the reference case increased as the total shipment miles to a repository increased for truck; the risks also increased with mileage for rail but at a lower rate. For the MRS scenario the differences between repository sites were less pronounced for both modal options, because of the reduction in total shipment miles possible with the large dedicated rail casks. All the risks reported are small in comparison to the radiological risks due to 'natural background.'

Résumé

L'impact relatif sur l'environnement du transport du combustible épuisé et des autres déchets nucléaires jusqu'aux neuf sites susceptibles d'être choisis comme dépôts aux États-Unis a été étudié. Deux scénarios ont été envisagés pour chacun de ces sites: 1) combustible épuisé vieux de 5 ans et déchets de haute activité provenant des armes nucléaires expédiés directement de leurs points d'origine jusqu'aux sites (cas de référence); 2) combustible épuisé vieux de 5 ans expédié possibilité de reprise et combustible épuisé consolidé vieux de 10 ans expédié (par voie ferrée réservée) des installations de stockage contrôlé avec possibilité de reprise jusqu'à un site. Le transport par camion ou par wagon à partir des points d'origine a servi de cas limite. Le système informatique utilisé pour analyser cet impact était constitué du code logistique WASTES II et du code d'évaluation des risques RADTRAN III. Dans le cas de l'expédition par camion, les risques radiologiques du cas de référence augmentent avec la distance totale en milles jusqu'au site du dépôt; les risques augmentent aussi avec le transport par wagon, mais às un rythme plus lent, toutefois. En ce qui a trait au deuxième scénario, les différences entre les sites des deux options modales sont moins accentuées en raison de la réduction du nombre total de milles parcourus avec les châsteaux sur voie ferrée réservée. Tous les risques signalés sont faibles comparativement à un 'milieu naturel.'

Introduction

Spent fuel from commercial nuclear power reactors in the United States will be permanently disposed of in mined geologic repositories. The Nuclear Waste Policy Act (NWPA) of 1982 outlined the implementation of this approach by the US Department of Energy (DOE). The DOE has begun selection of a site for a first repository from among 9 candidate sites in 3 geologic media – salt, tuff, and basalt. A monitored retrievable storage (MRS) facility may be included in the system; spent fuel could be stored for up to 5 years at an MRS, which would also consolidate the fuel before shipping it to the repository.

This paper reviews the analysis of the relative national environmental impacts of transporting nuclear wastes to each of the 9 candidate repository sites in the United States [Cashwell 1986]. This analysis was performed to support the repository environmental assessments, which were used as input to the selection of three priority sites. The sites selected for further

Keywords: Radioactive materials transport, environmental impacts, risk assessment, costs, comparative evaluations, road transport, rail transport, spent fuels, high-level radioactive wastes.

characterization were the Permian Basin in Texas; Yucca Mountain, Nevada; and Hanford, Washington.

Several of the potential sites were closely clustered and, for the purpose of distance and routing calculations, were treated as a single location. These are: Cypress Creek Dome and Richton Dome in Mississippi (Gulf Interior Region), Deaf Smith County and Swisher County sites in Texas (Permian Basin), and Davis Canyon and Lavender Canyon sites in Utah (Paradox Basin). The remaining sites are: Vacherie Dome, Louisiana; Yucca Mountain, Nevada; and Hanford Reservation, Washington.

For compatibility with both the repository system authorized by the NWPA and with the MRS option, 2 separate scenarios were analyzed. In brief, they are 1) shipment of spent fuel and high-level waste (HLW) directly from waste generators to a repository (reference case), and 2) shipment of spent fuel to a MRS facility, and then to a repository.

Problem Definition

In order to perform comparative cost and risk analyses of the impacts of transportation for a future US nuclear waste management system, a large array of data is required. These data include information on the transport links and surrounding populations, routing information (e.g., distances traveled), packaging (e.g., cask capacity), transport mode characteristics (e.g., train speeds), radionuclide inventory, and pertinent operational characteristics of the system, such as accident rates. These data are used as input for 2 major computational tools, the WASTES II logistics code and the RADTRAN III risk analysis code.

For the reference case, the primary waste stream is spent nuclear fuel (SF) from reactors. Secondary waste streams considered for this case include defence high-level wastes (DHLW) from the Savannah River Plant in South Carolina, the Hanford Reservation in Washington, and the Idaho National Engineering Laboratory in Idaho; and commercially generated high-level waste from West Valley, New York (WVHLW). Acceptance of DHLW in a commercial repository was endorsed by the President of the United States in 1985 [White House Memorandum 1985]. In this case, all reactors will ship 5-year-old, or older, unconsolidated spent fuel directly to a candidate repository site over a 26-year period. High-level commercial and defence wastes will also be shipped directly to the repository. Two primary modal options are examined for the Reference Case: all truck and all rail from reactors and HLW generators. The resultant costs and risks will bound the transportation impacts. No attempt has been made to forecast the actual fractions of truck and rail transport that might be used. The shipping system ultimately used for transportation of spent fuel and HLW will be a combination of modes determined by considerations such as the capabilities of handling facilities at the origins, freight rates, and operational constraints of the system.

MRS input data and scenarios are compatible with those being used by the MRS program. Final MRS documentation to be presented to Congress will, however, include additional alternatives not discussed here.

For the MRS cases, as in the reference case, reactors will ship 5-year-old, or older, unconsolidated spent fuel, but to an MRS rather than a repository. All spent fuel leaving the MRS will be consolidated and at least 10 years old. Additional secondary wastes would be generated at an MRS by the proposed spent fuel consolidation and possible overpacking operations, and would also be shipped to the repository. These secondary wastes would consist of assembly hardware, high-activity waste (HAW), and transuranic waste (TRU). Transport from an MRS would be by one of two possible shipping options: 1) 100-ton (100T) dedicated rail shipments of overpacked consolidated spent fuel and waste byproducts generated in the consolidation process, and 2) 150-ton (150T) dedicated rail shipments of non-overpacked consolidated spent fuel and byproducts. As in the reference case, high-level commercial and defence wastes are shipped directly to the repository. For shipments from the MRS, bounding values for total cask weight and payload characteristics were used either to minimize or to maximize cask capacity and, hence, to put upper and lower limits on the number of shipments from the MRS to the repository.

Methodology

In order to perform cost and risk analyses of the impacts of transportation, a number of assumptions must be made regarding the physical, operational, and geographical characteristics of the system to be analyzed over the time period assumed for operations. For this reason, many of the analyses performed to provide the systems simulations required by the National Environmental Policy Act or the Nuclear Waste Policy Act are comparative in nature during the EA stage. An increasing level of specificity will be required for the final environmental impact statement, as well as for actual budgeting and operational forecasting.

Figure 1 outlines the basic structure of models and data-base input necessary to perform a national transportation cost and risk analysis. The major components of this modeling system are discussed below.

Spent fuel data base – This documents utility responses to a voluntary survey on spent-fuel-discharge rates, storage-pool capacities, and anticipated future operational plans; compiled by Battelle Pacific Northwest Laboratories for the DOE [Heeb 1985].

Electric generating capacity data – The Energy Information Administration (EIA), a branch of the DOE, predicts the anticipated future industry requirements and capabilities by fuel source type, by year [Gieleki 1984].

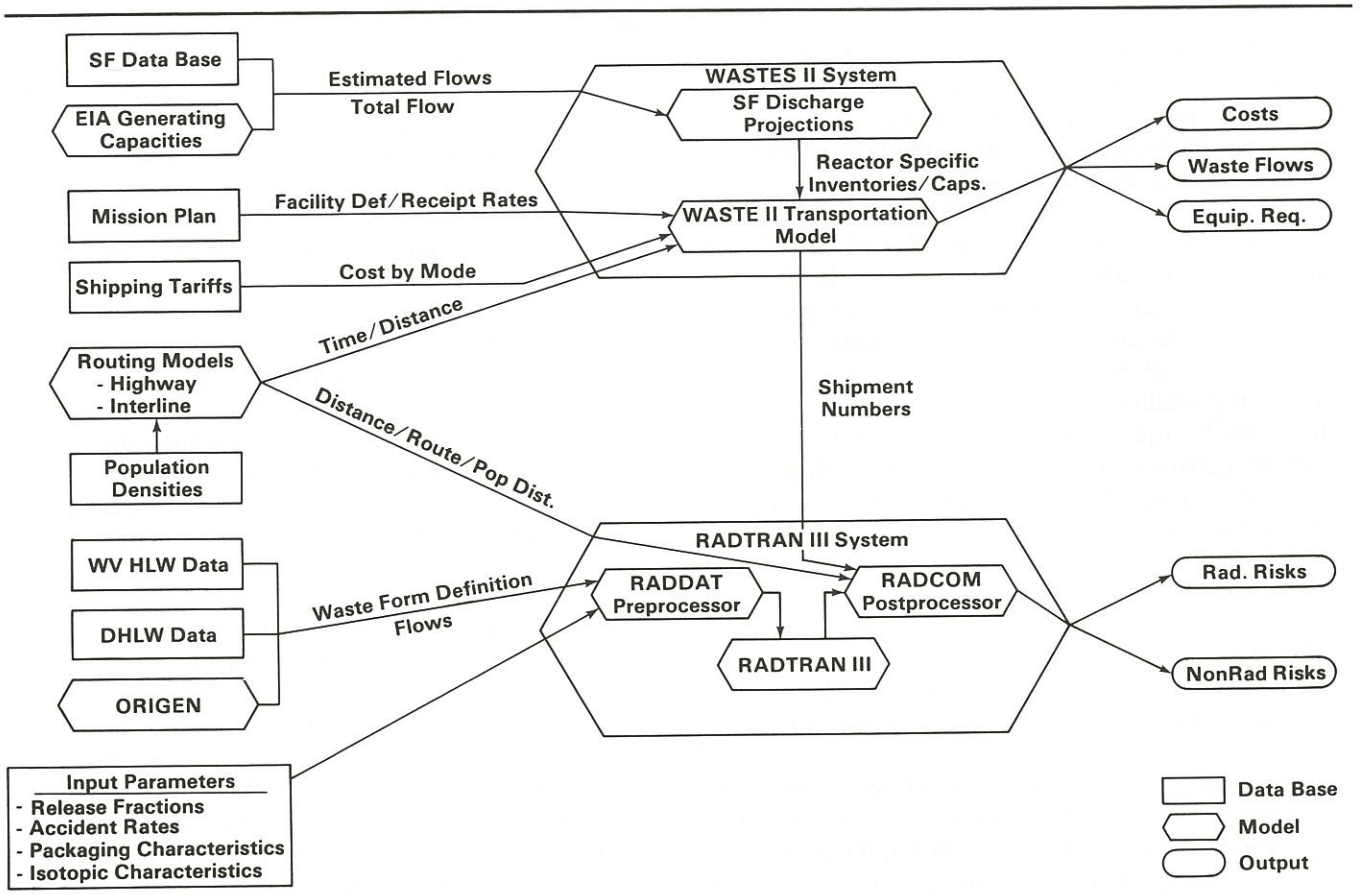

Figure 1 Computational system used in the analysis.

Spent fuel discharge projections – Based upon the spent fuel data base, as adjusted to conform to the EIA mid-case; anticipated waste flows from reactors were calculated [Heeb 1985].

DOE / Office of Civilian Radioactive Waste Management Mission Plan – Anticipated overall receipt rates of spent fuel and HLW at the first repository are furnished in tabular form in this document [DOE Mission Plan 1985]. These data were used to assign priorities to the projected flows discussed above.

Shipping tariffs – Published shipping tariffs are used to calculate the relative costs of transport for a given mode and distance [McNair 1986].

DOE / West Valley waste form definition – The characteristics of the WV commercial high-level waste form [Rykken 1985].

DOE / defence programs HLW waste form definition – Projections of waste-form characteristics for DHLW generated in support of US Defence programs [Baxter 1983].

ORIGEN – Computer code developed to provide the waste-form characteristics of spent nuclear fuel over time [Croff 1980].

HIGHWAY – This routing model is based upon a coded network of the nation's highways. It calculates a travel path, distance, and time for any given origin-destination pair. Both HIGHWAY and INTERLINE require input of all waste shipping (origin) and receiving (destination) facility locations [Joy 1982].

INTERLINE – The INTERLINE model calculates the railroad route and distance between any given origin-destination pair [Peterson 1985].

USGS population density profiles – Use of the US Census Bureau's population characteristics, together with the routes calculated above, permit population densities along the prospective travel routes between each origin-destination pair to be determined.

WASTES – The WASTES model is a simulation-language based model for estimating flows, equipment requirements, inventories, and costs of wastes for a user-defined system. The model requires origin-specific data such as system shipping priorities, storage constraints, distance to receiving facility, and operational parameters specific to the modal assumptions input; WASTES calculates the logistics of the necessary material movements outlined above [Shay 1986].

RADDAT – A computerized preprocesser for input parameters and data for RADTRAN. This code maintains an internal library of radioisotope characteristics which are automatically called and formatted for a given waste form.

Table 1: Total Shipment-Miles (Millions of Miles*) Reference Case – Direct to Repository

	Repository location					
Mode / waste type	*GIR*	*Vacherie*	*Permian*	*Paradox*	*Yucca Mt*	*Hanford*
100% Truck						
SF	67.4	71.7	94.4	115.1	141.8	149.7
DHLW	28.0	28.0	26.0	28.0	33.0	35.0
WVHLW	1.0	1.0	1.0	2.0	2.0	2.0
Total	96.4	100.7	121.4	145.1	176.8	186.7
100% Rail						
SF	11.0	11.7	15.4	18.8	23.2	24.6
DHLW	6.5	6.5	6.1	6.5	7.6	8.4
WVHLW	0.2	0.2	0.2	0.2	0.3	0.3
Total	17.7	21.2	21.7	25.5	31.1	33.3

*1 mile = 1.608 km.

RADTRAN – This model calculates the radiological risks associated with the transport of radioactive materials. Although RADTRAN may be used alone for simple calculations, it is used within the computational system described here to generate unit risk factors (i.e., the risks associated with the transport of 1 shipment over 1 unit of distance in each population-density zone) [Madson 1986]. Separate unit-risk factors are generated for incident-free non-occupational risk, incident-free occupationasl risk, and accident risk for each shipment type in each population density zone. Incident-free non-occupational risk includes risks to persons at stops, persons residing within 800 m of the transport link, and persons sharing the transport link. Incident-free occupational risk includes risk to crew, rail inspectors, etc. Doses for these calculations are based on the maximum regulatory transport index. The accident unit risk is calculated after the basic accident rate is partitioned according to fractional occurrence by population density zone. Fractional occurrence by severity is then accounted for in a severity category matrix. For spent fuel, 6 severity categories were used. Releases may occur in categories III–VI. Release fraction estimates are taken from Wilmot (1981). Exposure pathways included are direct inhalation, cloudshine, groundshine, inhalation of resuspended material, and ingestion.

RADCOM – Combines the unit risk factors from RADTRAN with the numbers of shipments and total distances traveled in each population-density zone, and then sums the terms to calculate total radiological risks. Nonradiological unit risk factors from other sources [National Transportation Statistics 1985] are calculated in a similar manner to determine the total nonradiological risks.

The interactions of these models, as applied to the user-defined input assumptions for the system to be analyzed, allow national transportation costs and risks to be compared for the scenarios of interest to the repository program.

Results

Results of the analysis performed for the reference case are summarized in Tables 1–3, below. The differences in cost and impacts among the various repository sites are related primarily to the total shipping distances (Table 1). As can be noted from the table, spent fuel shipments account for the largest fraction of the total shipping distance for both modal options, comprising from 70–80 per cent of the total truck travel, and from 62–75 per cent of the total rail travel. In either case, the largest percentages are associated with travel to the most western site (Hanford, Washington). The fraction of total travel attributable to spent fuel trans-

Table 2: Total Transportation Costs ($M) Reference Case – Direct to Repository

	Repository location					
Mode / waste type	*GIR*	*Vacheria*	*Permian*	*Paradox*	*Yucca Mt*	*Hanford*
100% Truck						
Capital	227.2	234.2	261.2	290.1	325.1	337.2
Operating	708.9	730.0	866.0	1015.1	1213.6	1277.8
Total	936.1	964.2	1127.2	1305.2	1538.7	1615.0
100% Rail						
Capital	267.3	277.7	300.9	322.5	354.2	362.8
Operating	714.7	734.9	821.6	885.3	991.0	1013.8
Total	982.0	1012.6	1122.5	1207.8	1345.2	1376.6

Table 3: Summary of the Total Risks of Transportation Reference Case – Direct to Repository

	Repository					
Mode	*GIR*	*Vacherie*	*Perimian*	*Paradox*	*Yucca Mt*	*Hanford*
100% truck from origin						
SF						
Radiological[1]	4.6	5.0	6.2	7.7	9.2	10
Nonradiological[2]	13	14	18	24	29	31
HLW						
Radiological	1.8	1.7	1.7	1.8	2.1	2.1
Nonradiological	6.2	5.8	6.2	6.1	7.4	7.4
100% rail from origin						
SF						
Radiological	.16	.17	.18	.21	.24	.25
Nonradiological	.81	.85	1.0	1.3	1.6	1.6
HLW						
Radiologica	.062	.067	.063	.066	.079	.074
Nonradiological	.63	.69	.64	.66	.84	.79
Totals						
Truck from origin:						
Radiological	6.4	6.7	7.9	9.5	11	12
Nonradiological	19	20	24	30	36	38
Rail from origin:						
Radiological	.22	.24	.24	.28	.32	.32
Nonradiological	1.4	1.5	1.6	2.0	2.4	2.4

[1]Radiological health effects include latent cancer fatalities and genetic effects in all generations.
[2]Nonradiological fatalities.

port increases as the potential repository site is shifted to the west, because most of the spent fuel inventory projected to require shipment to the first repository is from reactors in the eastern United States. The relative contribution of high-level wastes requiring shipment to the repository is between 19 and 29 per cent for truck, and 25 and 37 per cent for rail. Although the projected mileage increases as the more western repository options are analyzed, the relative influence of high-level wastes on the results decreases. Data in Table 1 indicate that miles traveled to the westernmost sites (Yucca Mt, Nevada, and Hanford, Washington) are almost double the total shipment miles required for transport to the easternmost sites in the Gulf Interior Region (GIR).

Transportation costs for the repository location options are summarized in Table 2. These costs increase with the total number of shipment-miles; however, because of the tariff structures of the transport modes, they do not increase in a linear manner. Truck costs increase by approximately 75 per cent between the most eastern site in the GIR and the Hanford site in the West. Consistent with the rail rate structure, total rail costs for these sites vary by only about 40 per cent. Truck costs are lower than rail for the easternmost sites and higher than rail for the western sites. The contribution of spent fuel cost to the total is consistent with the fraction of shipment mileage attributable to spent fuel transport for truck; it is somewhat less than the fraction of total mileage for rail.

Because the points of origin of most shipments (i.e., reactors) are primarily in the eastern United States, the average fractions of total travel in rural, suburban, and urban population-density zones are about the same for spent fuel transport to each candidate repository site. Consequently, total travel distance becomes the major discriminator of risk between sites for a given shipment scenario. Table 3 shows that the GIR and Vacherie, Louisiana, sites, which are closest to the origin points, have the lowest overall risks associated with them; while those sites farthest from the majority of the country's reactors have the highest associated risks. However, the total risks associated with the closest repository sites only differ from those for the most distant site by about a factor of 1.9 to 2.1, for truck, and by about a factor of 1.5 to 1.8 for rail. These factors generally parallel increases in shipment-miles, except for the radiological risk of rail transport, which increases at a significantly lower rate than the mileage. A component of radiological risk for rail transport, but not for truck transport, is associated with required endpoint classification and inspection stops. Because this component is distance-independent (i.e., the same for all trips, short or long), the influence of distance traveled on total radiological risk for rail is less pronounced than for truck.

Insertion of an MRS into the system tends to reduce the variation in cost and risk between the potential repository sites, because of the reduction in shipment-miles possible with the large dedicated rail casks. The 100T cask can carry between 18 and 45 consolidated, canistered spent fuel assemblies; the 150T cask capaci-

Table 4: Total Shipment-Miles (Millions of Miles) MRS Case – MRS at Oak Ridge

	Repository location					
Mode / waste typer	*GIR*	*Vacherie*	*Permian*	*Paradox*	*Yucca Mt*	*Hanford*
Truck from origin						
SF to MRS	48.8	48.8	48.8	48.8	48.8	48.8
DHLW to Repos.	28.0	28.0	26.0	28.0	33.0	35.0
WVHLW to Repos.	1.0	1.0	1.0	2.0	2.0	2.0
Rail from Origin						
SF to MRS	8.0	8.0	8.0	8.0	8.0	8.0
DHLW to Repos.	6.5	6.5	6.1	6.5	7.6	8.4
WVHLW to Repos.	0.2	0.2	0.2	0.2	0.3	0.3
Rail from MRS to Repository (150T, nonoverpacked SF)						
	0.2	0.3	0.6	0.8	1.5	1.0
Totals						
Truck from origin:						
150T from MRS	78.0	78.1	76.4	78.6	85.3	86.8
Rail from origin:						
150T from MRS	14.9	15.0	14.9	15.5	17.4	17.7

ty is between 48 and 171 assemblies. The actual payload depends on the fuel type (boiling water reactor (BWR) or pressurized water reactor (PWR)) and the geologic medium of the repository, because the consolidated fuel is packaged differently according to whether the repository is developed in salt, tuff, or basalt. Further, the MRS also reduces the difference in costs and risks between modal options from the reactors and high-level-waste sites. Shipments from origin sites to the MRS dominate the total transportation-related impacts. The 150T rail cask in particular reduces the impacts of transportation from the MRS to the repository because of its large payload per shipment.

Use of repository-specific canisters and overpacks for the MRS cases influences the relative ranking of the Yucca Mountain (tuff) and the Hanford (basalt) repository sites, because the canister and overpack for tuff are lower in capacity than the canister and overpack for basalt (all of the other sites use the canister and overpack for salt). In addition, the projected rail routings between the MRS locations and Yucca Mountain are more circuitous than the rail routings between the MRS locations and Hanford. The combination of increased shipment-miles and reduced canister and overpack capacities causes Yucca Mountain to rank higher in cost and risk than the Hanford repository site. Tables 4–6 summarize the shipment-miles, costs, and risks for the MRS case for a MRS located in Oak Ridge, Tennessee, with 150T dedicated rail casks between the MRS and the repository.

Summary

To summarize, transportation costs increase with the

Table 5: Total Transportation Costs ($M)[1] MRS Case – MRS at Oak Ridge

	Repository location					
Mode / waste type	*GIR*	*Vacherie*	*Permian*	*Paradox*	Yucca Mt	*Hanford*
Truck from reactors, HLW Sites						
Capital	201.0	202.1	204.3	209.8	214.2	217.5
Operating	613.7	608.1	601.1	615.8	639.0	652.9
Rail from reactors, HLW Sites						
Capital	232.3	237.7	235.9	239.5	246.7	250.3
Operating	643.7	646.1	647.5	644.2	667.9	664.4
Rail from MRS to repository (150 T, nonoverpacked)						
Capital	78.6	78.6	78.6	78.6	100.6	84.1
Operating	172.7	199.0	265.3	306.8	468.7	346.8
Totals						
Truck from origin:						
150T from MRS	1066.0	1087.8	1149.3	1211.0	1422.5	1301.3
Rail from origin:						
150T from MRS	1127.3	1161.4	1227.3	1269.1	1483.9	1345.6

[1]The totals presented in this table are for the case in which all spent fuel and HLW wastes are shipped by the mode indicated; dedicated rail shipments from the MRS to the repository are added.

Table 6: Summary of the Risks of Transportation of Spent Fuel and High-Level Wastes: MRS Case – (All SF to MRS, 150T Cask)

	Repository					
Mode	*GIR*	*Vacherie*	*Permian*	*Paradox*	*Yucca Mt*	*Hanford*
100% truck from origin						
SF						
Radiological[1]	3.6	3.6	3.6	3.6	3.6	3.6
Nonradiological[2]	9.1	9.1	9.1	9.1	9.1	9.1
HLW						
Radiological	1.8	1.7	1.7	1.8	2.1	2.1
Nonradiological	6.2	5.8	6.2	6.1	7.4	7.4
1–% rail from origin						
SF						
Radiological	.14	.14	.14	.14	.14	.14
Nonradiological	.92	.92	.92	.92	.92	.92
HLW						
Radiological	.062	.067	.063	.066	.079	.074
Nonradiological	.63	.69	.64	.66	.84	.79
150T rail from MRS						
Radiological	.017	.035	.035	.038	.054	.042
Nonradiological	1.4	2.6	3.8	5.3	1.0	6.1
Totals						
Truck from origin:						
150T from MRS						
Radiological	5.4	5.3	5.3	5.4	5.8	5.7
Nonradiological	17	18	19	20	26	22
Rail from origin:						
150T from MRS						
Radiological	.22	.25	.24	.25	.27	.26
Nonradiological	2.9	4.2	5.3	6.9	12	7.7

[1]Radiological health effects include latent cancer fatalities and genetic effects in all generations.
[2]Nonradiological fatalities.

total number of shipment-miles; however, because of the tariff structures of the transport modes, they do not increase in a linear manner. Truck costs increase by approximately 75 per cent between the most eastern site in the Gulf Interior Region and the Hanford site in the West. Consistent with the rail rate structure, total rail costs for these sites vary by only about 40 per cent. Truck costs are lower than rail for the easternmost sites and higher than rail for the western sites. The contribution of spent fuel cost to the total is consistent with the fraction of shipment mileage attributable to spent fuel transport for truck; it is somewhat less than the fraction of total mileage for rail.

Between 17 and 38 truck accident fatalities, between 1.4 and 7.7 rail accident fatalities, and between 0.22 and 12 radiological health effects can be expected to occur as a result of radioactive material transportation during the 26-year operating period of the first repository. During the same period in the United States, about 65,000 total deaths from truck accidents and about 32,000 total deaths from rail accidents would occur; also an estimated 58,300 cancer fatalities are predicted to occur in the United States during a 26-year period from exposure to background radiation alone (not including medical and other man-made sources) [Oakley 1972]. The risks reported here are upper limits and are small by comparison with the 'natural background' of risks of the same type.

Acknowledgements

This work performed at Sandia National Laboratries, Albuquerque, New Mexico, was supported by the United States Department of Energy under Contract DE-AC04-76DP00789. An earlier version of this paper was presented at the Second International Conference on Radioactive Waste Management, Winnipeg, 7–11 September 1986.

Notes and References

1. *Baxter RG.* Description of defense waste processing facility reference waste form and canister, DP-1606, Revision 1. Aiken, SC: E.I. duPont de Nemours, 1983.
2. *Cashwell JW,* et al. Transportation impacts of the commercial waste management program, SAND85-2715. Albuquerque, NM: Sandia National Laboratories, April 1986.
3. *Croff AG.* ORIGEN2: a revised and updated version of the Oak Ridge isotope generation and depletion code, ORNL-5621. Oak Ridge, TN: Oak Ridge National Laboratory, July 1980.

4. *Gielecki M*, et al. Commerical nuclear power 1984: prospects for the United States and the world, DOE / EIA-0438. Washington, DC: US Department of Energy, 1984.
5. *Heeb CM*, et al. Reactor-specific spent fuel discharge projections: 1984 to 2020, PNL-5396. Richland, WA: Pacific Northwest Laboratories, April 1985.
6. *Joy DS*, et al. HIGHWAY, a transportation routing model: program description and user's manual, ORNL / TM-8419. Oak Ridge, TN: Oak Ridge National Laboratory, December 1982.
7. *Madsen MM*, et al. RADTRAN III. SAND84-0036. Albuquerque, NM: Sandia National Laboratries, Feb. 1986.
8. *McNair GW*, et al. Truck and rail charges for shipping spent fuel and nuclear waste, PNL-4064. Richland, WA: Pacific Northwest Laboratory, Feb. 1986.
9. Mission plan for the civilian radioactive waste management program, DOE / RW-0005. Washington, DC: US Department of Energy, June 1985.
10. National transportation statistics, 1985 annual report, DOT-TSC-RSPA085-5. Washington, DC: US Department of Transportation, June 1985.
11. *Oakley DT*. Natural radiation exposure in the United States, ORP / SID 72-1. Washington, DC: US Environmental Protection Agency, June 1972.
12. *Peterson BE*. INTERLINE, a railroad routing model: program description and user's manual, ORNL / TM-8944. Oak Ridge, TN: Oak Ridge National Laboratory, November 1985.
13. *Rykken LE*. West Valley Nuclear Service Company, Communication, August 1985.
14. *Shay MR, Buxbaum MF*. WASTES: waste system transportation and economic simulations – Version II, PNL-5714. Richland, WA: Pacific Northwest Laboratory, February 1986.
15. White House Memorandum, "1842, April 30, 1985.
16. *Wilmot EL*. Transportation accident scenarios for commercial Spent fuel, SAND80-2124. Albuquerque, NM: Sandia National Laboratories, February 1981.

Book Review

Fallout from Chernobyl
L. Ray Silver, Toronto: Deneau Publishers & Company, 1987.

The worst nuclear power plant accident in history has led to a wide variety of publications that seek to inform, frighten, confuse, advance social causes, make money, garner political power, or direct attention from other issues. In *Fallout from Chernobyl*, Ray Silver seeks to show how the Canadian reaction to the accident fits into the framework of our highly political nuclear policy. Despite the title, therefore, this book is directed toward a Canadian audience, who will see a side to the nuclear debate rarely seen in newspapers or on television. The book has given Silver, a veteran writer on nuclear issues, an opportunity to champion the nuclear industry, and in particular the CANDU reactor.

The book begins with a short description of the accident itself, in which Silver struggles to give an account of a complex sequence of events to a lay audience. Success in this goal is limited, as the short illustrated glossary of nuclear terms cannot be expected to educate the public on the concepts of nuclear power technology. The author works around this problem by comparing the reactor's condition and response to those of machines with which the public has broad familiarity, e.g., the similarity between the unstable nature of a RBMK-type reactor at low power, and a slow-moving airplane on the verge of stalling.

Praise is heaped on the Soviets, particularly Mikhail Gorbachev, who is lauded for his frank discussions of the accident situation. The efficiency of the Russians in entombing the damaged reactor and getting the remaining power plants quickly back on line is starkly contrasted to the drawn-out western response to Three Mile Island. The detailed first-hand accounts by the Russians who fought to bring the damaged reactor under control make fascinating reading, and provide a unique study of human behaviour under conditions of severe stress.

In the following chapters, dealing evacuation efforts and the international spread of contamination, there are intermittent jumps to the Canadian nuclear scene. Both past and current issues are described in a somewhat random order, as the book eventually shifts completely to a description of Canadian nuclear policy (or lack of it). More than one book has been placed inside this single cover; the Chernobyl accident and development of the Canadian nuclear industry each merit their own by-line. This uneasy combination of two themes, and the apparent rush to bring the book to press, contribute in places to a somewhat uneven editing job; numerous events and data are unnecessarily repeated, and there is an excessive 'hopping' from one scene, and one time period, to another.

Three Canadian groups come under particularly strong attack by Silver, not only for their response to the accident, but for their entire approach to nuclear issues. He condemns much of the press for their sensationalist tactics, distortion of statistics, and poor professionalism in not checking their sources; he has little trouble in finding numerous examples of these faults. The press is willingly used by the second targeted group, anti-nuclear activists. Together, they do more to hurt than help the public, both by prolonging debate when decisive action is required, and by causing unwarranted anxiety. Silver tells of one frightened women who called a government hot-line after reading headlines on the Chernobyl fallout: '... the lady was hysterical. She had been caught in the Toronto rain without an umbrella the previous day. Would she get cancer? Should she burn the clothes that got wet?'

Politicians form the third group to earn Silver's condemnation. Particularly at the federal level, they are generally described as being ignorant of nuclear issues, opportunistic in their reaction to the Chernobyl accident, and lacking any policy except to mouth epithets they judge will appeal to blocks of voters. The message is that political forces are destroying Canada's chances to make significant contributions to international reactor safety programs, or to help the Russians cope with the aftermath of Chernobyl. Indeed, Silver claims that members of the Mulroney cabinet are deliberately hoping to shut down the Canadian nuclear industry – not by a frontal assault, but by attrition and by evasion of responsibility. The few hardwork-

ing champions of nuclear power – Ontario Hydro, Jon Jennekens, a few isolated politicians, and the CANDU reactor itself – face an uphill battle against Ottawa stonewalling.

The conspiracy theory (the press, organized labour, activists, the NDP, and several other politicians are out to 'get' nuclear power) may be pushed too vehemently for the good of Silver's cause. Despite his condemnation of the press, Silver himself falls into the trap of unnecessarily dramatic language to describe the Chernobyl accident victims, 'Some had been burned by a flameless fury; some were unmarked, but an unseen and unfelt fire cooked the marrow in their bones.' Choice phrases such as 'cancerous rays' and 'curies of errant energy' from fallout, or bombs 'slicked to slip through supersonic air faster than sound'. show how easy it is to sacrifice correct terminology and accuracy in favour of dramatic effect.

Despite some shortcomings, this book may prove invaluable in exposing the public to a perspective on the nuclear debate which receives little press. Certainly, if the book can help stir politicians to adopt a consistent nuclear policy, this alone would be a tremendous triumph. Perhaps the most important message that Silver leaves with the reader is that 'there is no free lunch' – Nuclear power is not risk-free, but its record, including the Chernobyl accident, show that it has made a tremendous positive contribution to humanity.

A.N. Sinclair
Assistant Professor
Mechanical Engineering
University of Toronto

CNS Conferences and Seminars

CEGB Workshop 'Chemical Reactivity of Oxide Fuel and Fission Product Release,[1] 7–9 April 1987, Berkeley, UK

This Central Electricity Generating Board (CEGB) Workshop, co-sponsored by the British Nuclear Energy Society and the Canadian Nuclear Society, was the latest of the annual workshops on dry storage, which includes the 1984 Ontario Hydro Workshop on Irradiated Fuel Storage. It was attended by about 50 experts from the UK, France, Germany, Holland, the US (ORNL, LLL and PNL), and Canada. Three Canadian papers were presented by AECL and Ontario Hydro staff (see attached program) and the session 'Oxidation of UO_2 in air and fission product release' was chaired by C.R. Frost (Ontario Hydro).

The UO_2 oxidation / fission product release work reported at the workshop provides data to assist a) design of interim irradiated fuel dry storage facilities, and b) estimates of the radiological consequences of postulated low-probability in-reactor accidents. The workshop proceedings, including an account of the discussion periods, will be issued by the CEGB within 4 months.

Mechanisms of Oxidation of UO_2 in Air

'Structural Aspects of the Oxidation of UO_2.' N. Holmes and G.C. Allen, CEGB, Berkeley Nuclear Laboratories, UK.

'Investigation of the Mechanisms of UO_2 Oxidation in Air – The Role of Grain Size.'
P. Wood and G.H. Bannister, CEGB, Berkeley Nuclear Laboratories, UK.

'The Effect of Oxygen Partial Pressure on the Kinetics of Unirradiated UO_2 Oxidation.' P.M. Tucker, CEGB, Berkeley Nuclear Laboratories, UK.

'Surface Morphology and Characterisation of UO_2 Fuel Pellets Oxidised in Air at 230°C and 270°C.' P.A. Tempest, P.M. Tucker and J.W. Tyler, CEGB, Berkeley Nuclear Laboratories, UK.

'Release of Fine Particulate on the Oxidation of UO_2 in Air.' J.F.B. Payne and D. Butterworth, CEGB, Berkeley Nuclear Laboratories, UK.

Oxidation of UO_2 in Air and Fission Product Release

'Progress of Air Oxidation Tests of LWR Spent Fuel in an Imposed γ-Field.' E.R. Gilbert, T.K. Campbell, C.A. Knox, G.F. Piepel, Battelle, Pacific Northwest Laboratories, U.S.A.

'Influence of Manufacturing Route and Burnup on the Oxidation and Fission Gas Release Behaviour of Irradiated UO_2 in Air at 175 – 400°C.' M.J. Bennett, J.B. Price, P. Wood, UKAEA, Harwell and CEGB, BNL, UK.

'Fission Product and U_3O_8 Particulate Emission Arising from the Oxidation of irradiated UO_2 – Preliminary Studies.' R. Williamson and S.A. Beetham, UKAEA, Harwell, UK.

'Fission Product Release and UO_2 Oxidation.' F.C. Iglesias, C.E.L. Hunt, D.S. Cox, N.A. Keller, R.D. Barrand, J.R. Mitchell, R.F. O'Connor, AECL, Chalk River, Canada.

'The Oxidation of Unirradiated UO_2 in CO_2 / O_2 Atmospheres.' J. Edwards, W.E. Ellis, F. Frazer, UKAEA, Windscale, UK.

Oxidation of (U, Pu)O_2 in Air and Dry Fuel Storage

'Heating of Untight LMFBR Fuel Elements under Oxidising Atmospheres.' J. Rouault and J. Girardin, CEA, Cadarache, France.

'Experimental Study of Fission Product Release from a Breached LMFBR Fuel Pin under Oxidising Conditions.' J. Birardin and J. Rouault, CEA, Cadarache, France.

'Predicting Spent Fuel Oxidation States in a Tuff Repository.' R.E. Einziger, R.E. Woodley, Westinghouse Hanford, U.S.A.

'The Chemical State of Fission Products in LWR Fuels Related to Long-Term Dry Storage.' R. Kohli, Battelle, Columbus Division, U.S.A.

'UO_2 Oxidation in Air at 50°C to 400°C and the Implications for CANDU Irradiated Fuel Dry Storage.' C.R. Frost and K.M. Wasywich, Ontario Hydro and AECL, Canada.

'Application of the UO_2 Oxidation Data to the Interim Storage of Irradiated Fuel in an Air Environment.' D.J. Wheeler, GEC – Energy Systems Limited, UK.

Oxidation of UO_2 and Fission Product Release in Reactor Coolant

'Fission Gas Release from Irradiated UO_2 during Post-Irradiation Annealing in CO_2 / CO Atmospheres.' J.C. Killeen and J.A. Turnbull, CEGB, Berkeley Nuclear Laboratories, UK.

'Fission Product Release from Defective Fuel.' B.J. Lewis, AECL, Chalk River Nuclear Laboratories, Canada.

'The Influence of Environment on Release Behaviour and Chemical Forms of Fission Products Released under LWR Accident Conditions.' J.L. Collins, M.F. Osborne, R.A. Lorenz, Oak Ridge National Laboratory, U.S.A.

Oxidation of UO_2 and Fission Product Release in Reactor Coolant

'Transient Release of Iodine and Caesium from Spent Fuel in the Presence of Zircaloy and Oxygen.' G. Kaspar and M. Peehs, KWU, Federal Republic of Germany.

'The Role of Zircaloy Cladding on Fission Product Tellurium Release during a Severe Reactor Accident.' B.R. Bowsher, S. Dickinson, R.A. Gomme, A.L. Nichols, J.S. Ogden, UKAEA, Winfrith and University of Southampton, UK.

'Chemical Speciation of Fission Products using Matrix Isolation Infrared Spectroscopy and Mass Spectroscopy.' B.R. Bowsher, R.A. Gomme, J.S. Ogden, UKAEA, Winfrith and University of Southampton, UK.

Instructions for Authors

Scope of the Journal
The *Nuclear Journal of Canada*, published quarterly, is an international journal devoted to original contributions in all fields related to nuclear science, engineering, and medicine, including related science, engineering and technologies, materials, underlying principles, and social and ethical issues. Original articles, notes, and critical reviews will be considered for publication in the *Journal*. Submissions will be refereed. The Editor reserves the right to reject any submission deemed unsuitable for publication.

Original articles must be of a reasonably broad scope and of significance to the nuclear community. Notes should describe significant work in progress or of a novel nature.

Papers and discussions are published in English or French at the author's preference. The International System of Units (SI) must be used.

Manuscripts
Normal manuscript length is in the range of 5,000 – 15,000 words. The original and four copies should be submitted to the Editor, who will acknowledge receipt. The manuscript will then be sent to an Editorial Board member, who will arrange for independent reviews of the manuscript. Following review, the manuscript will either be approved for publication, or will be returned to the author if judged unsuitable for the *Nuclear Journal of Canada*. Upon acceptance, the Editor will contact the author to advise on the issue in which the paper will appear and the publication deadlines.

The manuscript should be typewritten, or computer printed (NLQ), in black ink, double-spaced, single-sided, on paper 210 × 297 mm (8 × 11 in.) with 25 mm left and right margins. Each page should be numbered starting with the title page. The following items are to be included:

Title Page should specify title, author names, affiliations, full postal addresses, and telephone numbers, number of pages of text, number of figures, and number of tables.

Abstracts should be not more than 150 words and on a separate page. The abstract should emphasize the new results and be self-contained so that it can be used by the abstract services without change. One should not have to read the paper in order to understand the abstract. The use of the first person singular pronoun must be avoided. Authors able to submit abstracts in both English and French should do so, in the interests of clarity, accuracy and speed of production. References should not be cited in the abstract.

Keywords should not exceed fifteen and should be placed directly below the abstract. All keywords used should be referenced in the 'Thesaurus of Engineering and Scientific Terms,' published by the Engineers Joint Council (New York).

Equations and formulae should be numbered in square brackets flush with the right hand margin. Unusual and Greek characters should be clearly identified.

References should be cited in parentheses in the text, by authors' last names and year of publication. For example: 'Previous studies (Critoph 1977; Duret 1978; and Notley 1983) indicate that ...' All citations should be listed on a 'Notes and References' page following the text. They should appear unnumbered, alphabetically by author, in the format:

Author(s) (names followed by initials). Title of article, book, or thesis. Name of publication, publisher, or university. Location. Volume or edition. Year. First and last page of article, or pages in book. (If there are two authors, both should be named in full; if more than two, the citation should give the first author's name followed by *'et al.'*

Tables should be typed on separate sheets. Their desired location should be indicated in the text. Tables should be numbered with Arabic numerals. Complicated column headings should be avoided. Descriptive footnotes should be indicated by superscripts, (a), (b), (c), etc. and begun anew for each table.

Figures should be numbered with Arabic numerals. The figure number is to be shown on the back of each figure. On a separate piece of paper, attached to the back of the figure, is to be shown the author name(s), the title of the paper, the figure number, the figure caption, the orientation on the page and any instructions with regard to cropping. Lettering should be large enough to be legible after reduction of the figure to a single-column width of 8.5 mm. Capital letters after this reduction should have a height of 1.5 – 2.0 mm. Photographs should be glossy prints and should have maximum contrast.

Acknowledgements should be written in the third person and kept to a concise recognition of relevant contributions and financial support.

Copyrighted material If a manuscript contains any material that is protected by copyright, the author must submit to the Editor, before publication, written permission from the copyright holder for its reproduction.

Discussions An original and one copy of discussions should be submitted in typewritten form. Double-spaced, single-sided as for original manuscripts, to the Editor.

Galley Proofs
Galley proofs are provided to the authors for the correction of printing errors and not for improvements in the paper. The cost of changes introduced by the author(s) will be charged to them. Corrected galley proofs are to be returned within 48 hours of receipt. Authors are solely responsible for the technical accuracy of their material as it finally appears in print.

Books for Review
Books for review should be offered or sent to the Editor. Book reviews will be published as space permits.